Resource Allocation in Relay Networks

Anahid Attarkashani

A Thesis

in

The Department

of

Electrical and Computer Engineering

Presented in Partial Fulfillment of the Requirements

For the Degree of

Doctor of Philosophy (Electrical & Computer Engineering) at

Concordia University

Montréal, Québec, Canada

July 2018

CONCORDIA UNIVERSITY

SCHOOL OF GRADUATE STUDIES

This is to certify that the thesis prepared

By: Anahid Attarkashani

Entitled: Resource Allocation in Relay Networks

and submitted in partial fulfillment of the requirements for the degree of

Doctor of Philosophy (Electrical & Computer Engineering)

complies with the regulations of this University and meets the accepted standards with respect to originality and quality.

Signed by the final examining committee:

_____ Chair
Dr. Andrea Schiffauerova

_____ External Examiner
Dr. Franois Gagnon

_____ External to Program
Dr. Alina Stancu

_____ Examiner
Dr. Yousef R. Shayan

_____ Examiner
Dr. Dongyu Qiu

_____ Thesis Supervisor
Dr. Walaa Hamouda

Approved by _____
Dr. Mustafa Mehet Ali, Graduate Program Director

Monday, September 24, 2018 _____
Dr. Amir Asif, Dean
Faculty of Engineering and Computer Science

Abstract

Resource Allocation in Relay Networks

Anahid Attarkashani, Ph.D.

Concordia University, 2018

Demand for high data rates is increasing rapidly, due to the rapid rise of mobile data traffic volume. In order to meet the demands, the future generation of wireless communication systems has to support higher data rates and quality of service. The inherent unreliable and unpredictable nature of wireless medium provides a challenge for increasing the data rate. Cooperative communications, is a prominent technique to combat the detrimental fading effect in wireless communications. Adding relay nodes to the network, and creating s virtual multiple-input multiple-output (MIMO) antenna array is proven to be an efficient method to mitigate the multipath fading and expand the network coverage. Therefore, cooperative relaying is considered as a fundamental element in the Long Term Evolution (LTE)-Advanced standard.

In this thesis, we address the problem of resource allocation in cooperative networks. We provide a detailed review on the resource allocation problem. We look at the joint subcarrier-relay assignment and power allocation. The objective of this optimization problem is to allocate the resources fairly, so even the cell-edge users with weakest communication links receive a fair share of resources. We propose a simple and practical algorithm to find the optimal solution. We assess the performance of the proposed algorithm by providing simulations. Furthermore, we investigate the optimality and complexity of the proposed algorithm.

Due to the layered architecture of the wireless networks, to achieve the optimal performance it is necessary that the design of the algorithms be based on the underlying physical and link layers. For a cooperative network with correlated channels, we propose a cross-layer algorithm for relay

selection, based on both the physical and link-layer characteristics, in order to maximize the link-layer throughput. The performance of the proposed algorithm is studied in different network models. Furthermore, we investigate the optimum number of relays required for cooperation in order to achieve maximum throughput.

Buffering has proven to improve the performance of the cooperative network. In light of this, we study the performance of buffer-aided relay selection. In order to move one step closer to the practical applications, we consider a system with coded transmissions. We study three different coding schemes: convolutional code, Turbo code, and distributed Turbo code (DTC). For each scheme, the performance of the system is simulated and assessed analytically. We derive a closed-form expression of the average throughput. Using the analysis results, we investigate the diversity gain of the system in asymptotic conditions. Further, we investigate the average transmission delay for different schemes.

Acknowledgments

I would like to express my gratitude to all those who gave me the opportunity to complete this thesis. First and foremost, I would like to express my sincere gratitude to my supervisor, Prof. Walaa Hamouda for his support and guidance through this work. His wide knowledge and vision on telecommunications have been a great value for me. I am also thankful to him for giving me detailed and constructive comments. I am also grateful to my committee members, Prof. Yousef Shayan, Prof. M. Omair Ahmad, and Prof. Alina Stancu for providing invaluable feedback that made this thesis better.

I gratefully acknowledge the Concordia Graduate Students Support Program (GSSP) and the Department of Electrical and Computer Engineering at the Concordia University for their financial support.

My deepest gratitude belongs to my husband, Siavash Gorji, for his love, understanding, support and care during the whole study period. I also thank my father for his constant love and support. At the end, I would like to dedicate this thesis to my late mother. Her unconditional love is something I can never pay back.

Contents

List of Figures

List of Tables

List of Acronyms

3GPP	Third Generation Partnership Project
ACK	Acknowledgment
A/D	Analog-to-Digital converter
AF	Amplify and Forward
AWGN	Additive White Gaussian Noise
BCJR	Bahl, Cocke, Jelinek, and Raviv
BER	Bit Error Rate
BICM	Bit-Interleaved Coded Modulation
BPSK	Binary Phase-Shift Keying
BRS	Best Relay Selection
CDF	Cumulative Density Function
CRC	Cyclic Redundancy Check
CSI	Channel State Information
D/A	Digital-to-Analog converter
DF	Decode and Forward
DoF	Degrees of Freedom
DTC	Distributed Turbo Code
EH-WSN	Energy Harvesting Wireless Sensor Network
FER	Frame Error Rate
FFT	Fast Fourier Transform
GCD	Greatest Common Divisor
HD	Half Duplex
i.i.d	Independent and Identically Distributed
i.n.i.d	Independent but Not Identically Distributed
ISI	Inter Symbol Interference
LBAP	Linear Bottleneck Assignment Problem

LLR	Log-Likelihood Ratio
LPF	Low Pass Filter
LSAP	Linear Sum Assignment Problem
LTE-A	Long Term Evolution-Advanced
MAP	Maximum A Posteriori
MIMO	Multiple-Input Multiple-Output
MRC	Maximal Ratio Combining
MRS	Multiple Relay Selection
NACK	Negative Acknowledgment
OFDM	Orthogonal-Frequency-Division Multiplexing
PDF	Probability Density Function
PER	Packet Error Rate
PEP	Pairwise Error Probability
PRS	Partial Relay Selection
PSK	Phase-Shift Keying
QAM	Quadrature Amplitude Modulation
RD	Relay to Destination
RSC	Recursive Systematic Convolutional
SD	Source to Destination
SER	Symbol Error Rate
SIR	Signal-to-Interference Ratio
SNR	Signal-to-Noise Ratio
SOVA	Soft Output Viterbi Algorithm
SR	Source to Relay
SRS	Single Relay Selection
WSN	Wireless Sensor Network

List of Common Symbols

$\boldsymbol{x}$	vector $\boldsymbol{x}$
$\boldsymbol{X}$	matrix $\boldsymbol{X}$
x_{ij}	entry of row i and column j of matrix $\boldsymbol{X}$
$\in$	within the group
$\min$	minimization
$\max$	maximization
$O()$	order of complexity
$Q()$	Q-function
$\mathbb{P}()$	probability
$\forall$	for all
$\boldsymbol{X}^{\mathsf{T}}$	transpose of $\boldsymbol{X}$
$\boldsymbol{X}^{-1}$	inverse of $\boldsymbol{X}$
$\boldsymbol{X}^{H}$	conjugate transpose of $\boldsymbol{X}$
$\mathcal{N}$	Normal distribution
$\mathbb{E}()$	expected value
$\boldsymbol{I}_k$	identity matrix of size k
$det()$	determinant
$f()$	probability distribution function
$F()$	cumulative distribution function
$\mathbb{R}$	set of real numbers
$\Gamma()$	Gamma function

Chapter 1

Introduction

1.1 Cooperative Communication

With the advent of easily accessible personal wireless devices that support a variety of wireless services, more and more people rely on these devices for their daily activities. The increasing number of mobile broadband subscribers leads to the rapid growth of mobile data traffic. According to [1], between 2016 and 2022, the traffic generated by smart phones will increase by a factor of $\times 10$. In order to provide the required data traffic, the target data rate is increased in every generation of wireless mobile telecommunications technology. In addition to data rate, mobile broadband subscribers require reliable communication, increase in mobility, and higher quality of service.

One barrier to achieve high data rates while satisfying the requisite quality of service is the unpredictability and unreliability of the wireless medium. An emitted signal through the wireless medium arrives at the receiver from multiple paths, therefore the received signal suffers from distortion. This effect is known as *multipath fading*. This channel characteristic varries with time, if the transmitter, receiver, and the obstacles blocking the line-of-sight path are moving [2]. Multipath fading has detrimental effects on the network performance. One of the most effective techniques to mitigate the effects of fading is *diversity*.

The main idea behind the diversity technique is to transmit the same signal over independent fading channels. One method to provide independent fading channels is to use multiple transmit and/or receive antennas, which are separated in space. In applications where placing multiple antennas

at transmitter/receiver sides is challenging due to the limitations of size or power, the independent channels are established by adding *relay* nodes to the network. These single antenna nodes share their antennas and create a virtual multiple-input multiple-output (MIMO) antenna array. This technique is known as *cooperative diversity*. Substantial studies on cooperative communication confirm its advantages. First, significant diversity gain is achieved. Furthermore, communication through a relay node reduces the distance between the transmitter and the receiver nodes, hence the effect of path loss is reduced. In addition, the network coverage is enhanced by providing reliable communication links for cell edges users. Considering these advantages, in the study performed by the Third Generation Partnership Project (3GPP) for the Long Term Evolution (LTE)-Advanced standard development, cooperative relaying is included as an essential element in cellular networks [3]. However, with the advantages offered by relay communications, many challenges need to be addressed.

1.2 Motivation

The motivations behind this study are to:

(1) study the challenges in cooperative networks;

(2) propose practical solutions in order to enhance the performance of cooperative networks, while respecting the limitations;

(3) provide analytical and simulation frameworks for the proposed algorithms.

In design of wireless networks, one of the most important considerations is the allocation of resources, such as power and bandwidth. Optimal power allocation plays a key role in performance improvement of the network. It is known that the data rate and coverage of a network are improved by more power consumption, however the increased interference and cost appear as restricting factors. In the context of cellular networks, power consumption at the user ends is considered an important issue, in order to maximize the battery life time. Another network resource that should be considered is the radio spectrum. The radio spectrum is a scarce resource, therefore, it is regulated by regulatory authority to guarantee the efficient use.

Second challenge in design of wireless networks is the layered architecture. Network layers are associated with different system operations. The physical layer administers the transmission and reception of bits over the physical medium, the data link layer insures the reliable transmission over the physical layer, network and transport layers handle routing, addressing, and connectivity, and the application layer manages data rates and delay constraints related to the applications [2]. These layers are designed in a separate manner, in order to reduce the intricacies of the design, and to simplify the standardization. Nevertheless, the overall network performance is not always optimal, in the absence of a global optimization [2]. The performance of the layered network can be enhanced by a cross-layer design that considers the quality of service requirements of different layers, at the same time.

Recently, the application of *buffer-aided* relays in cooperative networks has attracted attention [4]. Substantial studies in this area indicate significant improvement in the performance of cooperative networks. It has been proven that buffer-aided relays improve the networks throughput, diversity, stability, and balances the traffic load passing through each relay [4]. Equipping relays with data buffers enable them to store and transmit packets in appropriate link condition. The main drawback of buffering is additional total transmission delay. However, in the applications that delay is tolerated, the system can benefit from many advantages of buffer-aided relaying. Considering the above challenges and techniques, the focus of this thesis is design of proper algorithms to improve the performance of the cooperative network with efficient exploitation of resources.

1.3 Thesis Contributions

The contributions of this thesis can be summarized as follows.

- We consider a cooperative network combined with orthogonal-frequency-division multiplexing (OFDM). For this model, we study the problem of joint power allocation and subcarrier-relay assignment. This resource allocation problem is a non-convex optimization problem and can be solved through an exhaustive search. We propose a practical algorithm to find the optimal solution with polynomial time complexity [5, 6].

- Considering both the physical and link-layer characteristics, we propose a cross-layer algorithm for relay selection in order to maximize the link-layer throughput. We consider a system model with equally spatially correlated channels, featuring closely placed relays (or a relay cluster). We show that the cross-layer design significantly improves the system performance in comparison to the capacity-based design [7].

- As a step to get closer to practical applications, and in consideration of the advantages of buffering, we study the performance of buffer-aided relay selection in a system with coded transmissions. We consider a general model for channels where channels are independent but not identically distributed, reflecting different distances among the nodes. We study three coding schemes: convolutional code, Turbo code, and distributed Turbo code (DTC). For each coding scheme, we derive a closed-form expression for the average throughput. Using this average throughput, we analyze the asymptotic behavior of the system for infinite buffer size and in high-SNR regime, which provides us with an important insight on the maximum achievable diversity gain [8, 9].

1.4 Thesis Organization

The rest of the thesis is organized as follows:

In Chapter 2, we present some background on cooperative network and different methods of relay selection and resource allocation. Then, we briefly present the OFDM transmission technique. The principles of channel coding techniques including convolutional code, Turbo code and DTC are covered. At last, we present the basics of buffer-aided relaying and the related works on this topic.

In Chapter 3, we propose an optimal algorithm for the joint power allocation and subcarrier-relay assignment problem in OFDM relay networks, with L half-duplex (HD) decode-and-forward (DF) relays, and M subcarriers. Our objective is to find the best subcarrier-relay assignment and power allocation, that maximizes the minimum received SNR. This non-convex optimization problem could be solved by exhaustive search, which is not practical when the number of subcarriers and relays is large. Suboptimal methods, that solve the relay assignment problem and power allocation separately have less time complexity at the expense of performance degradation. We propose

a simple algorithm to jointly solve the subcarrier-relay assignment and power allocation problem. We show that the proposed algorithm finds the optimal solution with complexity order of $O(M^3L)$.

In Chapter 4, we propose a cross-layer-based relay selection scheme in a wireless sensor network (WSN) with equally spatially correlated channels. The equally correlated model can be used as a worst-case benchmark or as a rough approximation by assuming equal correlation coefficients for all channels. By considering the physical and link layer characteristics, one or multiple relays are selected to maximize the link layer throughput. Based on the channel characteristics, the best performance is achieved by using one cooperative relay in poor links and multiple relays in high quality links. We compare the performance of the proposed scheme with the capacity-based scheme and we see that considerable improvement in performance is achieved in both correlated and uncorrelated channels. We examine the proposed scheme for both DF and amplify-and-forward (AF) relaying, and for relay selection and subcarrier allocation in OFDM-based systems. In all cases, the cross-layer technique is shown to offer significant improvement relative to physical-layer optimization techniques.

In Chapter 5, we study the performance analysis of a relay selection scheme in a buffer-aided multi-relay network with coded transmissions. We consider three different coding schemes: convolutional codes, Turbo codes and DTC. Moreover, it is assumed that the channels undergo quasi-static Rayleigh fading and all the links are independent but non-identically distributed. For each of the coding schemes, we analyze the performance of the system in terms of the average throughput, and derive a closed-form expression. In addition, simple and explicit approximations of the average throughput for infinite buffer size and in the high-SNR regime are obtained to provide some insights on how various system parameters impact the system performance. An analysis of the asymptotic average throughput provides the maximum achievable diversity gain of the system. Finally, we verify the accuracy of the derived analytical framework by providing Monte-Carlo simulations. We show that analytical average throughput holds tight under different system parameters.

In Chapter 6, we summarize the results and contributions described above. We also suggest different areas for future studies.

Chapter 2

Background and Literature Review

In this chapter, we present a brief background on topics related to this thesis, and we provide a literature review on the related works.

2.1 Cooperative Communication

Cooperative communication is based on the work done on relay networks proposed in [10]. In this work, the capacity of the network consisting of one source node, one destination node, and one relay node is analyzed. The benefits of relaying networks have been widely acknowledged in [11]. First, using relays reduce the communication distance between nodes. A reliable direct transmission in long distances requires high power, which causes faster battery drainage and increased interference. Adding relay nodes to the network reduces the communication distance. Therefore, less power is required for reliable transmission and the network coverage expands. Apart from that, relays add independent paths to the network, therefore, spatial diversity is achieved. Diversity is of high importance due to the inevitable fading effect in wireless networks. The schematic of a relay network is shown in Fig. 2.1.

In [12], the authors suggest that spatial diversity can be achieved by cooperation of mobile users and call it *User Cooperation Diversity*. In the suggested scheme, mobile users share their antenna and act as a relay for other users (see Fig. 2.1). Cooperative network is similar to relay network in many aspects, although the main difference is that in cooperative network users are responsible

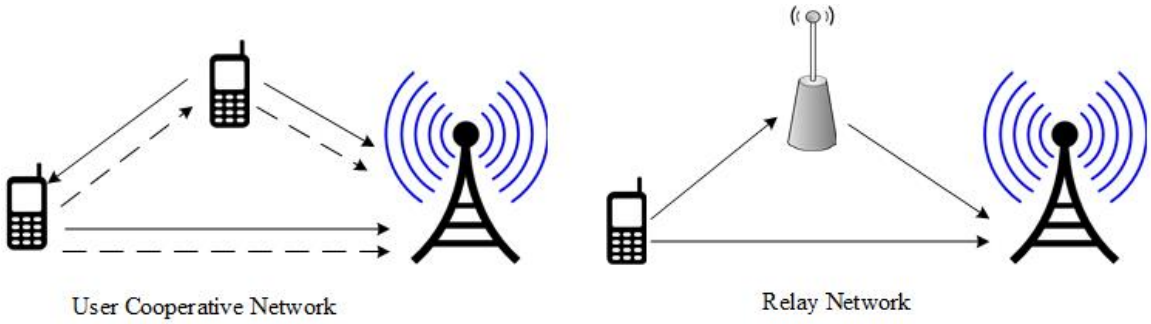

Figure 2.1: Cooperative Networks

for transmitting their own information, while acting as a relay for other users. However, in relay networks the only role of a relay is receiving and forwarding the information from other source nodes. In this work, we consider a relay network for simplicity, but the proposed methods can be extended to cooperative networks.

2.1.1 Cooperative Signaling Methods

There are two main transmission protocols in cooperative networks:

- **Decode and forward**: In this protocol, the relay decodes and re-encodes the received signal before forwarding (Fig. 3.9). The relay nodes require the knowledge of channel state information (CSI) in order to decode the received signal. In this protocol, in case of incorrect decoding the cooperation would result in error propagation.

- **Amplify and forward**: In this protocol, the relay amplifies the received signal before forwarding (Fig. 3.9). The advantage of this protocol is its simplicity. However, when the relay amplifies the received signal, the noise is also amplified. Furthermore, sampling, amplifying and transmitting an analog signal is difficult.

2.2 Resource Allocation

The resource allocation problem in cooperative networks has been widely addressed in the literature [13–17, 17–20]. Resource allocation is an optimization problem with an objective of achieving

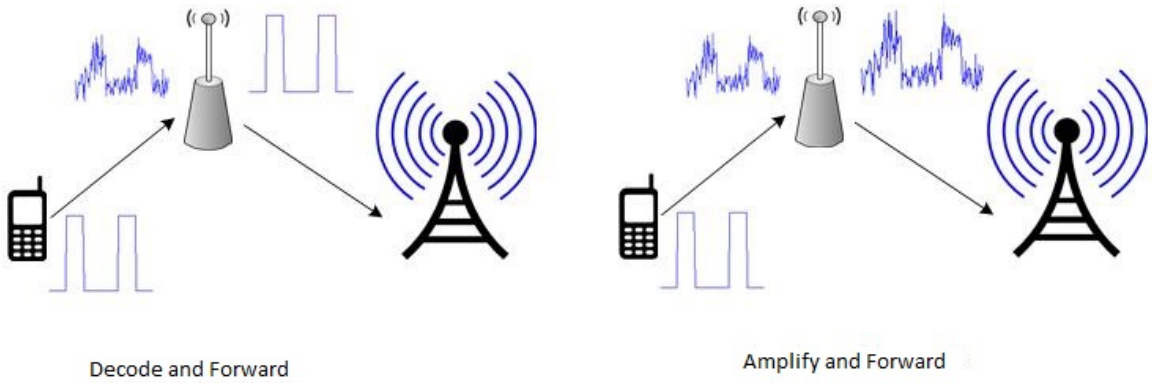

Figure 2.2: Cooperative signaling methods

the best performance, given the available resources. There are two main resources in cooperative networks: relays and power.

2.2.1 Relay Selection

The relay selection problem deals with the selection of one or a set of relays based on different metrics to satisfy different criteria. A proper technique for relay selection can improve the performance of a wireless network by achieving full diversity. Relay selection problem has been widely studied in literature [13, 14, 21–25]. Two main schemes proposed are, the single relay selection (SRS) and multiple relay selection (MRS). In SRS, the best relay is selected according to a certain criterion. It is shown that employing this scheme, full diversity is achieved [13]. In MRS, a subset of reliable relays is selected. In this scheme, the weakest paths are excluded, therefore better performance is achieved compared to conventional cooperative networks [14].

Although multi-relay transmission offers better performance than single relay transmission, its implementation requires additional resources and increased complexity. Multiple relays utilize either orthogonal subchannels (in time or frequency) or space-time codes to transmit their information to the destination node. Orthogonality in time or frequency, leads to consumption of scarce resources and results in performance loss in terms of transmission rate or spectral efficiency. To overcome this problem, space-time coded protocols are proposed for cooperative relaying in [26–30]. Design of space-time codes for multi-relay networks is different from MIMO schemes and difficult

in practice. Different from MIMO schemes, in a multi-relay network, antennas belong to dispersed terminals. Therefore, the creation of a virtual MIMO terminal from distributed relays requires coordination and additional synchronization among different nodes. In addition, in a multi-relay network, the number of participating relays is variable. A relay may not participate in cooperation if the it has not received the signal successfully [13]. To avoid the complexity of the space-time code design, and the excessive use of resources (e.g. time and bandwidth), single relay selection or best relay selection (BRS) schemes have been proposed in [13]. It has shown that BRS achieves the same diversity gain as a multi-relay transmission. Substantial work has been done based on the BRS scheme. This method is also adapted to various applications, for instance, in [31–33], BRS is employed under the concept of cognitive radio, and in [34] it is combined with network coding.

Different selection criteria are used to select the best relay [13, 21–25]. The commonly used selection metrics in the literature are categorized as follows:

- **Geographical location**: By this metric, relays are selected based on their spatial distribution. It is assumed that the locations of the relays are known or can be estimated. This metric is used in [21–23]. The disadvantage of this metric is that the effects of shadowing and fading are neglected.

- **Average channel characteristics**: By this metric, relays are selected based on an estimate of the average channel fading, or average SNR. While this method works well for static terminals, it is not recommended for mobile terminals, since channels are subject to considerable change.

- **Instantaneous channel characteristics**: By this metric, relays are selected based on an estimate of instantaneous channel characteristics. This metric is vastly used in numerous works like [13, 24, 25]. The main drawback of this metric is the large amount of overhead communicated between terminals, to propagate the channel information.

The relay selection algorithms proposed in the literature follow different criteria [13, 35–41]. The most commonly used criteria are:

- **Max-Sum criterion**: By this criterion, a relay or a set of relays are selected that maximize

the sum of data rates. This criterion is used in [35–38] to maximize the summation of data rates.

- **Max-Min criterion**: By this criterion, a relay or a set of relays are selected in order to maximize the minimum SNR or date rate. This method is used in [13, 39–41].

2.2.2 Joint Relay Selection and Power Allocation

The problem of resource allocation in cooperative networks is not limited to relay selection. Power allocation is another issue, that with the proper solution could enhance the system performance as well. The problem of joint relay selection and power allocation is described to be non-convex. To find the optimal solution to this non-convex optimization problem, different solutions are proposed in the literature:

- **Exhaustive search**: This method selects the best relay or relays among all the possible selections. The solution is optimal, however, the complexity of this method increases with the increase in the number of relays [15, 16].

- **Dual decomposition method**: This method results in an asymptotical solution. With the increase in the number of relays, the solution asymptotically reaches to the optimal solution. However, the complexity is still an issue with the increase in the number of relays [17, 18].

The main problem of these methods is the increase in time complexity of the algorithm, with an increase in the number of relays. In communication systems, the number of relays or users could be very large, which makes the aforementioned methods impractical. To deal with this issue, some suboptimal algorithms are proposed. These algorithms provide less complexity, at the expense of performance degradation. Suboptimal methods can be categorized as follows:

- **Two part method**: In this method, relay assignment and power allocation are performed separately. In [17, 19, 20], different suboptimal algorithms are proposed based on this method.

- **Partial relay selection**: In this method, the complete knowledge of the system is not being considered in the selection process. In [42], the authors propose a partial relay selection (PRS) algorithm. In this algorithm, first a subset of relays is pre-selected based on the average CSI,

then the best relay is selected based on the instantaneous CSI out of the pre-selected subset. In [15], the authors propose another PRS algorithm that uses only the knowledge of relay to destination node channels.

- **Other methods**: Other suboptimal methods are proposed that address the problem of joint relay selection and power allocation. In [16], the authors propose a suboptimal algorithm based on a relay ordering function, similar to the greedy approximation algorithm for knapsack problems [43].

2.3 Assignment Problem

The problem of resource allocation in cooperative networks can be considered as an assignment problem. Assignment problem deals with the question of how to assign n items to n other items [43]. An assignment problem can be described mathematically as a mapping π between two finite sets U and V of n elements. π is called a *permutation*. Each permutation can be represented by a permutation matrix $X = [x_{ij}]$, defined by

$$x_{ij} = \begin{cases} 1 & \text{element } j \text{ is assigned to element } i \\ 0 & o.w \end{cases} \tag{2.1}$$

This permutation matrix is described by a system of linear equations

$$\begin{aligned} &\textstyle\sum_{j=1}^{n} x_{ij} = 1 && i = 1, 2, ..., n \\ &\textstyle\sum_{i=1}^{n} x_{ij} = 1 && j = 1, 2, ..., n \\ &x_{ij} \in \{0, 1\} && \text{for all } i, j = 1, 2, ..., n \end{aligned} \tag{2.2}$$

This means that every row and every column of the permutation matrix has sum of 1. An $n \times n$ cost matrix $C = [c_{ij}]$ measures the cost of assigning element j to element i. The assignment problem can be defined as an optimization problem that searches for the best permutation to satisfy an objective function. The objective functions vary with different applications. If the objective is to minimize

the total cost, the objective function is defined by

$$\min \sum_{i=1}^{n} \sum_{j=1}^{n} c_{ij} x_{ij}, \tag{2.3}$$

$$\tag{2.4}$$

or if we show each permutation with π, the objective function can be written as

$$\min_{k=1,2,\dots K} \sum \pi_k, \tag{2.5}$$

in which π_k represents the k^{th} permutation out of whole $K = n!$ permutations. This problem is called *linear sum assignment problem(LSAP)* [43] and it corresponds to the max-sum criterion mentioned in section 2.2.1. The $\min$ function can be easily replaced by the $\max$ function.

Another objective is to minimize the maximum cost. This objective function is defined by

$$\min \max_{1 \le i,j \le n} c_{ij} x_{ij}. \tag{2.6}$$

$$\tag{2.7}$$

or as another representation

$$\min_{k=1,2,\dots K} \max \pi_k \tag{2.8}$$

This problem is called *linear bottleneck assignment problem(LBAP)* [43] and it corresponds to the max-min criterion mentioned in 2.2.1 by substituting the $\min$ function and $\max$ function. The algorithms for solving the LSAP and LBAP are presented in the following subsections.

2.3.1 Hungarian Algorithm

The Hungarian algorithm is proposed in [44] to solve LSAP. The algorithm is based on this theorem: "If a number is added to or subtracted from all of the entries of any row or column of a cost matrix, then an optimal assignment for the resulting cost matrix is also an optimal assignment for the original cost matrix." [43]. The following algorithm applies this theorem to a $n \times n$ cost

matrix to find an optimal assignment. It is shown that the time complexity of this algorithm is

Algorithm 1 Hungarian Algorithm

step 1: Subtract the smallest element in each row from all the elements of the same row
step 2: Subtract the smallest element in each column from all the elements of the same column
step 3: Draw lines through appropriate rows and columns so that all the zero elements of the cost matrix are covered and the minimum number of lines is used
step 4:
if the minimum number of covering lines is n **then**
The assignment is possible. Go to step 6
else
go to step 5
end if
step 5: Determine the smallest element not covered by any line. Subtract this element from each uncovered row, and then add it to each covered column
go to step 3
step 6: The assignment is the zero element of the cost matrix

$O(N^4)$. The best time complexity of Hungarian algorithm is $O(N^3)$ [45].

2.3.2 Threshold Algorithm

The Threshold algorithm is proposed to solve LBAP [43]. This algorithm consists of two phases. In phase 1, a threshold value c^* is chosen from the elements of the cost matrix, and a threshold matrix $\bar{C} = [\bar{c}_{ij}]$ is formed as follow

$$\bar{c}_{ij} = \begin{cases} 1 & c_{ij} > c^* \\ 0 & o.w \end{cases} \tag{2.9}$$

In phase 2, it is checked whether the threshold matrix $\bar{C}$ contains an assignment with the total cost of 0. If this assignment is found, the search is completed. If it is not found, phase 1 is repeated with a different threshold value c^*. Phase 1 can be performed using the binary algorithm. In this case, the time complexity of the threshold algorithm is $O(T(n)\log(n))$, in which $T(n)$ is the time complexity for checking if the cost matrix contains an optimal assignment or not. The threshold algorithm with the binary search is presented as follows:

If the corresponding assignment is needed, the method proposed in [46] can be used. This method has the time complexity of $O(\frac{n^{2.5}}{\sqrt{\log n}})$.

Algorithm 2 Threshold Algorithm

Initialize i_{min} = the minimum element of C
Initialize i_{max} = the maximum element of C
repeat
  $m = \lfloor \frac{i_{min}+i_{max}}{2} \rfloor$
  Define $\bar{C}$ using (2.9)

  if $\bar{C}$ contains an assignment with cost 0 **then**
    $i_{min} = m$
  else
    $i_{max} = m$
  end if
until The smallest c^* is found

2.4 OFDM

Multicarrier modulation is a technique where a wide-band signal is divided into a number of narrow-band signals and sent through different orthogonal subchannels [2]. The data rate and the bandwidth of each subchannel is much smaller than the total date rate and bandwidth of the system. In multicarrier modulation, the effect of inter-symbol interference (ISI) can be alleviated, if the bandwidth of each subchannel is smaller than the coherent bandwidth of the channel [2]. In this case, each subchannel experiences flat fading.

OFDM is a digital implementation of multicarrier modulation that uses fast Fourier transform (FFT)-based modulator and cyclic prefix. This technique is used substantially in wireless communications, for instance in Wi-Fi, WiMax, LTE, and LTE-Advanced [47]. The advantages of OFDM technique include the elimination of ISI, low complexity of FFT algorithms, and the omission of the complex equalizers [2].

The block diagram for OFDM transmitter and receiver is shown in Fig. 2.3 and 2.3. In the transmitter, the input data bits are modulated, usually with a quadrature amplitude modulation (QAM) or phase-shift keying (PSK) modulator. This symbol stream goes through a serial-to-parallel converter. The output is a sequence of N parallel symbol streams. Each symbol stream is transmitted through each subchannel, therefore these streams are frequency components of the output of the transmitter. By passing these symbol streams through an IFFT block, frequency components are converted into time samples. Then, cyclic prefix is added and samples are put back into one sample stream. This

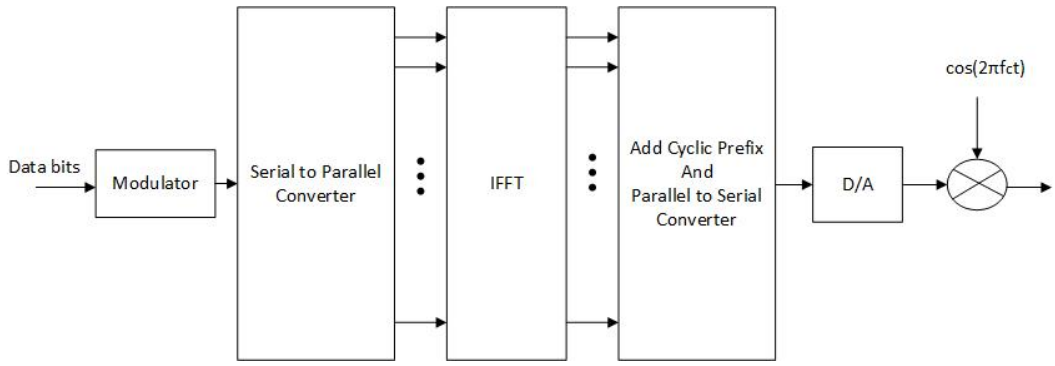

Figure 2.3: OFDM Transmitter

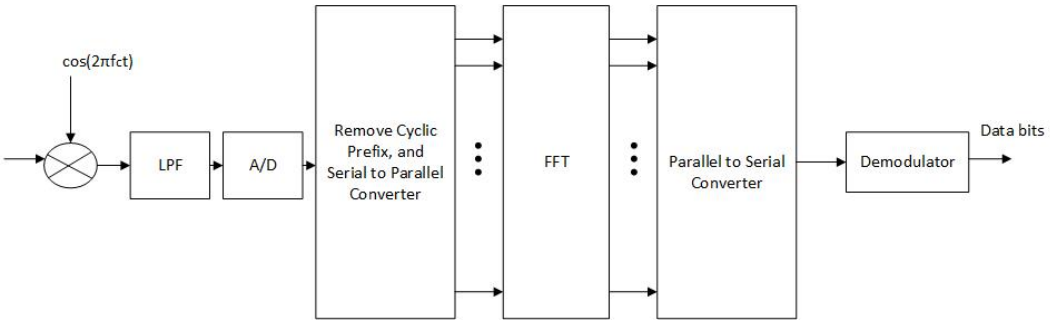

Figure 2.4: OFDM Receiver

stream is digital-to-analog converted and transmitted over the carrier frequency of f_c.

At the receiver, the received signal is down converted and passed thorough a low pass filter (LPF) to remove the carrier frequency. An analog-to-digital (A/D) converter samples the signal, then the cyclic prefix is removed and the samples are passed through a serial-to-parallel converter. The result is a sequence of N parallel streams. These streams are passed through an FFT block, parallel-to-serial converted and demodulated to recover the transmitted data bits.

2.5 Wireless Sensor Network (WSN)

WSN consists of many sensor nodes that are randomly distributed and communicate wirelessly over short distances. These sensors are usually low-cost, low-power and multifunctional [48]. Two main different architectures are used in sensor networks: flat architecture and hierarchical architecture. In flat architecture, each node is responsible for sensing, routing and transmitting its own data

to the base station. In a hierarchical architecture, each node belongs to a cluster. Each cluster consists of a cluster head and multiple sensor nodes. Each sensor transmits data only to the cluster head, and the cluster head gathers all the information in a cluster and transmits to the base station [49].

2.5.1 Relays in WSN

The use of relays in WSNs has drawn a lot of attention. Relay nodes fight multipath fading by adding cooperative diversity to the system. In addition, relay node can shorten the distance between a sensor node and the destination. Therefore, by an optimal power allocation scheme, the power consumption of sensor node decreases, which results in extended lifetime of the network. Moreover, relay node can balance data gathering by lessening loads from overloaded nodes. Adding relays to the network provides some extra routes. By finding an optimal route we can redirect burden from some overloaded nodes to more powerful relays.

By providing each sensor node with more than one disjoint connection, deploying relays makes network fault tolerant. If one connection is lost, an alternative connection saves sensor from dying [50]. In two-tiered cluster-based networks, high-power relays are placed in upper tier and sensors are placed in lower tier. Sensors in the lower tier communicate only with relays in the upper tier. The objective of the optimization problem is to find the minimum number of relays so that each sensor is connected to at least two relays. An alternative objective in order to maximize scalability is to find the minimum number of relays so that each sensor is connected to at least one relay [49].

In some sensor networks, usually with flat architecture, relay nodes are nodes similar to sensor nodes. The role of each node can be pre-defined as a sensor/relay or it can be changed by a role-assignment algorithm according to current network status, in order to achieve higher performance. In other networks, usually with hierarchical architecture, relays can be special nodes with higher capacity. Unlike sensor nodes that only gather information from surrounding information and transmit to the relays which usually are located closely, relay nodes repeatedly receive and transmit data from multiple sensors to another relay node or base station located in farther distances. Therefore, using a more powerful node for relays helps improve network performance [49].

2.6 Buffer-aided Relays

In a conventional cooperative network, it is assumed that relays can store only one packet for the duration of one time slot. Therefore, the source-relay (SR) and the relay-destination (RD) transmissions occur in two consecutive time slots, independent of the channel characteristics. In a system where channels vary with time, this scheduled transmission inhibits the system from using the best possible SR or RD links. This restriction can be removed by equipping relays with buffers. Buffer-aided relay can benefit a reliable SR link by receiving multiple packets and storing them in its buffer. Similarly, when RD link is reliable, relay can transmit multiple packets that are previously stored in its buffer.

Buffer-aided relays introduce significant improvements to the system performance in terms of throughput and stability, and balances the traffic load passing through each relay [4]. However, these improvements are achieved at the expense of an increase in total transmission delay, that should be handled in the applications that are delay-sensitive. Moreover, the relaying protocols for buffer-aided relaying are more complicated than conventional relaying, since the status of the buffers should be considered.

2.6.1 Single Relay Network

In order to get a better perspective of buffer-aided relays, initially we consider a single relay network where the relay node is equipped with buffer. In this network, a single source node is communicating with a single destination through a DF relay. We assume that direct communication is not possible. Channels are modeled as quasi-static fading, where fading gains are constant during one time slot, but change from one time slot to another.

In contrast with the conventional relaying transmission protocol where the source and the relay nodes transmit in consecutive time slots, in the buffer-aided relaying network, at each time slot a node with better link quality is selected for transmission. If the SR link has better quality than the RD link, the source node transmits, otherwise the relay node transmits. Fig. 2.5 depicts these transmission modes. This protocol is known as *buffer-aided relaying with adaptive link selection* and was introduced in [51–53]. Based on the nodes knowledge of CSI, the adaptive or fixed rate

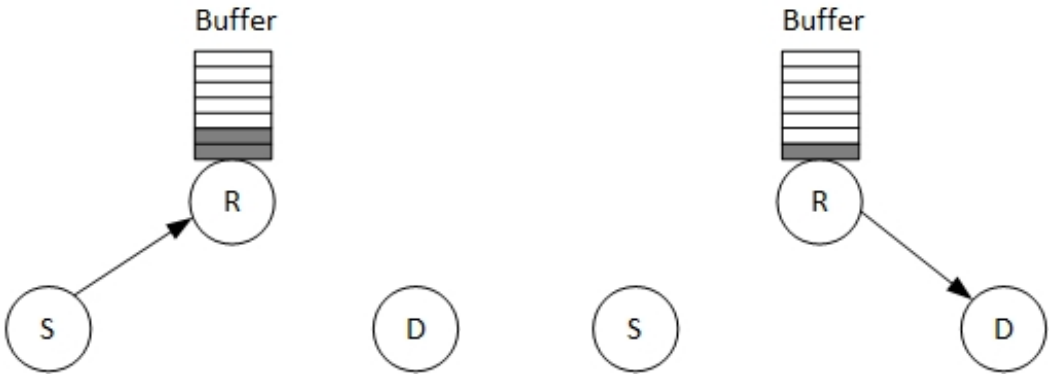

(a) A buffer-aided relaying when the relay receives a packet

(b) A buffer-aided relaying when the relay transmits a packet

Figure 2.5: A buffer-aided single relay network

transmissions are proposed.

Adaptive Rate Transmission

This protocol requires all the nodes to be aware of the CSI of their transmitting and receiving channels. In this scheme, based on the CSI of the SR and RD links, the decision is made whether the source or the relay node transmits. The source and the relay nodes while selected for transmission, transmit with data rate equal to the capacities of SR or RD channels, respectively. In [51], it is assumed that the buffer size is infinite, and the buffer is never empty nor full. Denoting the capacity of SR and RD links by C_{SR} and C_{RD}, respectively, and a constant $\rho > 0$, the transmission protocol is as follows:

- The source node is selected for transmission if $C_{SR} > \rho C_{RD}$
- The relay node is selected for transmission if $C_{SR} < \rho C_{RD}$

where ρ is a decision threshold that should be optimized. It has been shown that this scheme has diversity order of two, which provides considerable gain in comparison to conventional relaying. In a more practical scenario, it is assumed that buffer size is limited. Therefore, the transmission protocol is modified as follows:

- If the buffer is empty, the source node is selected for transmission

- If the buffer is full, the relay node is selected for transmission
- Otherwise, the selection policy is similar to finite buffer size scenario

In this protocol, the transmission delay is limited by reducing the buffer size.

Fixed Rate Transmission

For fixed rate transmission, the source and the relay do not have CSI knowledge of their transmission link, therefore the transmission rate is fixed. In order to decide which node to transmit, the relay node has the knowledge of the outage state of the SR and RD link. The outage state of the SR and RD links are determined by the relay and the destination nodes, respectively, and sent as a one bit feedback to the source and relay nodes. In [53] , the following transmission protocol is proposed based on the outage states.

- If the SR link is in outage and RD link is not, the relay transmits.
- If the RD link is in outage and SR link is not, the source transmits.
- If both links are not in outage, the relay transmits P_C percent of the times and the source transmits $100 - P_C$ percent of the times.

In this protocol, the transmission delay can be adjusted by the parameter P_C

2.6.2 Multi-relay Network

The performance of the system is improved in a network equipped with multiple relays. As mentioned in section 2.2.1, with a proper relay selection technique, the benefits of multi-relay network are achieved without excessive use of scarce resources. The BRS scheme is adapted to the buffer-aided relay network has first been proposed in [54] wherein the authors propose the max-max relay selection algorithm. In the max-max scheme, a relay with the best available SR channel is selected for reception, and the one with the best RD channel is selected for transmission.

The max-max algorithm is constrained by scheduled transmission, where the source and the relay transmit in consecutive time slots. This constraint is removed in [55], with the aim of providing

additional degrees of freedom (DoF) in relay selection. In [55], the authors propose the max-link algorithm where the best link is selected among the available SR and RD channels. Also, it is shown that a diversity gain twice the number of relays, is achieved. In [56], the authors consider a more realistic model where the source and the destination nodes can communicate directly. Furthermore, the modified max-link algorithm is proposed, where the relay selection scheme is similar to [55] with the RD transmission being conditioned to unsuccessful SD transmission.

Different from [54–56] where nodes transmit with fixed rate, in [57] the source and the relay nodes transmit with data rate equal to the capacities of SR and RD links. The best relay is the one that maximizes SR or RD channel capacity, similar to the selection criterion proposed in [51]. In [58], the authors propose a max-ratio policy, to optimize the secrecy transmission. In this scheme, the best relay is the one that maximizes the SR or RD signal to eavesdropper channel gain ratio.

In [59], the authors propose the balancing relay selection algorithm to balance the arrival and departure rates at each buffer. By keeping the buffers in non-full and non-empty states, more links are available for selection, therefore, the outage probability is reduced. Based on this idea, the relay selection algorithm selects a link with highest channel gain, while keeping buffers in non-full and non-empty state. In [60] and [61], the authors propose a priority-based max-link selection algorithm. In this algorithm, links are prioritized into three classes: 1) R-D links with full buffers, 2) S-R links with empty buffers, and 3) SR and RD links with non-full or non-empty buffers. The link with highest channel gain is selected among the links in each class. It has been shown that prioritizing reduces the outage probability in comparison with the max-link algorithm. In another work in [62], the authors introduce the max-weight algorithm, where each link is assigned a weight according to the relevant buffer status. The weight of each S-R (R-D) link is equal to the number of empty (occupied) buffer spaces. Then, the algorithm selects a link with the largest weight. It has been shown that the max-weight algorithm can achieve more diversity than max-link when buffer size is small. In [63], an improved max-weight algorithm is proposed as an extension to the max-weight algorithm. In this algorithm, if weight of more than one links are equal to the maximum weight, the link with highest channel gain is selected. Moreover, to reduce the delay, R-D links are prioritized to S-R links when having equal weights. In another work in [64], the authors propose an algorithm based on the max-weight algorithm. However, the proposed algorithm allows

simultaneous transmission of multiple S-R or R-D links.

Buffer-aided relay selection is also adapted to cognitive networks to select the best relay for the secondary network [65, 66]. In [65], one relay is selected for the secondary reception or transmission based on the max-link policy. However, the selection is constrained by a maximum tolerable interference level at the primary receiver. In [66], the authors propose a max-ratio scheme that selects the relay with highest SR or RD channel signal-to-interference ratio (SIR), while keeping the interference to the primary nodes below a certain threshold.

2.7 Channel Coding

In design of a communication system, the reliable transmission of the information from one point to another at an acceptable rate is a major task. Channel coding is a useful tool to fulfill this task. The idea behind channel coding is increasing the distance between constellation points, by mapping the constellation points of the input sequence to a higher dimensional signaling space [2]. This added redundancy provides error detection and correction capabilities. However, the addition of this redundancy increases the required bandwidth for transmission and the complexity of the encoder/decoder design. Therefore, the trade-off in designing a channel coding is to attain low error rate while considering the bandwidth and system complexity. There are two main classes of codes: *block codes* and *convolutional codes*. In the remaining of this section the principals of the convolutional code and Turbo code are briefly presented.

2.7.1 Convolutional Code

A convolutional code is generated by passing the information bits through a linear finite-state shift register [2]. Fig. 2.6 shows the diagram of a convolutional encoder, consists of K stages of k bits shift registers and n addition operators. A k-bit information sequence enters and shifted into each stage of the shift register. For each k-bit input, a code word of length n is generated. Therefore, the code rate is equal to $R_c = \frac{k}{n}$. The parameter K is defined as *constraint length* of the convolutional code.

A convolutional code is described by its generator matrix. This generator matrix consists of

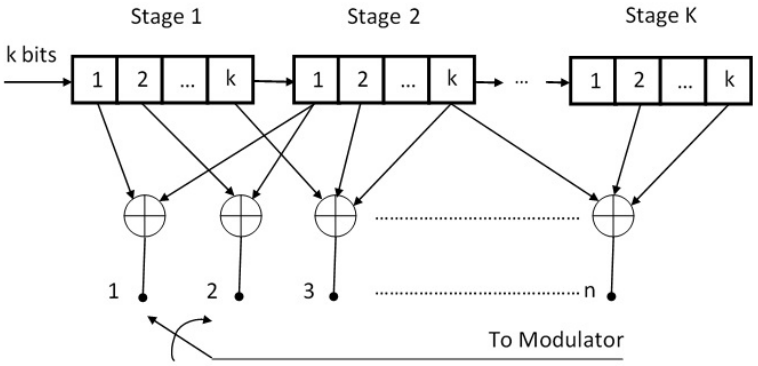

Figure 2.6: Convolutional encoder

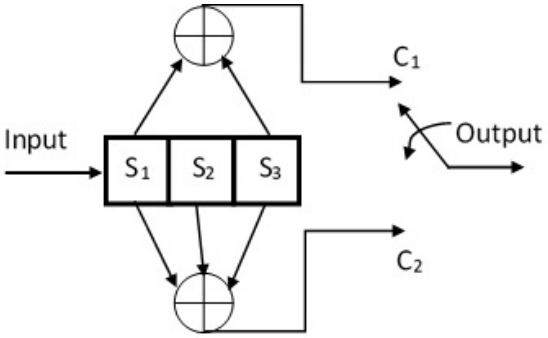

Figure 2.7: Convolutional encoder (5,7)

n vectors, representing the generator polynomial for each addition operator. The entries of these vectors represent the connection of the corresponding addition operator to each stage. For instance, consider the convolutional encoder depicted in Fig. 2.7, with $k = 1$, $K = 3$, and $n = 2$. The generator polynomials for this convolutional encoder are $g_1 = [1, 0, 1]$ and $g_2 = [1, 1, 1]$. It is more convenient to present the generator polynomials in octal form as $(5, 7)$.

Traditionally, there are three graphical methods to describe the properties of a convolutional code: the tree diagram, the trellis diagram and the state diagram. Fig. 2.8, shows the trellis diagram for convolutional code $(5, 7)$, assuming that the encoder is in all-zero state initially. The solid lines indicate the input bit $S_1 = 0$, and the dashed line indicate the input bit $S_1 = 1$. The term S_2S_3 denotes the current state of the shift register, and the output bits C_1C_2 are written next to the transition lines. The stages are denoted by t_i. Starting at the all-zero state $S_2S_3 = 00$ at stage t_0, if the input is 0, after the transitioning to the stage t_1, the new state will remain $S_2S_3 = 00$, and the output bits will be $C_1C_2 = 00$. Conversely, if the input is 1, after the transitioning to the stage t_1,

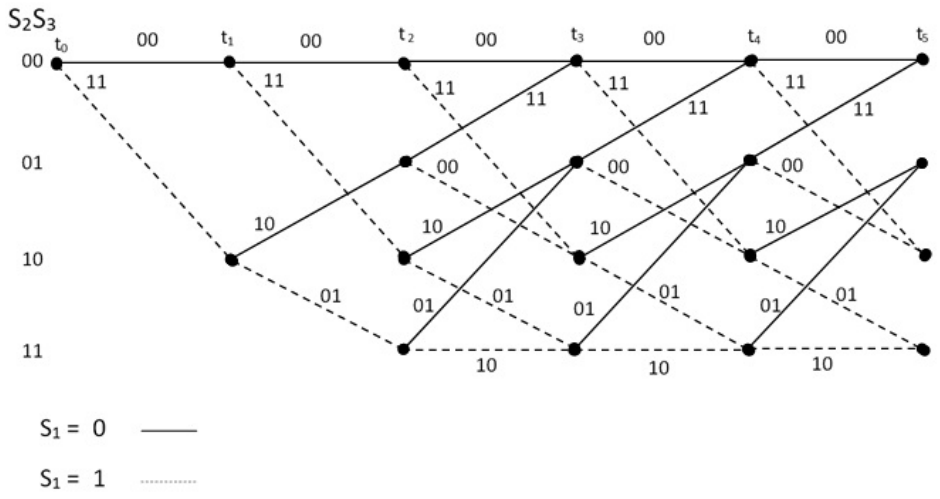

Figure 2.8: Trellis diagram for convolutional code (5,7)

the new state will become $S_2S_3 = 10$, and the output bits will be $C_1C_2 = 11$. Fig. 2.8 shows that the trellis repeats itself after stage t_3, which is expected when the constraint length is $K = 3$.

Viterbi Algorithm

The Viterbi algorithm is a maximum-likelihood decoder for decoding a convolutional code, by selecting a path in the code trellis which has minimum difference with the received sequence. This algorithm calculates a *metric* for every path in the trellis. For hard decision decoding, this metric corresponds to the Hamming distance between the coded bit sequence of each path and the received sequence. At each state, the algorithm compares the metrics of all paths entering that node (state). The path with the lowest metric is retained and all the other paths are removed. The path that is not removed is called the *survivor* path. At each state, 2^{K-1} survivor paths are kept, one for each state. These calculations are repeated for all the stages. When the trellis reaches the termination point, the path with the smallest value is selected. Then, the related sequence of symbols to this path constitutes the decoded bits.

Error Probability of Convolutional Codes

A state diagram is one of the methods to describe the properties of a convolutional code, including the distance properties. Fig. 2.9, depicts the state diagram of the convolutional code (5,7).

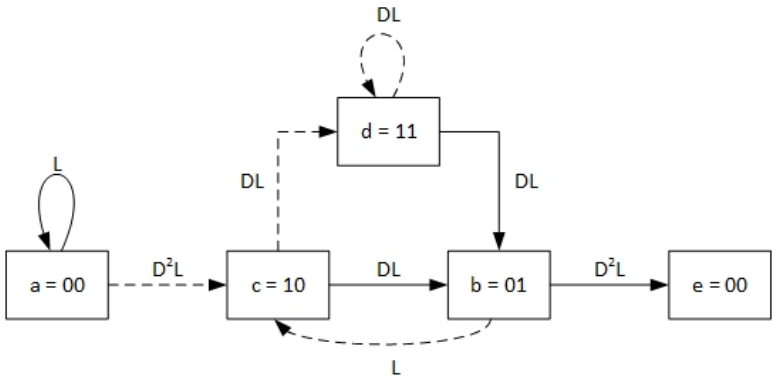

Figure 2.9: State diagram for convolutional code (5,7)

This diagram includes all the possible transitions from the all-zero state to the all-zero state. It is assumed that the input to the convolutional encoder is an all-zero sequence. Due to the linearity of the convolutional code, this assumption is made with no loss of generality. Each branch is labeled by branch gain $D^d L^l$, where the exponent of D denotes the Hamming distance of the corresponding branch's output with respect to the all-zero sequence, and the exponent of L denotes the length of the branch. Here, the exponent of L is always equal to 1, since the branch lengths are 1. The state equations for the state diagram in Fig. 2.9 are written as follows:

$$\begin{aligned} X_b &= DLX_c + DLX_d, \\ X_c &= D^2LX_a + LX_b, \\ X_d &= DLX_c + DLX_d, \\ X_e &= D^2LX_d, \end{aligned} \tag{2.10}$$

where $X_a, ..., X_e$ denote the node signals. The transfer function for this diagram is defined as $T(D, L) = X_e/X_a$. After solving the state equations given in (2.10), the transfer function is obtained as

$$\frac{X_e}{X_a} = \frac{D^5L^3}{1 - DL(1 + L)}. \tag{2.11}$$

Using the binomial expansion and setting $L = 1$, the transfer function becomes

$$T(D,1) \quad = \quad D^5 + 2D^6 + 4D^7 + ... \tag{2.12}$$

This transfer function can be written in the form of

$$T(D) = \sum_{d=d_{min}}^{\infty} a_d D^d, \tag{2.13}$$

where a_d denotes the number of paths with Hamming distance d from the all-zero path, and d_{min} denotes the minimum Hamming distance. By the aid of the transfer function and the distance properties of a convolutional code, the probability of error of a convolutional code can be calculated. An error-event is defined as the event that an erroneous path is selected at the decoder. The probability of the error event is upper-bounded by [67]

$$P_e \leq \sum_{d=d_{min}}^{\infty} a_d P_2(d), \tag{2.14}$$

where, $P_2(d)$ is called the *pairwise error probability*, and defined as the probability of the occurrence of the path with Hamming distance d. This probability depends on the channel model, modulation scheme, and whether the soft-decision or hard-decision decoding is employed. For instance, for an Additive White Gaussian Noise (AWGN) channel, Binary Phase-Shift Keying (BPSK) modulation, and soft-decision decoding, the pairwise error probability is given as

$$P_2(d) = Q(\sqrt{2\bar{\gamma} R_c d}), \tag{2.15}$$

where $Q(.)$ is the Gaussian $Q-$function, and $\bar{\gamma}$ is the average bit SNR. The upper bound given in (2.14) gives the probability of an error event, while it is more common to use the probability of bit-error. The probability of the bit-error for a convolutional code is given by

$$P_b = \sum_{d=d_{min}}^{\infty} a_d f(d) P_2(d), \tag{2.16}$$

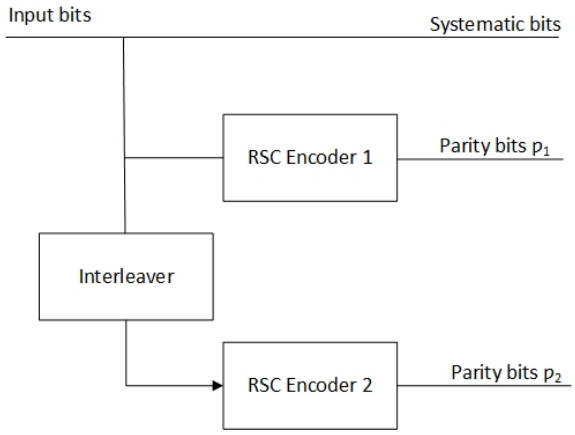

Figure 2.10: Block diagram of a Turbo Encoder

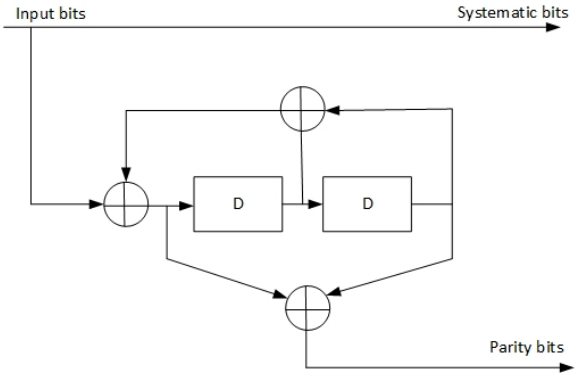

Figure 2.11: An RSC encoder with generator polynomial $(1, \frac{5}{7})$

where $f(d)$ denotes the number of bit errors in each erroneous path.

2.7.2 Turbo Code

Turbo codes are parallel concatenated convolutional codes that can achieve near-capacity performance with feasible complexity and code word length [67]. The turbo encoder shown in Fig. 2.10, consists of two constituent systematic encoders separated by an interleaver. Commonly, the recursive systematic convolutional (RSC) encoders are used as constituent encoders. An example of an RSC encoder with constraint length 3 is shown in Fig. 2.11. The RSCs are described with a ratio of polynomials $(\frac{g_1}{g_2})$, where g_1 and g_2 represent the parity and the feedback polynomials. The encoder in Fig. 2.11 has generator polynomial $(1, \frac{5}{7})$.

The interleaver is an essential component of the Turbo code. This block generates the output

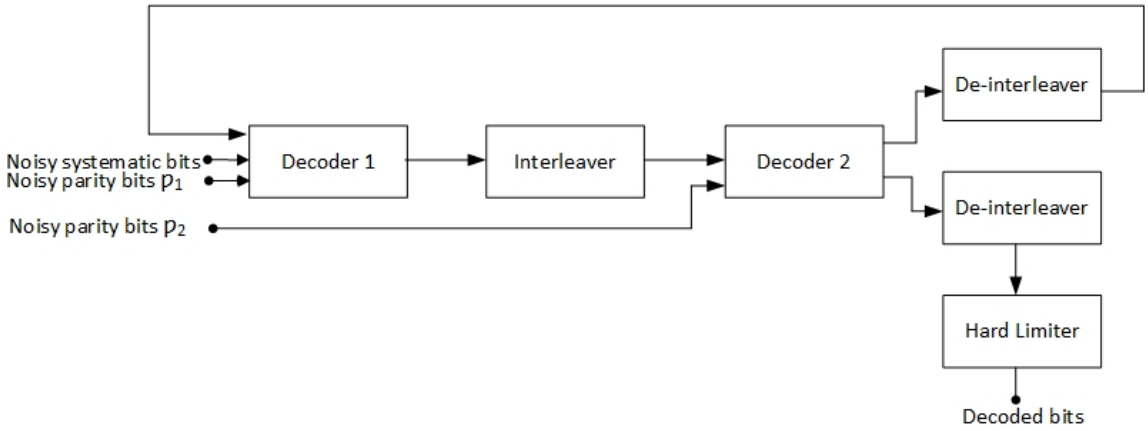

Figure 2.12: Block diagram of a Turbo Decoder

sequence by permuting the input sequence. Therefore, the output consists of the same symbols as the input, but in a different order. There are many different types of interleavers. For a Turbo code with small block length, it is advantageous to design the interleaver. Conversely, for large block lengths, pseudo-random interleavers are shown to perform best [68].

Unlike convolutional code, Turbo code is a block code. In order to determine the beginning and the ending of a block, the Turbo encoder is always initialized in all-zero state. Moreover, after encoding a block of data, a number of tail bits enter the encoder to make it return to the all-zero state.

Fig. 2.12 shows the block diagram for the Turbo decoder. The Turbo decoding algorithm iterates between two decoding stages. Each stage consists of a soft-decision decoder for the RSC encoders used in the Turbo encoder. The information sharing between the two stages are through an interleaver. The most commonly used decoding algorithms for a Turbo decoder are *soft output Viterbi algorithm (SOVA)*, or the *Bahl, Cocke, Jelinek, and Raviv (BCJR)* algorithm. The BCJR algorithm is a soft-input soft-output maximum *a posteriori* probability (MAP) detection algorithm. Unlike the Viterbi algorithm that maximizes the likelihood of the whole sequence, the BCJR algorithm maximizes the *a posteriori* probabilities of each individual bits [67]. Therefore, the BCJR algorithm shows slightly better performance than Viterbi algorithm. Since the BCJR is a soft-output algorithm, after completing a certain number of iterations, the output of the decoder is passed through a hard limiter to achieve the decoded bits.

Error Probability of Turbo Codes

The upper bound of the Turbo code is commonly driven by the Union bound method, given the weight distribution function $\lambda(d)$. Obtaining $\lambda(d)$ of the Turbo code for a particular interleaver is complicated. In [69], the authors obtain the average weight distribution $\bar{\lambda}(d)$, by averaging over all possible interleavers. As Fig. 2.10 shows, a turbo code consists of three fragments: the systematic (input) bits $\mathfrak{s}$, first parity bits sequence $\mathfrak{p}_1$, and second parity bit sequence $\mathfrak{p}_2$. If the interleaver $\mathcal{I}$ is known, the union upper bound for a block code with rate k/n is given as

$$P_w(\mathcal{I}) \leq \sum_{d=d_{min}} \lambda(d|\mathcal{I}) P_2(d), \tag{2.17}$$

where $\lambda(d|\mathcal{I})$ is the number of codewords with Hamming distance d, given a specific interleaver $\mathcal{I}$. The average $\bar{P}_w$ is obtained by averaging $P_w(\mathcal{I})$ over all the interleavers, as

$$\bar{P}_w \leq \sum_{d=d_{min}} \bar{\lambda}(d) P_2(d), \tag{2.18}$$

where $\bar{\lambda}(d)$ is the average weight distribution function. The $\bar{\lambda}(d)$ is obtained by averaging over all the interleavers. For a specific interleaver $\mathcal{I}$, the conditional weight distribution is given as

$$\lambda(d|\mathcal{I}) = \sum_{i} \binom{k}{i} p(d|i, \mathcal{I}), \tag{2.19}$$

where $p(d|i, \mathcal{I})$ is the probability of generating a codeword with weight d, from an input sequence with weight i, given the interleaver $\mathcal{I}$. As the Turbo code consists of three fragments, the weight of the output sequence can be written as $d = i + d_1 + d_1$, where d_1 is the weight of the parity set $\mathfrak{p}_1$, and d_2 is the weight of the parity set $\mathfrak{p}_2$. Therefore, $\lambda(d|\mathcal{I})$ is written as

$$\lambda(d|\mathcal{I}) = \underbrace{\sum_{i} \sum_{d_1} \sum_{d_2}}_{d=i+d_1+d_2} \binom{k}{i} p(i, d_1, d_2|i, \mathcal{I}), \tag{2.20}$$

where $p(i, d_1, d_2|i, \mathcal{I})$ is the probability that an input sequence with weight i is mapped to a codeword with fragment weights d_1 and d_2. If the interleavers are selected randomly and uniformly from

all the possible permutations of k elements, the $p(i, d_1, d_2|i, \mathcal{I})$ is given as

$$p(i, d_1, d_2|i, \mathcal{I}) = p(i|i, \mathcal{I})p(d_1|i, \mathcal{I})p(d_2|i, \mathcal{I}). \tag{2.21}$$

By averaging over all the interleavers, the $\bar{\lambda(d)}$ is obtained as

$$\begin{aligned} \bar{\lambda}(d) &= E[\lambda(d|\mathcal{I})] \\ &= \sum_{i} \sum_{d_1} \sum_{d_2} \binom{k}{i} p(d_1|i)p(d_2|i). \end{aligned} \tag{2.22}$$

By substituting (2.22) into (2.18), the average upper bound is obtained as

$$\bar{P}_w \leq \sum_{d=d_{min}} \sum_{i} \sum_{d_1} \sum_{d_2} \binom{k}{i} p(d_1|i)p(d_2|i)P_2(d). \tag{2.23}$$

The $p(d_{1/2}|i)$ denotes the probability of generating a codeword fragment of weight $d_{1/2}$, given an input sequence of weight i, and it is given by

$$p(d_{1/2}|i) = \frac{t(k, i, d_{1/2})}{\sum_{d_{1/2}} t(k, i, d_{1/2})} \approx \frac{t(k, i, d_{1/2})}{\binom{k}{i}}, \tag{2.24}$$

where $t(k, i, d)$ denotes the number of paths of length k, input weight i, and output weight d, when the trellis starts and ends in all-zero state. In [69], the authors show that for any block length $k = l$, the $t(l, i, d)$ can be derived from the transfer function of the convolutional encoder $T(L, I, D)$, defined as

$$T(L, I, D) = \sum_{l \geq 0} \sum_{i \geq 0} \sum_{d \geq 0} L^l I^i D^d t(l, i, d). \tag{2.25}$$

By solving (2.25) recursively, $t(l, i, d)$ is obtained. For instance, the transfer function for a convolutional code $(1, 5/7)$ is given by

$$T_{5/7}(L, I, D) = \frac{1 - LI - L^2I - L^3(D^2 - I^2)}{1 - L(i + I) - L^3(D^2 - I - I^2 + I^3D^2) + L^4(D^2 - I^2 - I^2D^4 + I^4D^2)} \tag{2.26}$$

With some manipulations, (2.26) can be written in form of (2.25), then $t(l,i,d)$ is calculated recursively, as

$$\begin{aligned} t(l,i,d) &= t(l-1,i-1,d) + t(l-1,i,d) \\ &+ t(l-3,i-3,d-2) - t(l-3,i-2,d) - t(l-3,i-1,d) + t(l-3,i,d-2) \\ &- t(l-4,i-4,d-2) + t(l-4,i-2,d-4) + t(l-4,i-2,d) - t(l-4,i,d-2) \\ &+ \delta(l,i,d) - \delta(l-1,i-1,d) - \delta(l-2,i-1,d) - \delta(l-3,i,d-2) + \delta(l-3,i-2,d) \end{aligned} \tag{2.27}$$

where $\delta(l,i,d) = 1$ if $l = i = d = 0$ and $\delta(l,i,d) = 0$ otherwise, and $t(l,i,d) = 0$ if any index is negative.

2.7.3 Distributed Turbo Code

Distributed coding techniques are introduced in [70–72] to improve the performance of the cooperative networks. The distributed Turbo code introduced in [73, 74] represents an important member of distributed codes. In [73, 74], the authors propose a DTC scheme for a single-relay network with one source and one destination nodes. The source node broadcasts a convolutionally coded block to the destination and relay nodes. The relay decodes the received signal, interleaves the information bits, and re-encodes with a convolutional encoder and forwards the coded bits to the destination node. At the destination node, the received codeword from the source and the relay constitute a Turbo code word. The destination uses a Turbo decoder to decode the received signal. Different DTC scheme are proposed in the literature [73–77]. In [73, 74], the author assumed that error-free decoding is performed at the relay. In [75], the relay calculates the *a posteriori* probabilities of the information bits. Then the soft estimate of the parity bits are generated and forwarded to the destination node. In [76], the relay calculates the log-likelihood ratio (LLR) of the information bits. Then, by applying a threshold on LLRs, the relay only forward the reliable bits and discard the others. In [77], the authors consider a network with multiple relays. The relays who can successfully decode the received signal, interleave and re-encode the decoded bits and forward to the destination. The rest of the relays amplify and forward the received signal. The destination

node combines all the received signals to form a DTC codeword.

2.8 Markov Chains

Markov chain is a process for which the future results are affected by all the preceding results. A Markov chain is defined as a sequence of states: $\{X_0, X_1, ...\}$. Each state X_i is a random variable that can take any value in state space $S = \{1, 2, ..., N\}$ [78]. The process begins from one state and moves to the next state. A transition from current state X_i to the next state X_j is called a *step*. The probability of this step is called the *transition probability*, which is denoted by $T_{ij} = \mathbb{P}(X_{n+1} = j|X_n = i)$. The process can remain in the same state with the probability of T_{ii}.

The transition probabilities do not depend on the past states that Markov chain was in, before the current state. That means

$$T_{ij} = \mathbb{P}(X_{n+1} = j|X_n = i, X_{n-1} = i-1, ..., X_0 = i_0) = \mathbb{P}(X_{n+1} = j|X_n = i). \tag{2.28}$$

This property is called the *Markov Property* [78]. A *transition matrix* is defined as a $N \times N$ square matrix $\mathbf{T}$ for which the entities are transition probabilities T_{ij}.

At each time n, the probability distribution of the chain is denoted by a vector $\boldsymbol{\pi}^{(n)}$, for which the entities are defined as $\boldsymbol{\pi}_i^{(n)} = \mathbb{P}(X_n = i)$. To predict the behavior of the process at any time, we need to obtain this probability distribution vector $\boldsymbol{\pi}^{(n)}$.

At time 0, the probability distribution of the process is defined by the *Initial distribution* vector denoted by $\boldsymbol{\pi}^{(0)}$. This initial distribution $\boldsymbol{\pi}^{(0)}$ is a vector whose i^{th} entry is $\pi_i^{(0)} = \mathbb{P}(X_0 = i)$, where

$$0 \leq \pi_i^{(0)} \leq 1 \quad \forall i \in S, \tag{2.29}$$

$$\sum_{i \in S} \pi_i^{(0)} = 1. \tag{2.30}$$

For a Markov chain, the probability distribution at time n is given by [78]

$$\boldsymbol{\pi}^{(n)} = \boldsymbol{\pi}^{(0)} \boldsymbol{T}^n. \tag{2.31}$$

Equation (2.31) indicates that any probabilistic behavior of the Markov chain can be obtained by performing matrix operations.

Suppose a Markov chain with distribution $\boldsymbol{\pi}$ such that, if the initial distribution is $\boldsymbol{\pi}^{(0)} = \boldsymbol{\pi}$ then the distribution at time 1 is also $\boldsymbol{\pi}^{(1)} = \boldsymbol{\pi}$. Then $\boldsymbol{\pi}$ is called the *stationary distribution* defined as [78]

$$\boldsymbol{\pi} = \boldsymbol{\pi}\boldsymbol{T}, \tag{2.32}$$

$$\sum_{i \in S} \pi_i = 1. \tag{2.33}$$

The existence of the stationary distribution is proven for special types of Markov chain, in *Fundamental Limit Theorem*. The definition of the special types of Markov chains are as follows:

- *Ergodic* or *irreducible* Markov chain: A Markov chain is irreducible if it is possible to go to every state from every state [78].
- *Aperiodic* Markov chain: For each state i, we define the period d_i as the greatest common divisor (GCD)

$$d_i = GCD\{n : T_{ii}^n > 0\}. \tag{2.34}$$

  where T_{ii}^n denotes the entity (i, i) of $\boldsymbol{T}^n$. An irreducible Markov chain is called *aperiodic* if its period is 1 [78].

Fundamental Limit Theorem: For an irreducible and aperiodic Markov chain with transition matrix $\boldsymbol{T}$, the stationary distribution $\boldsymbol{\pi}$ exists and it is a unique vector [78]. Then we have

$$\lim_{n \to \infty} \boldsymbol{T}^n = \boldsymbol{\Pi}, \tag{2.35}$$

where $\boldsymbol{\Pi}$ is a matrix with each row equal to $\boldsymbol{\pi}$.

In order to find the stationary distribution vector, linear equations (2.32) and (2.33) should be

solved. Expression (2.33) can be written as

$$\boldsymbol{B}\boldsymbol{\pi} = \boldsymbol{b}, \tag{2.36}$$

$$B_{ij} = 1, \forall i, j, \tag{2.37}$$

$$\boldsymbol{b} = [1, 1, 1, ..., 1]^{\mathsf{T}}, \tag{2.38}$$

where T is the transpose operator. By adding (2.32) to (2.36) we have

$$\boldsymbol{T}\boldsymbol{\pi} - \boldsymbol{\pi} + \boldsymbol{B}\boldsymbol{\pi} = \boldsymbol{b}, \tag{2.39}$$

then

$$\boldsymbol{\pi} = (\boldsymbol{T} - \boldsymbol{I} + \boldsymbol{B})^{-1}\boldsymbol{b}. \tag{2.40}$$

2.9 Conclusion

In this Chapter, we presented a general background on cooperative network and its elements. Different relaying protocols used in the literature are discussed. We also presented a literature review on different methods of relay selection and resource allocation. Then, we presented the basics of the assignment problems and related algorithms. These algorithms are later used in Chapter 3. Further, we briefly presented the OFDM transmission technique. Moreover, a brief review on WSN and its elements are also included. We have used the WSN model in Chapter 4. We presented the basics of buffer-aided relaying and the related works on this topic. The principles of channel coding techniques including convolutional code, Turbo code and DTC are covered. At last, we provided a summary on Markov chains. The Markov chain model is used in the analysis presented in Chapter 5.

Chapter 3

Joint Power Allocation and Subcarrier-Relay Assignment for OFDM-based Decode-and-Forward Relay Networks

OFDM is a well-known technique to combat frequency selective fading. By combining relaying with OFDM, we can have the advantages of both techniques. However, in order to achieve the improvements to the fullest extent the resource allocation should be optimized. Power allocation plays a key role in performance improvement by optimally distributing power among subcarriers. However, the problem of resource allocation is not solely defined by power allocation. In a network with multiple relays, the problem of subcarrier-relay assignment arises.

Various methods are proposed to solve the resource allocation problem. Graph-based methods are widely used [79,80], where the addressed problem is formulated as a problem of finding a perfect matching in a bipartite weighted graph. Another vastly used method is Lagrange dual decomposition that finds an asymptotically optimal solution [81, 82]. Although it is proven that the duality gap is negligible for large number of subcarriers, the high amount of calculations and time complexity makes this method not applicable. To deal with this problem, suboptimal algorithms are proposed.

In [82, 83], the joint optimization problem is decomposed into multiple simpler subproblems which are solved separately. In [79, 80], power allocation is not pursued to simplify the problem. These suboptimal algorithms reduce the complexity at the expense of performance degradation.

The criterion mostly used for resource allocation is maximizing the total capacity of the system known as max-sum criterion [79, 80, 82]. In a cooperative network, relays can represent other users that shared their antennas in order to create a virtual MIMO antenna array. These users require fair share of resources. The weak point of the max-sum criterion is that cell edge users with poor link qualities achieve less resources. To achieve the fairness more resources should be allocated to the users with poorest channels. This objective can be achieved by a criterion known as max-min which is addressed in few previous works [83–85]. This drew us to address the problem of resource allocation with max-min fairness objective.

In [86], the author proposed an optimal solution for joint power allocation and relay-assignment problem subject to the sum-power constraint. This work is based on the assumption that the relay-destination channel is perfect which is not a valid assumption when the channel quality is poor. Also, this algorithm is designed for AF relays.

Motivated by aforementioned shortcomings, in this chapter we investigate the joint optimization problem of subcarrier-relay assignment and power allocation to maximize the SNR of the poorest channel in an OFDM-based DF relay network. An optimal algorithm with polynomial time complexity is proposed to solve this problem. The optimality of the proposed algorithm is proved.

The rest of the chapter is organized as follows. In section 3.1 the system model is presented and the problem is formulated. In section 3.2 the proposed algorithm is presented and explained in details. In section 3.4 the simulation results are presented and discussed. Finally section 3.5 concludes the chapter.

3.1 System Model and Problem Formulation

The system model is depicted in figure 3.1. We consider an OFDM-based network with one source and one destination nodes and L half-duplex DF relay nodes denoted by S, D, and $R_i (i \in \{1, ..., L\})$, respectively. The communication takes place in two phases. In phase one, the source

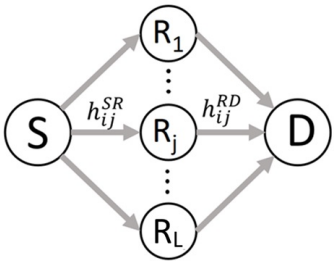

Figure 3.1: System model

node transmits data over all M subcarriers to relays. Each relay decodes a selected set of subcarriers. In phase two, each relay re-encodes and forwards the received data using another set of selected subcarriers to the destination node.

It is assumed that there is no direct communication link between source and destination nodes because of the poor link quality. All channels are considered to be Rayleigh fading with path loss. A centralized resource allocator with the knowledge of all the instantaneous CSI performs two tasks: 1) assigns subcarriers to relays and 2) distribute the power among subcarriers. The objective of the resource allocator is to reach max-min fairness between subcarriers, that means maximizing the SNR of the poorest (or bottleneck) subchannel at the destination node. We define two binary variables u_{ij} and v_{ij}. If subcarrier j is assigned to relay i in phase 1, $u_{ij} = 1$ otherwise $u_{ij} = 0$. Similarly, if subcarrier j' is assigned to relay i in phase 2 $v_{ij} = 1$ otherwise $v_{ij} = 0$. In order to avoid interference, it is assumed that each subcarrier is only assigned to one relay. The number of subcarriers assigned to relay R_i is denoted by b_i. These conditions are formulated by

$$\sum_{i=1}^{L} u_{ij} = 1 \quad \forall j, \quad \sum_{j=1}^{M} u_{ij} = b_i \quad \forall i, \quad u_{ij} \in \{0,1\} \tag{3.1}$$

$$\sum_{i=1}^{L} v_{i'j} = 1 \quad \forall j', \quad \sum_{j'=1}^{M} v_{i'j} = b_i \quad \forall i, \quad v_{i'j} \in \{0,1\} \tag{3.2}$$

Each selection of relays is denoted by a permutation matrix $u_k = [u_{ij}]_{M\times L}$ in phase 1, and $v_k = [v_{i'j}]_{M\times L}$ in phase 2, $k \in \{1, 2, ..., K\}$, K is the total number of permutations in each phase, $K = \frac{M!}{b_1!b_2!...b_L!}$.

Let S_{u_k} denote a set of (i, j) pairs indicating the indices of the elements of the permutation u_k and S_{v_k} denote a set of (i', j) pairs indicating the indices of the elements of the permutation v_k

$$(i,j)|u_{ij}=1, i\in\{1,...,L\}, j\in\{1,...,M\}, s.t.(1)\}, \tag{3.3}$$

$$S_{v_k}=\{(i',j)|v_{i'j}=1, i'\in\{1,...,L\}, j\in\{1,...,M\}, s.t.(2)\}. \tag{3.4}$$

The SNR of the SR_i channel when subcarrier j is assigned to relay i is denoted by γ_{ij}^{SR}, and the SNR of the R_iD channel when subcarrier j' is assigned to relay i is denoted by $\gamma_{i'j}^{RD}$. The power P is available at the source node and distributed among subcarriers using the Water-filling algorithm. All γ_{ij}^{SR} can be improved by using power P_{ij} according to

$$\gamma_{ij}^{SR}(new)=(1+\frac{P_{ij}}{P_0})\gamma_{ij}^{SR}(old) \tag{3.5}$$

$$\sum_{(i,j)\in S_{u_k}} P_{ij}\leq P \tag{3.6}$$

$$P_{ij}\geq 0$$

P_0 is an initial power assigned to each subcarrier to avoid zero power allocation. The power P_r is available at each relay and distributed among subcarriers using the Water-filling algorithm, in phase two. All $\gamma_{i'j}^{RD}$ can be improved by using power $P'_{i'j}$ according to

$$\gamma_{i'j}^{RD}(new)=(1+\frac{P'_{i'j}}{P_0})\gamma_{i'j}^{RD}(old) \tag{3.7}$$

$$\sum_{(i',j)\in S_{v_k}} P'_{i'j}\leq Pr \quad \forall j \tag{3.8}$$

$$P'_{i'j}\geq 0$$

The optimization problem can be formulated as

$$\max_k \min\{\min_{(i,j)\in S_{u_k}} \gamma_{ij}^{SR}(new), \min_{(i',j)\in S_{v_k}} \gamma_{i'j}^{RD}(new)\}. \tag{3.9}$$

This optimization problem is subject to (3.1),(3.2),(3.6),(3.8). Due to independence of γ_{ij}^{SR} and $\gamma_{i'j}^{RD}$, the optimization problem is divided into two sub-problems (3.10) and (3.11) without losing

optimality. In section 3.2 we propose a joint optimization algorithm to solve these subproblems.

$$\max_{k} \min_{(i,j)\in S_{u_k}} \gamma_{ij}^{SR}(new) \quad s.t.(3.1),(3.6) \tag{3.10}$$

$$\max_{k} \min_{(i',j)\in S_{v_k}} \gamma_{i'j}^{RD}(new) \quad s.t.(3.2),(3.8) \tag{3.11}$$

3.2 Proposed Optimization Algorithm

The idea of the proposed algorithm comes from the Threshold algorithm used to solve the max-min assignment problem on a cost matrix C [43] . A threshold algorithm has two stages. In the first stage an element from cost matrix is selected as a threshold c^* and applied to the cost matrix to define the threshold matrix.

$$\bar{c} = \begin{cases} 1 & c_{ij} < c^* \\ 0 & o.w \end{cases} \tag{3.12}$$

In the second stage, the feasibility of an assignment with zero cost is checked for this threshold matrix. The largest value of the threshold is the optimum value.

In the proposed algorithm, the cost matrix is an SNR matrix $\Gamma^{SR} = [\gamma_{ij}^{SR}]$ or $\Gamma^{RD} = [\gamma_{ij}^{RD}]$. Each assignment can be improved by using the available power. An assignment is considered feasible, if the required power to reach a specific threshold is less than the available power.

Using γ_{thr} as a threshold, matrix Γ^{SR} is broken into two matrices Δ and Ψ by thresholding with γ_{thr}. This threshold is selected so the best permutation in Δ can reach the target SNR (γ_{thr}) consuming less power than the available power P. The parameters Δ and Ψ are given by

$$\Delta = \begin{cases} \gamma_{ij} & \gamma_{ij} \leq \gamma_{thr} \\ 0 & o.w \end{cases} \tag{3.13}$$

$$\Psi = \begin{cases} \gamma_{ij} & \gamma_{ij} > \gamma_{thr} \\ 0 & o.w \end{cases} .$$

By this approach, the optimization problem is divided into two parts. First, we apply the joint

power allocation and subcarrier-relay assignment on Δ until all the power is used. Then, we apply the max-min algorithm on Ψ when no extra power is available. The γ_{thr} is calculated by *Search for Threshold* Algorithm. The threshold value can be any element of ML elements in Γ^{SR}. Binary search algorithm is utilized to find the threshold:

1) Let us sort all the values of Γ^{SR}. When a matrix or array is indexed by a single argument (r), we refer to this as the r^{th} smallest element of that array or matrix. γ_{thr} is initialized by the midpoint value $\gamma_r = \Gamma^{SR}_{(r)} = \Gamma^{SR}_{(\lfloor \frac{1+MN}{2} \rfloor)}$.

2) Matrix $\Phi_r = [\phi_{ij}]$ contains the required power for each element of Γ^{SR} to reach γ_r.

$$\Phi_r = \begin{cases} (\frac{\gamma_r}{\gamma^{SR}_{ij}} - 1)P_0 & \gamma^{SR}_{ij} \leq \gamma_r \\ 0 & o.w \end{cases} \tag{3.14}$$

3) The best permutation in Φ_r denoted by u_r, requires minimum power to reach γ_r. Therefore the optimization problem can be written as (3.15). This problem is known as semi-assignment problem and it is solved by the Shortest Augmenting path algorithm proposed in [87]. The complexity order of this algorithm is $O(M^2L)$.

$$\min \sum_{j=1}^{L} \sum_{i=1}^{M} \phi_{ij} u_{ij}, \quad \sum_{i=1}^{L} u_{ij} = 1 \quad \forall j, \quad \sum_{j=1}^{M} u_{ij} = b_i \quad \forall i, \quad u_{ij} \in \{0, 1\}. \tag{3.15}$$

If the required power for this permutation is less than the available power P, we search for a higher threshold in the searching span of $[\Gamma^{SR}_{(r+1)} : \Gamma^{SR}_{(ML)}]$, otherwise, the searching span is $[\Gamma^{SR}_{(1)} : \Gamma^{SR}_{(r-1)}]$.

The *Search for Threshold* algorithm returns the index of the highest reachable threshold with the available power P. However, the power is not totally consumed. It is viable that by consuming the whole power we reach a higher SNR (T) , $\Gamma_{(r)} \leq T < \Gamma_{(r+1)}$. The *Joint Optimization* algorithm performs a fine-tuning process on T to reach the highest achievable SNR. In this algorithm, first we start with a target SNR achieved from the *Search for Threshold* Algorithm T_0 and the min-sum permutation is found. In the next step, the whole power is used to improve this permutation to reach a new higher target SNR (T_1). It is viable that another permutation exists that can reach T_1 with less power. The search continues until the selected permutation does not change in consecutive iterations.

Algorithm 3 Search for Threshold

Input: Γ^{SR}
Output: r
Initialize $r_{min} = 1$ and $r_{max} = ML$
repeat
  $r = \lfloor \frac{r_{min}+r_{max}}{2} \rfloor$
  $\gamma_r = \Gamma^{SR}_{(r)}$
  Calculate Φ_r with the threshold of γ_r
  Find u_r as the $min\text{-}sum$ permutation in Φ_r
  if $\sum_{(i,j)\in S_{u_r}} p_{ij} \leq P$ **then**
    $r_{min} = r$
  else
    $r_{max} = r$
  end if
until $\sum_{(i,j)\in S_{u_r}} p_{ij} \leq P$ and $\sum_{(i,j)\in S_{u_{r+1}}} p_{ij} > P$
return r

Algorithm 4 Joint Optimization

Input: Γ^{SR} , P , γ_r
Output: T, u_k
Initialize $T = \gamma_r$
$k = 1$
repeat
  Calculate Φ with T as threshold
  Find u_k as the $min\text{-}sum$ permutation in Φ
  if $\sum_{(i,j)\in S_{u_k}} p_{ij} \leq P$ **then**
    Calculate $\gamma^{SR}_{ij}(new)$ using Water-filling algorithm
    $T = min_{(i,j)\in S_{u_k}}\{\gamma^{SR}_{ij}(new)\}$
  else
    $u_k = u_{k-1}$
    Convergence = **true**
  end if
  $k = k + 1$
until $u_k = u_{k-1}$

The *Joint Optimization* algorithm ensures that we have achieved the highest possible bottleneck SNR (denoted by T) and the power is consumed completely. To this point, the elements of Γ^{SR} which are greater than T are not considered in the optimization process. Therefore, in the next step the Ψ matrix is calculated, and the optimum assignment is found by performing the max-min algorithm. It should be noted that in this step no power allocation is needed. This procedure is illustrated in *Main Algorithm*. The similar algorithm is used to find the best permutation in phase 2, denoted by T^*_{RD}. The highest achievable SNR at the destination node is calculated using (3.16)

$$T^* = \min\{T^*_{SR}, T^*_{RD}\}. \tag{3.16}$$

The time complexity of the proposed algorithm is analyzed as follows: the complexity of *Search*

Algorithm 5 Main Algorithm

1: **Input**: Γ^{SR}, u_k
2: **Output**: T^*_{SR}
3: Call *Search for Threshold* algorithm and find r
4: Call *Joint Optimization* algorithm and find T and u_k
5:
$$\Psi = \begin{cases} \gamma^{SR}_{ij} & \gamma^{SR}_{ij} > T \\ T & (i,j) \in S_{u_k} \\ 0 & o.w. \end{cases}$$
6: Calculate $u_k = max\text{-}min$ permutation in Ψ
7: $T^*_{SR} = \min_{(i,j)\in S_{u_k}} \gamma^{SR}_{ij}$
8: **return** T^*_{SR}

for Threshold algorithm, *Joint Optimization*, and max-min are $O(M^2L\log(ML))$, $O(M^3L)$, and $O(M^2L\log(ML))$, respectively. It can be seen that the time complexity of each iteration of the main algorithm is dominated by $O(M^3L)$. In comparison with the complexity order of the exhaustive search which is $O(\frac{M!}{(M/L)!^L})$, the proposed algorithm has less complexity for large number of subcarriers.

3.3 Proof of Optimality

In this section, it is proved that *Joint optimization* algorithm reaches the optimal T. Assume that the algorithm stops after $\mathfrak{I}$ iterations reaches the SNR value of T_k, but the optimal SNR is T_{k+1}. The required amount of power for the optimal permutation to reach T_{k+1} is P_{k+1}. Two cases are possible:

1) $P_{k+1} < P$: In this case the algorithm cannot stop at iteration $\mathfrak{I}$, since the condition at line 10 is satisfied. This contradicts the first assumption.

2) $P_{k+1} > P$: In this case T_{k+1} is not feasible, therefore cannot be the optimal solution.

By rejecting the assumption it can be concluded that T_k is the optimal solution.

3.4 Simulation Results

In this section, simulation results are presented to evaluate the performance of the proposed algorithm. The model used in simulation complies with the system model presented in section 3.1. In all the simulations, it is assumed that for all the relays $b_i = \frac{M}{L}$. This assumption is for simplicity, however, b_i can take any integer value.

In Fig. 3.2 the performance of the proposed algorithm is compared with the *Exhaustive search* algorithm, in terms of error probability to validate the optimality of the proposed algorithm. It can be seen that the performance of our algorithm matches the *Exhaustive search*, for different number of relays, subcarriers and various values of SNR.

In Fig. 3.3, the performance of our algorithm is evaluated in terms of the achievable minimum SNR across the subcarriers at the destination node. The performance of the proposed algorithm is compared to the :*Relay assignment + equally distributed power (EDP)* algorithm. The *Relay assignment + equally distributed power (EDP)* algorithm is a two-step algorithm. In the first step, relays are assigned according to max-min criterion. This method is an optimal relay selection for DF relays and it is often used as a baseline relay selection scheme as a means of comparison [13]. In the second step the power is allocated equally between subcarriers. It can be observed that the minimum SNR achieved by the proposed algorithm is considerably higher that the *Relay assignment + equally distributed power (EDP)* algorithm. It can also be seen that by increasing the number of

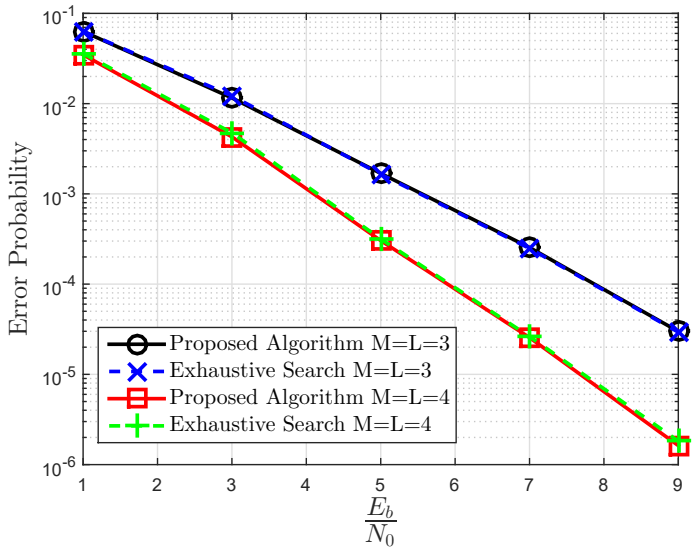

Figure 3.2: Error probability of the proposed algorithm in comparison with Exhaustive search

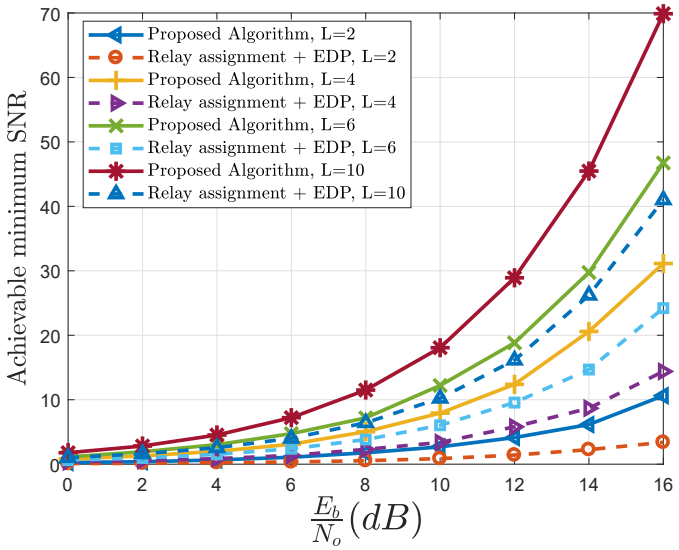

Figure 3.3: Achievable minimum SNR across the subcarriers in a system with $L = \{2, 4, 6, 10\}$ relays, 60 subcarriers, $P_s = 6, P_0 = 1, P_r = 1$

relays, the achievable minimum increases, as expected.

In Fig. 3.4, t he performance of the proposed algorithm is compared to the*Relay assignment + Waterfilling*, in terms of the achievable minimum SNR. The*Relay assignment + Waterfilling* is a two-step algorithm. In the first step relays are assigned according to max-min criterion and in the second step power is distributed by Water-filling algorithm. It can be seen that the proposed

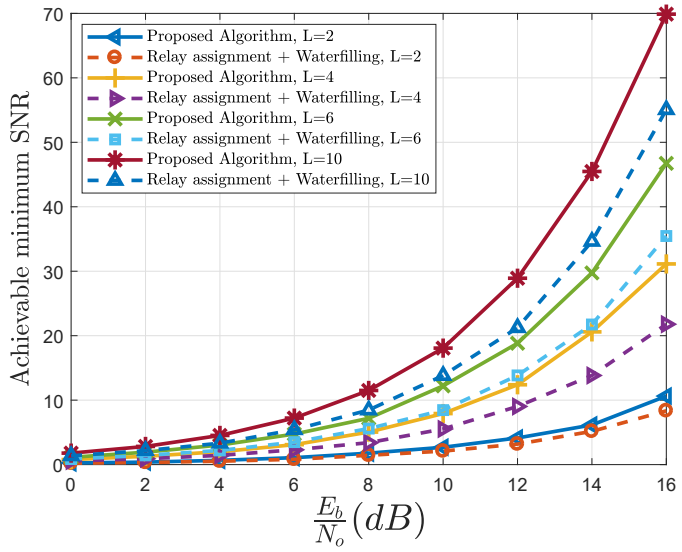

Figure 3.4: Achievable minimum SNR across the subcarriers in a system with $L = \{2, 4, 6, 10\}$ relays, 60 subcarriers, $P_s = 6, P_0 = 1, P_r = 1$

algorithm achieves higher minimum SNR than the *Relay assignment + Waterfilling*, for different number of relays and various values of SNR. The reason for this improvement is that in the proposed algorithm, the subcarrier-relay assignment and power allocation problem are solved jointly, where in the *Relay assignment + Waterfilling*, the optimization problem is solved separately.

In Fig. 3.5 the performance of our algorithm is compared with the *Relay assignment + EDP* and *Relay assignment + Waterfilling* algorithms in terms of the achievable minimum SNR across the subcarriers at the destination node, for different number of relays. It can be seen that the for various number of relays the proposed algorithm achieves higher minimum SNR that the other two algorithms. It can also be seen that for larger number of relays, the improvement in the achievable minimum SNR is more considerable.

In Fig. 3.6 it is shown that the *Joint Optimization* algorithm converges to the optimum value in less than 3 iterations.

In Fig. 3.7, the performance of the proposed algorithm is compared to the *Relay assignment + EDP*, in term of the outage probability. An outage event occurs when in each transmission, the minimum SNR is lower than a certain threshold. Here, we assume that the SNR threshold is $0dB$. It can be observed that the proposed algorithm achieves considerable improvement in terms of the

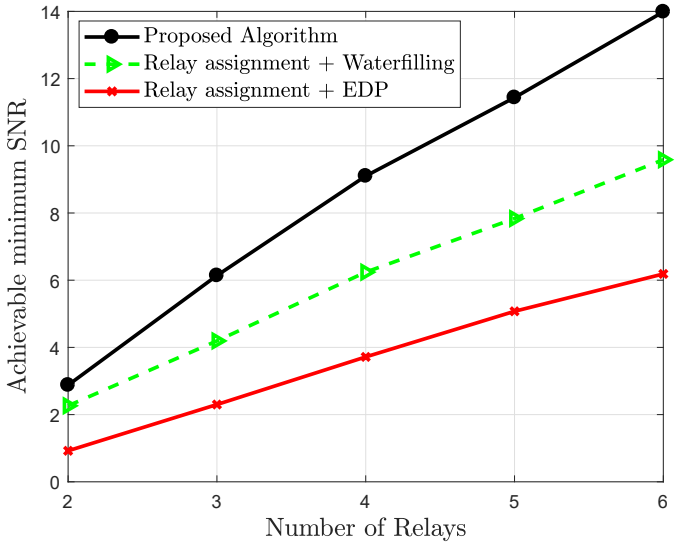

Figure 3.5: Achievable minimum SNR across the subcarriers in a system with 60 subcarriers, $P_s = 6, P_0 = 1, P_r = 2$ and different number of relays

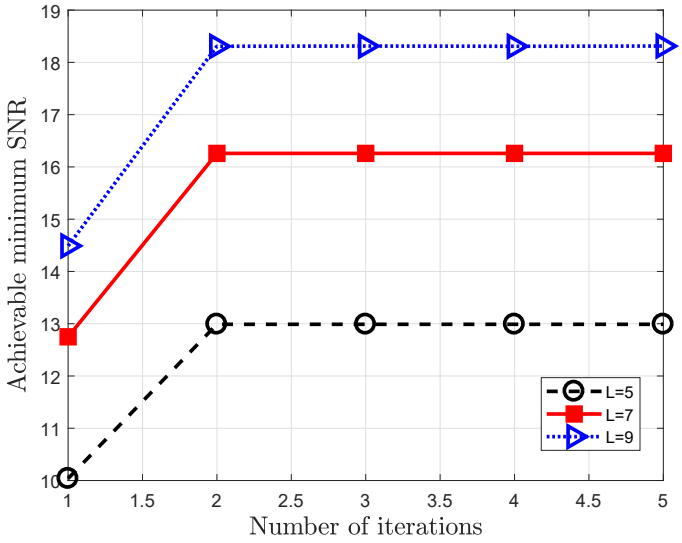

Figure 3.6: Convergence of the *Joint Optimization* algorithm, in a system with 5 subcarriers and different number of relays

outage probability. Also, it is shown in this figure that the performance improvement becomes more noticeable, as the number of relays increases.

In Fig. 3.8, the performance of the proposed algorithm is compared to the *Relay assignment + Waterfilling*, in term of the outage probability. This figure shows that the proposed algorithm

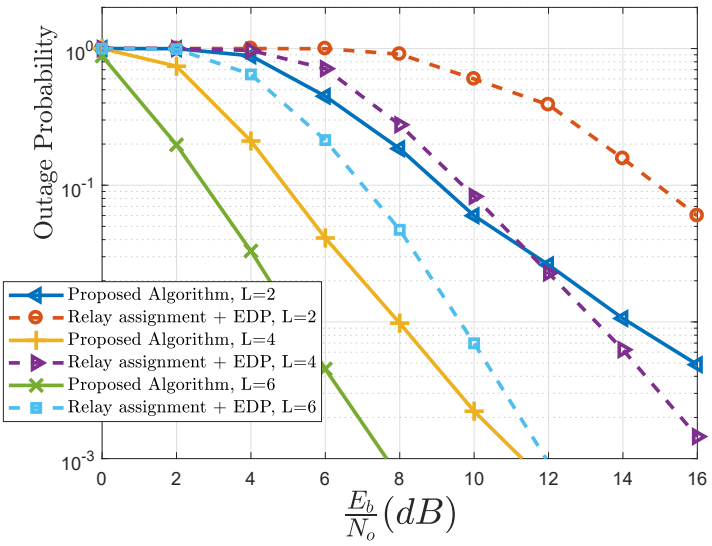

Figure 3.7: The outage probability of the proposed algorithm in comparison with the max-min algorithm, in a system with 60 subcarriers and different number of relays

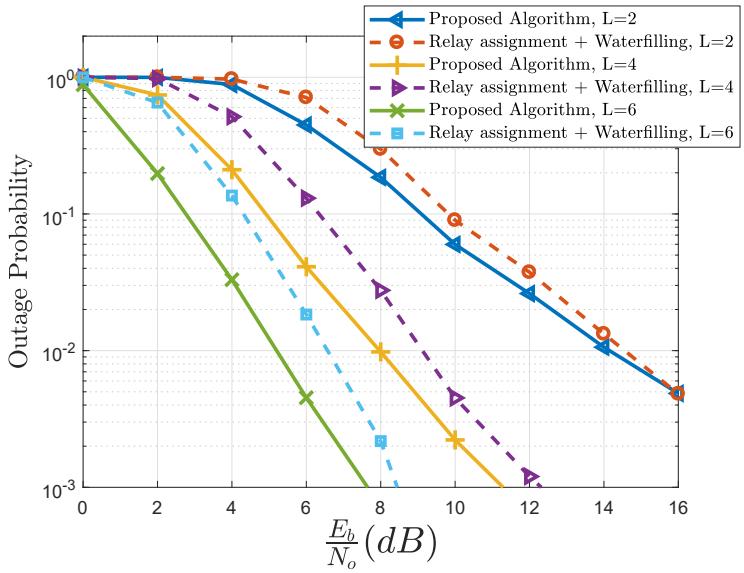

Figure 3.8: The outage probability of the proposed algorithm in comparison with the max-min algorithm, in a system with 60 subcarriers and different number of relays

outperforms the *Relay assignment + Waterfilling* one for all the values of SNR and for different number of relays. It can be observed that similar to Fig. 3.7, the performance improvement becomes more noticeable, as the number of relays increases.

In Fig. 3.9, the performance of our algorithm is compared with the algorithm proposed in [86]

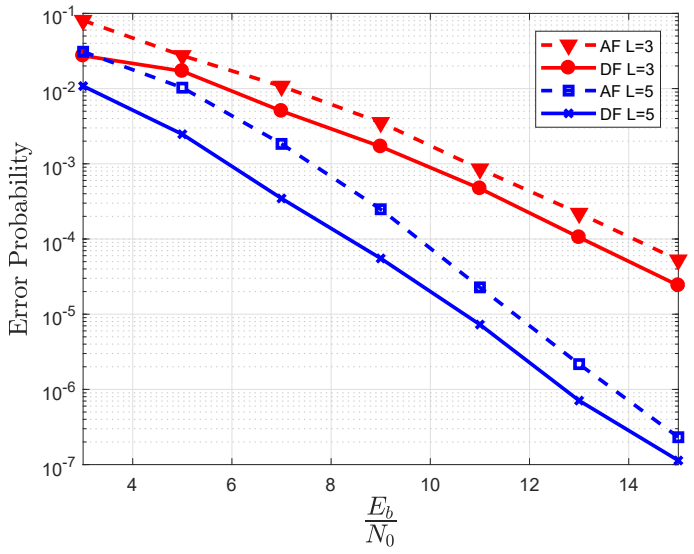

Figure 3.9: The error probability of the system with DF relays in comparison with AF relays, in a system with 3 subcarriers

for a system with AF relays. As AF relays amplify and forward the received signal, they are restricted to use the same subcarrier for reception and transmission. The proposed algorithm is not restricted by the same limitation. However, to make a fair comparison, we add an extra condition to our algorithm that states relays are constrained to use the same subcarriers for transmission and reception. Fig. 3.9 shows that even by adding this extra condition, the proposed algorithm outperform the algorithm proposed in [86], for different values of SNR and various number of relays. The performance improvement is more significant in low SNR regime. The reason is that in an AF relay noise is amplified besides the signal. This effect is more detrimental when the noise level is higher.

The proposed algorithm is based on the max-min fairness to ensure that each subcarrier secures a fair part of the resources. To evaluate the fairness of the proposed algorithm, we used Jain's fairness index given by $\frac{(\sum_m T^*_{(m)})^2}{M\sum_m (T^*_{(m)})^2}$. In Fig 3.10 the fairness of our method is compared with the Max-min algorithm and the Max-sum algorithm. In the Max-sum algorithm the selection criterion is to maximize the total capacity. It is observed in this figure that the proposed algorithm achieves higher fairness.

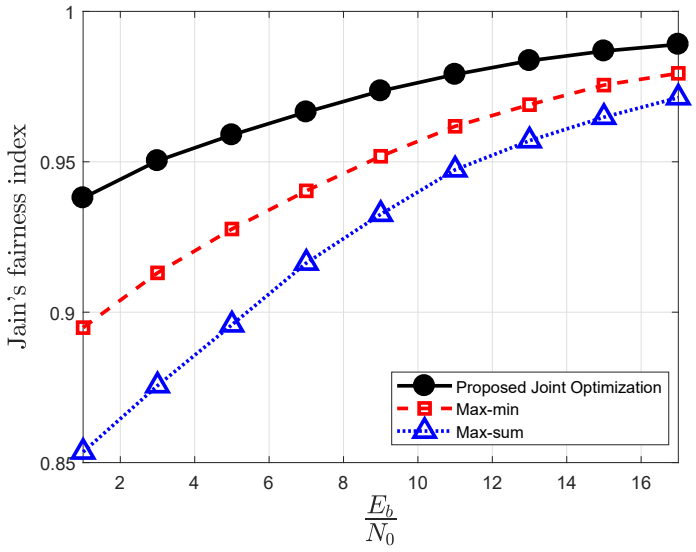

Figure 3.10: The Jain's fairness index of the proposed algorithm in comparison with Max-min and Max-sum algorithms

3.5 Conclusion

We proposed an algorithm for the joint power allocation and relay assignment problem in relay networks. The relay assignment is based on the max-min criterion and the power allocation is performed by the water-filling algorithm. We analytically proved the optimality of the proposed algorithm. It was also shown by simulation results that the performance of our algorithm matches the performance of the exhaustive search. Since the proposed algorithm acts iteratively, we performed convergence investigation and showed that the algorithm convergences in less than three iterations. By performing complexity analysis, we showed that the algorithm that we proposed offers polynomial time complexity that makes it practical for a larger number of relays or subcarriers. Moreover, we provided various comparisons between our algorithm and the max-min algorithm when power is equally distributed among subcarriers, and the max-min algorithm when power allocation follows waterfilling algorithm. Our algorithm showed significant improvement in terms of the outage probability and the achievable minimum SNR, in comparison with these two algorithms. It can be inferred from the simulation results that as the SNR and/or the number of relays increase, the performance improvement of the proposed algorithm with respect to the other two algorithms becomes more significant. It was also shown that our algorithm secures more fairness in comparison with the

max-min and max-sum algorithms.

Chapter 4

Throughput Maximization using Cross-Layer Design in Wireless Sensor Networks

4.1 Introduction

In WSN, depending on the application, there are three main metrics that are the objective of optimization: network lifetime is maximized, data latency is minimized, and network throughput is maximized. Due to the recent improvements in energy harvesting technique in WSN (EH-WSN), the sensor nodes can harvest energy from resources like wind, solar or vibration in their surrounding environment [88], therefore, in EH-WSN mostly the objective of optimization is network throughput rather than lifetime maximization. The throughput optimization is investigated in [88–90]. The problem is NP-hard. Therefore, in [89] the authors derive a bound rather than optimal solution. In [90] an exact solution for throughput optimization is obtained for medium-sized networks, but for large network a heuristic algorithm is proposed.

The many benefits of relays in WSN are previously discussed in Chapter 2. A proper relay selection technique in a WSN with multiple relays can improve the performance of the network. The

relay selection techniques that improve the performance of the wireless network from a physical-layer point of view, do not consider the quality-of-service (QoS) requirements of the data-link layer like packet error rate (PER) or total throughput. A proper cross-layer technique could guarantee these requirements. In [91], a cross-layer relay selection algorithm is proposed to select the optimal relay in device-to-device (D2D) communications, while addressing the problem of buffer management. Both channel-state-information (CSI) in the physical-layer, and queue state information (QSI) at the data-link layer are considered. In [92], a cross-layer relay selection for cooperative network is proposed. The algorithm uses exhaustive search at the destination node to select a subset of relays that maximizes the link-layer throughput. In [93], a Q-learning-based algorithm is proposed for relay selection problem to maximize the link-layer transmission efficiency. In [94], a distributed optimal relay selection scheme is proposed to improve multimedia transmission, while optimizing the application layer QoS and distortion. In [95], a cross-layer design for relay selection and power control is proposed for a multi-cell network to maximize the total capacity while considering the inter-cell interference. It is assumed that relays are affected by the nodes in adjacent cells. In [96], a cross-layer relaying transmission framework is proposed to maximize the effective capacity. In the same paper, the authors also propose a cross-layer fixed power allocation scheme based on the particle swarm optimization.

Previous works on relay selection assume independent channels. This is a valid assumption when relays are sufficiently separated, although in scenarios when relays are placed closely these channels tend to be correlated. In [97], the performance of a system with SRS with correlated channels is analyzed. It is assumed that SR channels are equally correlated, as well as RD channels, but for each relay, SR and RD channels are independent. This correlation model is used as a worst-case benchmark. In [98], the performance of a single relay network is analyzed. It is assumed that SR, RD, and SD channel are correlated. In [99], a relay selection scheme for OFDM based system is proposed over equally spatially correlated channels within the same hop and independent channel in two hops.

In this chapter, we propose a cross-layer-based scheme for relay/sensor selection to maximize the link-layer throughput. In this scheme, no limit is put on the number of relays. Taking into account the physical and link-layer characteristics, one or multiple relay sensors are selected. The

objective of the scheme is to maximize the link layer throughput. Unlike many works that assumed independent channels, we consider equally spatially correlated channels. Correlation among different sensors become significant when sensors are closely placed (a relay cluster). The equally correlated model can be used as a worst-case benchmark or as a rough approximation by assuming equal correlation coefficients for all channels.

The rest of the chapter is organized as follows. In section 4.2, the system model is presented and the problem is formulated. In section 4.3, the proposed scheme for cross-layer sensor/relay selection is presented and discussed in details. In section 4.4, the simulation results are presented and discussed. Finally, section 4.5 concludes the chapter.

4.2 System Model

We consider a two-hop wireless sensor network with a single source node S, L half-duplex DF relays/sensors $R_i, i = 1, ..., L$ and single destination node D (see Fig. 4.1). All nodes are equipped with single antennas. Each hop includes L channels which are equally correlated in space. Channels from different hops are statistically independent. Channels are modeled as Rayleigh fading with equally correlated gains as proposed in [100]. This model can be used for systems with closely placed sensor network (i.e., relay cluster). Many techniques are proposed for relay clustering. One of the mostly used methods is geographic approach which places closely placed sensors in one cluster. By this method, sensors in a cluster experience correlated fading. The equally correlated model can be used as a worst-case benchmark or as a rough approximation by assuming equal correlation coefficients for all channels [100], [97, 99]. For the i^{th} relay, R_i, we denote the SR gain by h_i^{SR} and RD channel gain by h_i^{RD}. According to [100], we can model equally correlated Rayleigh fading channel as

$$h_i^{\{SR,RD\}} = (\sqrt{1-\rho}x_i + \sqrt{\rho}x_0) + i(\sqrt{1-\rho}y_i + \sqrt{\rho}y_0) \tag{4.1}$$

where $i = \sqrt{-1}$, x_i and $y_i \sim \mathcal{N}(0, \sigma^2/2)$ are independent, x_0 and $y_0 \sim \mathcal{N}(0, \sigma^2/2)$ are independent and used to correlate all channels. Correlation coefficient is denoted by $\rho = \mathbb{E}[h_i h_j^*]/\sqrt{\mathbb{E}[h_i h_i^*]\mathbb{E}[h_j h_j^*]}$ where $\mathbb{E}$ is the expected value operator and $0 \leq \rho \leq 1$.

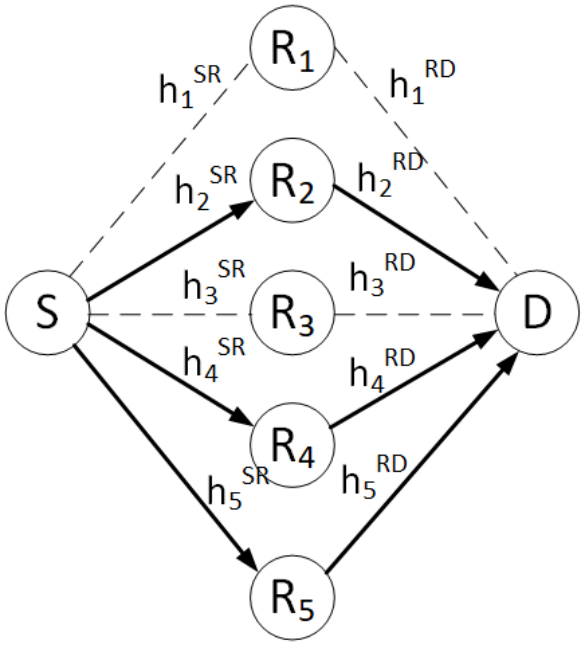

Figure 4.1: The block diagram of the system with 5 relays; 3 relays are selected for cooperation

It is assumed that channels are quasi-static and fixed during a single packet transmission. Also, a perfect CSI is assumed. The relay/sensor selection takes place at the destination node. A subset of K best sensors are selected, and this selection is sent to the source node through a reliable error-free feedback link.

The transmission takes place in two hops. In the first hop, the source node sends a packet with the length of N. Using a spatial multiplexer, this packet is split into K streams. The source node uses orthogonal transmission (in time, code, or etc.) to send each stream to relays. It is assumed that due to the poor link quality, a direct communication link between the source and the destination node does not exist. Each of the selected relays decodes the received signal. In the second hop, sensor relays transmit the re-encoded signal to the destination node. The received signal at the i^{th} sensor from the source node, and the received signal at the destination node from R_i are, respectively, given as

$$y_{SR_i} = h_i^{SR}\sqrt{\frac{P_s}{K}}s + n_{SR_i}, \tag{4.2}$$
$$y_{R_iD} = h_i^{RD}\sqrt{P_r}\hat{s} + n_{R_iD}$$

where P_S is the available power at the source node, P_r is the available power at each sensor node, $n_{\{SR_i,R_iD\}}$ is zero-mean complex Gaussian noise with variance $N_0/2$, and $\hat{s}$ is the estimated value of s. Equivalent instantaneous SNR at the destination node, received from relay R_i is given by

$$\begin{aligned} \gamma_i^{eq} &= \min\{\gamma_i^{SR}, \gamma_i^{RD}\}, \\ \gamma_i^{SR} &= \frac{P_s|h_i^{SR}|^2}{KN_0}, \\ \gamma_i^{RD} &= \frac{P_r|h_i^{RD}|^2}{N_0}. \end{aligned} \tag{4.3}$$

4.3 Cross-Layer Relay/Sensor Selection

In this section, we present a cross-layer relay selection technique that uses CSI at physical layer to maximize the throughput at the data-link layer. It is assumed that Go-Back-N (GBN) protocol is used with the transmit window size of W.

For each stream sent through relay R_i, the received symbol error rate SER_i at the destination node assuming BPSK modulation is given by

$$SER_i = Q(\sqrt{2\gamma_i^{eq}}) \tag{4.4}$$

where $Q(.)$ denotes Gaussian Q-function. The packet error rate (PER) at the destination node is given by (4.5).

$$PER = 1 - [\prod_{i=1}^{K}(1 - SER_i)]^{N/K}. \tag{4.5}$$

The instantaneous throughput at the destination node using GBN protocol is given as

$$\eta_{GBN} = K\frac{1 - PER}{1 + PER(W - 1)}. \tag{4.6}$$

Using (4.4) and (4.5) into (4.6), the instantaneous throughput is given by

$$\eta = K \frac{[\prod_{i=1}^{K}(1 - Q(\sqrt{2\gamma_i^{eq}}))]^{N/K}}{1 + (1 - [\prod_{i=1}^{K}(1 - Q(\sqrt{2\gamma_i^{eq}}))]^{N/K})(W-1)}. \tag{4.7}$$

At the destination node, the best set of sensors is selected to maximize the instantaneous throughput given in (4.7) for each packet. In this case, the total number of possible sensor selections is $\sum_{K=1}^{L} \binom{L}{K}$.

In order to verify the improvement of the cross-layer based sensor selection scheme, we use a capacity-based scheme for comparison. The general formula for the instantaneous capacity is given as [2]

$$C = \log_2 det[I_K + \bar{\gamma}\mathbf{H}^H\mathbf{H}] \tag{4.8}$$

where I_K is $K \times K$ identity matrix, $\bar{\gamma}$ is the average SNR $\bar{\gamma} = \frac{P_s}{N_0}$, and H denotes conjugate transpose. $\mathbf{H}$ represents the equivalent channel matrix and is given by (4.26). In a system with DF relays, $\mathbf{H}$ derives from the minimum of normalized SR and RD channel matrices. It can be seen that constant K, source power P_s and sensor power P_r are absorbed into channel matrices.

$$\begin{aligned} \mathbf{H} &= \min\{\mathbf{H}^{SR}, \mathbf{H}^{RD}\}, \\ \mathbf{H}^{SR} &= [\frac{h_i^{SR}}{\sqrt{K}}], \\ \mathbf{H}^{RD} &= [\sqrt{\frac{P_r}{P_s}} h^{RD}\}]. \end{aligned} \tag{4.9}$$

4.3.1 Cross-Layer Relay/Sensor Selection for AF Relaying

The proposed scheme is based on the DF relaying protocol. Another widely used relaying protocol is the AF. Although DF relaying shows promising results, the AF protocol attracts attention due to its simplicity, and is widely used in many works. In this section, we show that the proposed cross-layer scheme can be applied to AF relaying networks with some modifications.

In a system with AF relaying, the received signal at the i^{th} sensor/relay from the source node, denoted by y_{SR_i}, and the received signal at the destination node from R_i, denoted by y_{R_iD}, are

respectively given by

$$y_{SR_i} = h_i^{SR}\sqrt{\frac{P_s}{K}}s + n_{SR_i}, \tag{4.10}$$
$$y_{R_iD} = h_i^{RD}\beta_i y_{SR_i} + n_{R_iD}$$

where β_i is maximum achievable gain at sensor i and is given by

$$\beta_i = \sqrt{\frac{P_r}{|h_i^{SR}|^2 P/k + N_0}}. \tag{4.11}$$

The equivalent instantaneous SNR at the destination node, received from sensor node R_i is given by

$$\begin{aligned} \gamma_i^{eq} &= \frac{\gamma_i^{SR}\gamma_i^{RD}}{\gamma_i^{SR} + \gamma_i^{RD} + 1}, \\ \gamma_i^{SR} &= \frac{P_s|h_i^{SR}|^2}{KN_0}, \\ \gamma_i^{RD} &= \frac{P_r|h_i^{RD}|^2}{N_0}. \end{aligned} \tag{4.12}$$

Assuming BPSK modulation and GBN protocol at data-link layer, (4.4)-(4.7) can be applied to calculate the SER, PER, and throughput.

To verify the improvement of the cross-layer based sensor selection scheme, we use a capacity-based scheme for comparison. According to [101], the instantaneous capacity for a system that could be described by $y = \mathbf{A}x + \mathbf{B}n$ is given as

$$\begin{aligned} C = \log_2 det[\mathbf{I} + (\mathbf{A}\mathbf{R}_x\mathbf{A}^H)(\mathbf{B}\mathbf{R}_n\mathbf{B}^H)^{-1}], \\ \mathbf{R}_x = \mathbb{E}\{\mathbf{x}\mathbf{x}^H\}, \\ \mathbf{R}_n = \mathbb{E}\{\mathbf{n}\mathbf{n}^H\}, \end{aligned} \tag{4.13}$$

where $\mathbf{R}_x$ is the covariance matrix of the transmitted vector, and $\mathbf{R}_n$ is the noise covariance matrix.

For each sensor node i, the received signal at the destination node is given by

$$y_{R_iD} = h_i^{RD}\beta_i h_i^{SR}\sqrt{\frac{P_s}{K}}s + h_i^{RD}\beta_i n_{SR_i} + n_{R_iD}. \tag{4.14}$$

The received signal from all k sensor nodes at the destination node can be described as

$$\mathbf{y} = \begin{bmatrix} y_{R_1D} \\ y_{R_2D} \\ \vdots \\ y_{R_kD} \end{bmatrix} = \mathbf{A}\begin{bmatrix} x_1 \\ x_2 \\ \vdots \\ x_k \end{bmatrix} + \mathbf{B}\begin{bmatrix} n_{SR_1} \\ \vdots \\ n_{SR_k} \\ n_{RD_1} \\ \vdots \\ n_{RD_k} \end{bmatrix} \tag{4.15}$$

In which **A** and **B** are defined as follows

$$\mathbf{A} = \begin{bmatrix} h_1^{SR}\beta_1 h_1^{RD} & 0 & \dots & 0 \\ 0 & h_2^{SR}\beta_2 h_2^{RD} & \dots & 0 \\ \vdots & \vdots & \vdots & \vdots \\ 0 & 0 & \dots & h_k^{SR}\beta_k h_k^{RD} \end{bmatrix} \tag{4.16}$$

$$\mathbf{B} = \begin{bmatrix} h_1^{RD}\beta_1 & 0 & \dots & \dots & 1 & 0 & \dots \\ 0 & h_2^{RD}\beta_2 & \dots & \dots & 0 & 1 & \dots \\ \vdots & \vdots & \vdots & \vdots & \vdots & \vdots & \vdots \\ 0 & 0 & \dots & h_k^{RD}\beta_k & 0 & \dots & 1 \end{bmatrix}$$

covariance matrices of the transmitted vector and noise are defined as follows

$$\begin{aligned} \mathbf{R}_x &= \frac{P_s}{K}.\mathbf{I}_{k\times k} \\ \mathbf{R}_n &= N_0.\mathbf{I}_{2k\times 2k}. \end{aligned} \tag{4.17}$$

The instantaneous capacity becomes

$$C = \log_2 det[\mathbf{I} + \frac{P_s}{kN_0}(\mathbf{A}\mathbf{A}^H)(\mathbf{B}\mathbf{B}^H)^{-1}]. \tag{4.18}$$

4.3.2 Cross-layer Relay/Sensor Selection and Subcarrier Allocation

In this section, we consider an OFDM-based network with single source node, single destination node, L half duplex DF relays/sensors, and M orthogonal subcarriers. In each hop for a given subcarrier, there are L channels that are equally correlated in space [99]. Channels for different subcarriers are statistically independent. Channels are modeled as Rayleigh fading with equally correlated gains. The SR and RD channel gains for the i^{th} relay and j^{th} subcarrier is given by

$$h_{ij}^{\{SR,RD\}} = (\sqrt{1-\rho}x_{ij} + \sqrt{\rho}x_{0j}) + i(\sqrt{1-\rho}y_{ij} + \sqrt{\rho}y_{0j}) \tag{4.19}$$

where x_{ij} and $y_{ij} \sim \mathcal{N}(0, \sigma^2/2)$ are independent, x_{0j} and $y_{0j} \sim \mathcal{N}(0, \sigma^2/2)$ are independent and used to correlate all channels. Correlation coefficient is denoted by $\rho = \mathbb{E}[h_{ij}h_{i'j}^*]/\sqrt{\mathbb{E}[h_{ij}h_{ij}^*]\mathbb{E}[h_{i'j}h_{i'j}^*]}$.

It is assumed that, at the source node by using a multiplexer, a packet of length N is split into M streams, and each stream is transmitted by one subcarrier. The source node uses all the subcarriers to transmit information to K selected sensors. Each sensor decodes the received data from a pre-selected set of subcarriers. This selection is done by the destination node and sent to sensor relays using an error-free feedback channel. In order to avoid interference it is assumed that each subcarrier can be allocated to only one sensor node. It is also assumed that each sensor node uses the same subcarriers in the second time slot as the first time slot. The received signal at the i^{th} relay from the source node and using j^{th} subcarrier, and the received signal at the destination node from R_i using the same subcarrier are given as

$$\begin{aligned} y_{ij}^{SR} &= h_{ij}^{SR}\sqrt{\frac{P_s}{M}}s + n_{ij}^{SR}, \\ y_{ij}^{RD} &= h_{ij}^{RD}\sqrt{\frac{P_r}{m_i}}\hat{s} + n_{ij}^{RD}. \end{aligned} \tag{4.20}$$

It is assumed that the available power at the source node P_s, and the available power at each sensor

node P_r are equally distributed among subcarriers. The number of subcarriers assigned to relay sensor R_i is denoted by m_i.

Equivalent SNR at the destination node, received from relay R_i using subcarrier j is given as

$$\begin{aligned} \gamma_{ij}^{eq} &= \min\{\gamma_{ij}^{SR}, \gamma_{ij}^{RD}\}, \\ \gamma_{ij}^{SR} &= \frac{P_s|h_{ij}^{SR}|^2}{MN_0}, \\ \gamma_{ij}^{RD} &= \frac{P_r|h_{ij}^{RD}|^2}{m_iN_0}. \end{aligned} \tag{4.21}$$

For each stream sent by subcarrier j through relay R_i, the received symbol error rate SER_{ij} at the destination node assuming BPSK modulation is given as

$$SER_{ij} = Q(\sqrt{2\gamma_{ij}^{eq}}). \tag{4.22}$$

We define a binary variable α_{ij}, when subcarrier j is assigned to relay i, $\alpha_{ij} = 1$, otherwise $\alpha_{ij} = 0$. The PER at the destination node is given by

$$PER = 1 - [\prod_{i=1}^{L}\prod_{j=1}^{M}(1 - SER_{ij}\alpha_{ij})]^{N/M}. \tag{4.23}$$

Using (4.22) and (4.23) into (4.6), the instantaneous throughput for the GBN protocol is given as

$$\eta = K\frac{[\prod_{i=1}^{L}\prod_{j=1}^{M}(1 - SER_{ij}\alpha_{ij})]^{N/M}}{1 + (1 - [\prod_{i=1}^{L}\prod_{j=1}^{M}(1 - SER_{ij}\alpha_{ij})]^{N/M})(W-1)}. \tag{4.24}$$

In order to verify the improvement of the proposed scheme, we compare it with the capacity-based scheme. The general formula for instantaneous capacity is given as

$$C = \log_2 det[I_M + \bar{\gamma}\mathbf{H}^H\mathbf{H}] \tag{4.25}$$

where $\bar{\gamma} = \frac{P_s}{N_0}$, and matrix $\mathbf{H}$, the equivalent channel matrix is given as

$$\begin{aligned} \mathbf{H} &= \min\{\mathbf{H}^{SR}, \mathbf{H}^{RD}\}, \\ \mathbf{H}^{SR} &= [\frac{h_{ij}^{SR}}{\sqrt{M}}], \\ \mathbf{H}^{RD} &= [\sqrt{\frac{P_r}{P_s m_i}} h_{ij}^{RD}]. \end{aligned} \tag{4.26}$$

4.4 Simulations Results

In this section, simulation results are presented to evaluate the performance of the proposed scheme. The model used in simulation complies with the system model presented in section 4.2. The system performance is evaluated in terms of the system throughput with respect to E_s/N_0. It is assumed that the system has four relay sensors $L = 4$, packet length is $N = 120$, window size is $W = 4$, source and sensor powers are $P_s = P_r = 1$, and average channel gain is $\sigma^2 = 1$.

To verify the improvement achieved by the proposed scheme, the system performance is evaluated in terms of the link-layer throughput using cross-layer-based and capacity-based relay selection schemes. The results are shown in Fig. 4.2. In this figure, it is assumed that the channels are uncorrelated $\rho = 0$. It can be seen that the cross-layer approach leads to considerable improvement in terms of the system throughput. In the second scenario, it is assumed that channels are correlated with correlation coefficient $\rho = 0.8$. The results are shown in Fig. 4.3. It can be seen that the system performance degrades with channel correlation, however, the cross-layer-based scheme still outperforms the capacity-based considerably.

Fig. 4.4 shows the performance of the proposed scheme using AF transmission. Similar to the DF case, it can be seen that the cross-layer-based scheme outperforms the capacity-based.

Fig 4.5 shows the results of the proposed scheme for relay sensor selection and subcarrier allocation. For simplicity, an OFDM-based system is considered with 4 subcarriers and 4 relays. Two scenarios are considered: uncorrelated channels $\rho = 0$ and correlated channels $\rho = 0.8$. It can be seen that in both scenarios the proposed scheme outperforms the capacity-based scheme.

In Fig. 4.6-4.8, the percentage of the relay usage is demonstrated for each value of SNR. These results compare the relay/sensor usage percentage in cross-layer and capacity-based schemes in a

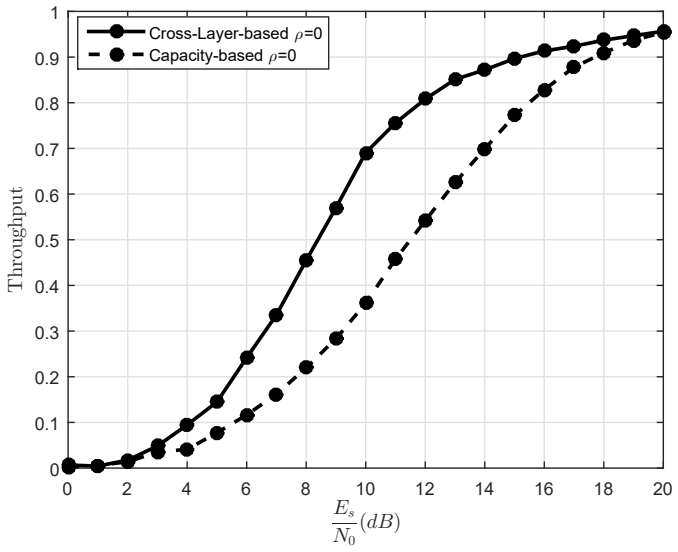

Figure 4.2: Throughput of the cross-layer-based relay selection in comparison with capacity-based scheme in a system with 4 DF relays for different values of SNR

system with four relay sensor nodes $L = 4$, and for two scenarios, with uncorrelated channels $\rho = 0$ and with correlation $\rho = 0.8$. It can be inferred from Fig. 4.6-4.8 that in the cross-layer-based scheme and in case of poor channels, the maximum throughput is achieved when only one relay node is used for cooperation (SRS). However, for higher values of SNR better performance is achieved by letting more than one sensor node transmit to the destination. A similar trend is seen for correlated channels. In the capacity-based scheme, no meaningful difference is seen in relay usage percentage for different values of SNR.

4.5 Conclusion

We proposed a cross-layer-based scheme for sensor node selection in wireless cooperative sensor networks with equally spatially correlated channels. The objective is to maximize link layer throughput. The performance of the proposed scheme is compared with the physical-layer capacity-based scheme. The results show that the proposed scheme outperforms the capacity-based scheme, considerably, for both correlated and uncorrelated models. In the proposed scheme, no limit is put on the number of selected sensor nodes. The simulation results show that for poor channels with low SNR, the best performance is achieved by selecting one relay (SRS) while in channels with

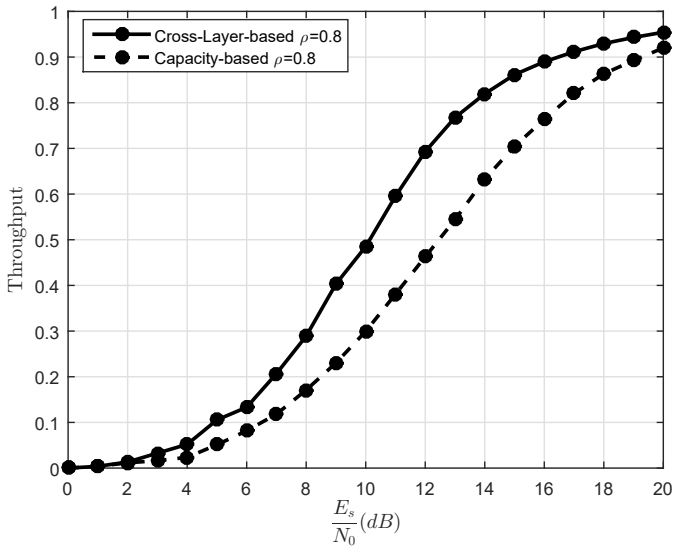

Figure 4.3: Throughput of the cross-layer-based relay selection in comparison with capacity-based scheme in a system with 4 DF relays with correlated channels for different values of SNR

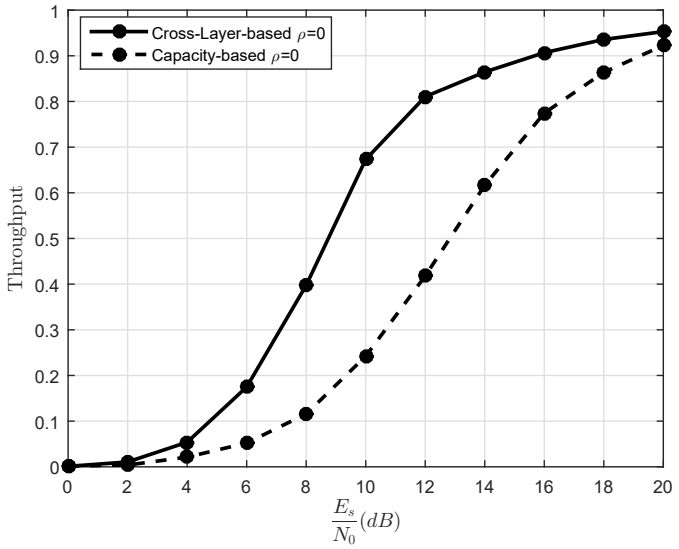

Figure 4.4: Throughput of the cross-layer-based relay selection in comparison with capacity-based scheme in a system with 4 AF relays for different values of SNR

higher SNR, letting more relays to cooperate is more beneficial (MRS). The proposed scheme is applied to both DF and AF relaying where performance gains are achieved in both cases. We also used the proposed scheme for sensor selection and subcarrier assignment in OFDM-based system where a large gain was observed compared to physical-layer based optimization techniques.

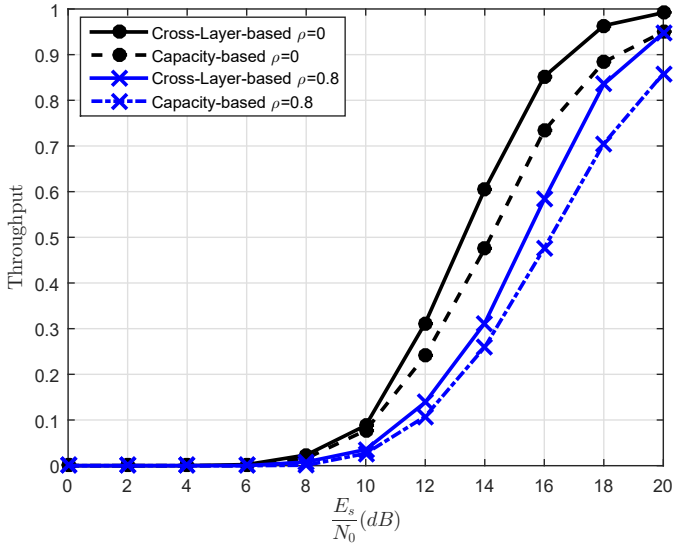

Figure 4.5: Throughput of the cross-layer-based relay selection in comparison with capacity-based scheme in a system with 4 DF relays and 4 subcarriers for different values of SNR

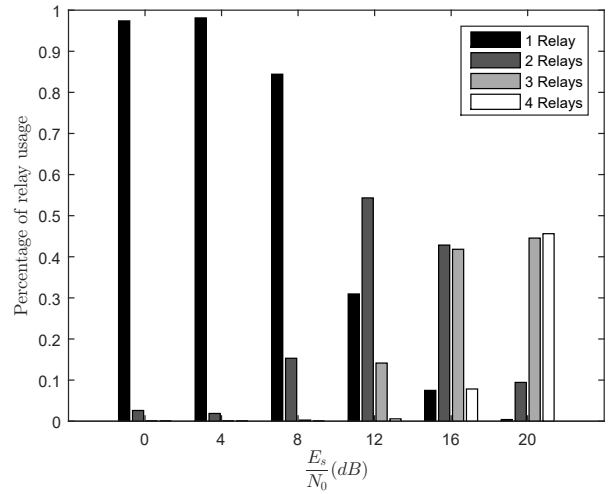

(a)

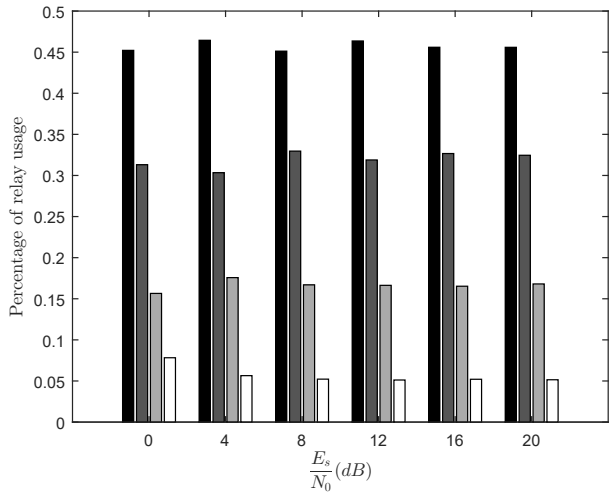

(b)

Figure 4.6: Relay usage percentage of Average number of selected relays in a system with 4 DF relays for different values of SNR with $\rho = 0$, a) Cross-layer-based , b) Capacity-based

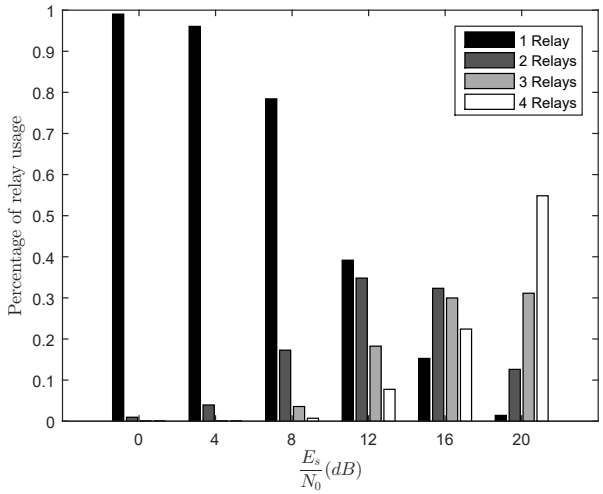

(a)

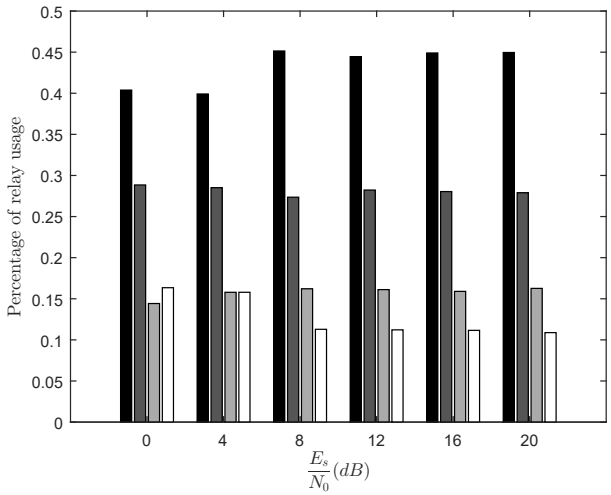

(b)

Figure 4.7: Relay usage percentage of Average number of selected relays in a system with 4 DF relays for different values of SNR with $\rho = 0.8$, a) Cross-layer-based , b) Capacity-based

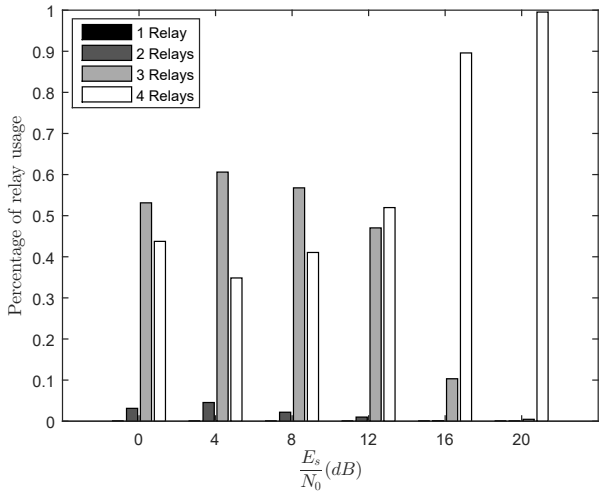

(a)

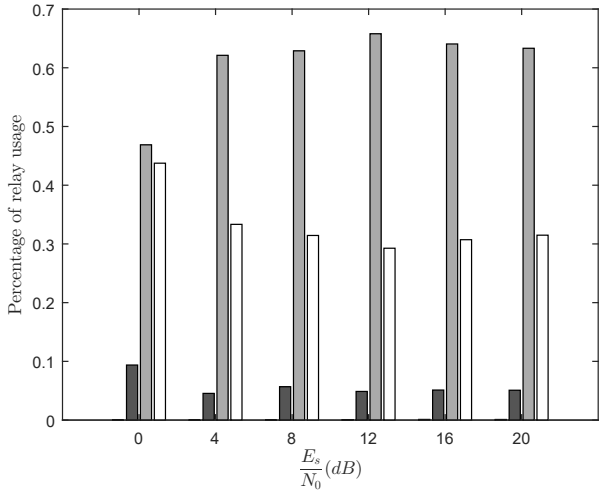

(b)

Figure 4.8: Relay usage percentage of Average number of selected relays in a system with 4 DF relays and 4 subcarriers, a) Cross-layer-based , b) Capacity-based

Chapter 5

Performance Analysis of Convolutional codes, Turbo Codes and Distributed Turbo Codes in Buffer-Aided Relay Selection

5.1 Introduction

Buffer-aided relays introduce significant improvements to the system performance in terms of throughput and stability, and balances the traffic load passing through each relay [4]. As mentioned in Chapter 2, buffer-aided relay selection algorithms are studied in substantial works. Although channel coding is an integral part of any communication system, there have been few works reported on the problem of coded buffer-aided relaying in the open literature. In [102], the authors propose an adaptive modulation and coding scheme in a cognitive buffer-aided relaying network, where the communication from the secondary source to the secondary destination switches between the direct and relaying transmission based on the instantaneous channel conditions. In [103], the authors propose a link selection protocol based on the quality of the links and buffer status in a buffer-aided relaying system that combines bit-interleaved coded modulation (BICM) with OFDM. Different

from [102] and [103], where the system includes a single relay, the authors in [104] consider a cooperative system with two half-duplex (HD) DF relays with the BICM transmission. In this system, the relays alternate between transmission and reception, and a detection algorithm based on the iterative parallel decoding is used at the destination node.

To further improve the performance of the relay networks, a coded cooperation technique is proposed in [105], where channel coding is integrated into cooperative transmission. Coded cooperation networks employ distributed coding schemes to encode and transmit the data. Among various distributed coding schemes, distributed Turbo code (DTC) has shown to perform close to the capacity of relay channel [74]. DTC scheme in a multi-relay network has been considered in [106–110]. In [106], the authors consider a multi-relay network with Nakagami-m fading channels, where the source node broadcasts a turbo-coded frame to the destination and relay nodes. All the relays receive the first part of the frame, and the ones who successfully decode the received signal, generate the second part of the codeword and forward it to the destination node. In [107], the authors propose an AF turbo-coded relay selection scheme, where the relay with the highest end-to-end instantaneous SNR amplifies and forwards the received signal to the destination node. In [108] and [109], the authors present the bit error rate (BER) and outage analysis for a Turbo-coded relay selection scheme, in Rayleigh and Nakagami-m fading channels. In their proposed scheme, the relays listen to a fraction of the codeword, and among a set of relays who decoded successfully, known as the decoding set, the one with the highest instantaneous R-D channel SNR is selected for transmission of the remaining bits. In [110], the authors propose a DTC scheme with two ordered best relays, where two relays with the highest and second highest R-D link qualities, respectively, are selected for transmission. The best relay uses an interleaver and a recursive systematic convolutional (RSC) encoder to encode the received signal; the second-best relay uses a similar RSC encoder, without interleaving. The two code segments are combined and decoded by an iterative decoder at the destination node.

In this work, we are motivated by observing that in [106–110] buffering capability is not assumed for the relay nodes. Therefore, these systems do not benefit from numerous advantages offered by data buffers. Different from the above-mentioned works, we consider a relay selection

problem in a system with multiple buffer-aided relays combined with three distinct coded transmissions, i.e., convolutionally coded, Turbo-coded and DTC transmissions. To the best of our knowledge, convolutionally coded, turbo-coded and DTC transmissions in the context of buffer-aided relay selection has not been investigated in the open literature. We assume that all the transmissions experience quasi-static Rayleigh fading, which is a realistic model for users that are stationary or moving slowly. To model the fading gains, we consider a general case, where channels are independent but not identically distributed (i.n.i.d). The contributions of this chapter are as follows:

(i) For each coding scheme, we analyze the average throughput of the underlying system.

(ii) Simple and explicit expressions of the asymptotic throughput for infinite buffer size and in the high signal-to-noise ratio for the aforementioned schemes are derived. Using the derived asymptotic expression of the throughput, the maximum achievable diversity gain is obtained.

(iii) Furthermore, we provide a comparison between the DTC scheme and a convolutionally coded scheme for various number of relays in terms of throughput and average delay. Finally, we verify the accuracy of our analytical framework by Monte-Carlo simulations for various system parameters.

The rest of this chapter is organized as follows. In Section 5.2, the system model is presented, and the relay selection scheme is discussed. In Section 5.3, the performance analysis of the system in terms of the average throughput is presented. In Section 5.4, the simulation results are presented and discussed. Finally, Section 5.5 concludes the paper.

5.2 System Model

Fig. 5.1 shows the block diagram of the system model. We consider a multi-relay network consisting of a single source node S, a single destination node D, and L HD DF relay nodes denoted by $R_i, i = 1, ..., L$. All nodes are equipped with a single antenna, and they are subjected to the same power constraint P. In our model, we assume that the direct transmission from the source to the destination node is possible. We assume that channels are quasi-static Rayleigh fading, i.e., they remain constant during the transmission of a frame but change from one frame to another. The SD,

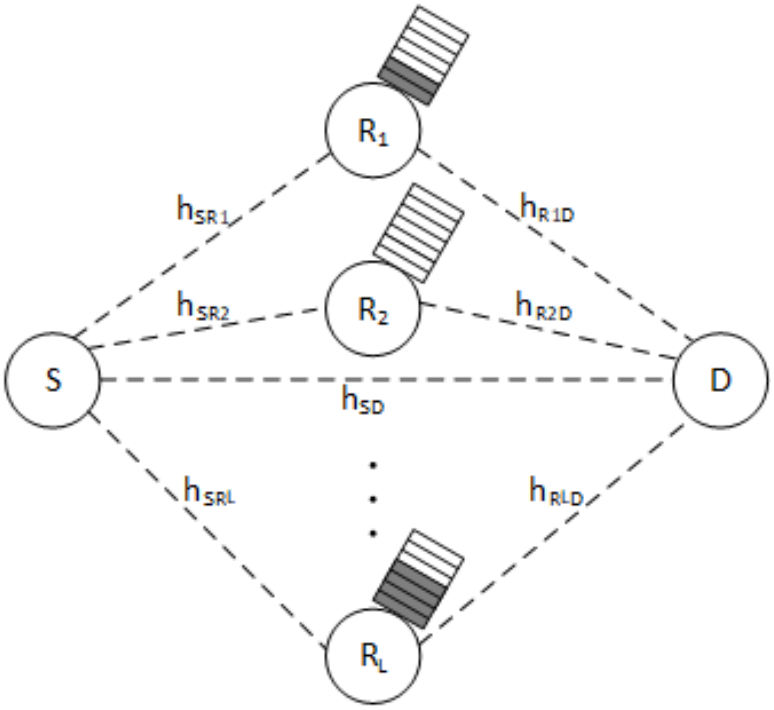

Figure 5.1: Buffer-aided relaying system.

SR, and RD channel gains are denoted by h_{SD}, h_{SR_i} and h_{R_iD}, which are modeled as circularly symmetric complex Gaussian distributed with zero mean and variances σ^2_{SD}, $\sigma^2_{SR_i}$ and $\sigma^2_{R_iD}$, respectively. In addition, AWGN with zero mean and variance $\frac{N_0}{2}$ for each channel is considered. We assume that the destination node has perfect knowledge of the SR and RD channel state information (CSI). The link selection is performed at the destination node on the basis of the instantaneous SR and RD channel SNRs, which are denoted by $\gamma_{SR_i} = \frac{P|h_{SR_i}|^2}{N_0}$ and $\gamma_{R_iD} = \frac{P|h_{R_iD}|^2}{N_0}$, respectively. This decision is sent to the relays through a reliable error-free feedback link.

Here, the relay selection policy is based on the modified max-link scheme proposed in [56]. In the modified max-link scheme, at each time slot, instead of selecting the best relay, the best link is selected among all the available links. The available links are all the SR links with non-full buffers and all the RD links with non-empty buffers. We assume that each relay is equipped with a buffer of size Q. The parameter $q_i \in [0, Q]$ denotes the number of packets stored in relay R_i. This parameter is incremented when relay R_i has successfully received a packet and decremented when R_i has successfully transmitted a packet. Let us denote the subset of all the relays with non-empty buffers by $\mathcal{NE} = \{R_i : q_i > 0\}$. Similarly, a subset of all the relays with non-full buffers is denoted by

$\mathcal{NF} = \{R_i : q_i < Q\}$. Given this, the relay R_i^* associated with the selected link is given by

$$R_i^* = \arg\max_{R_i} \big\{ \{\gamma_{SRi} : R_i \in \mathcal{NF}\} \cup \{\gamma_{R_iD} : R_i \in \mathcal{NE}\} \big\}. \tag{5.1}$$

We denote by γ^* the SNR of the selected SR or RD channel, associated with R_i^*. Considering quasi-static Rayleigh fading channels, γ^* follows the cumulative distribution functions (CDF)

$$F_{SR,RD}(\gamma^*) = \left(1 - e^{\frac{-\gamma^*}{\bar{\gamma}_{SR}}}\right)^{A_{\mathcal{NF}}} \left(1 - e^{\frac{-\gamma^*}{\bar{\gamma}_{RD}}}\right)^{A_{\mathcal{NE}}}. \tag{5.2}$$

By taking derivative of CDF, the probability density function (PDF) is written as

$$\begin{aligned} f_{SR,RD}(\gamma^*) = {} & \frac{A_{\mathcal{NF}}}{\bar{\gamma}_{SR}} \left(1 - e^{\frac{-\gamma^*}{\bar{\gamma}_{SR}}}\right)^{A_{\mathcal{NF}}-1} \left(1 - e^{\frac{-\gamma^*}{\bar{\gamma}_{RD}}}\right)^{A_{\mathcal{NE}}} e^{\frac{-\gamma^*}{\bar{\gamma}_{SR}}} \\ & + \frac{A_{\mathcal{NE}}}{\bar{\gamma}_{RD}} \left(1 - e^{\frac{-\gamma^*}{\bar{\gamma}_{SR}}}\right)^{A_{\mathcal{NF}}} \left(1 - e^{\frac{-\gamma^*}{\bar{\gamma}_{RD}}}\right)^{A_{\mathcal{NE}}-1} e^{\frac{-\gamma^*}{\bar{\gamma}_{RD}}}. \end{aligned} \tag{5.3}$$

For the direct SD link, the PDF of channel SNR is given as

$$f_{SD}(\gamma) \quad = \frac{1}{\bar{\gamma}_{SD}} e^{-\frac{\gamma}{\bar{\gamma}_{SD}}}. \tag{5.4}$$

In the modified max-link scheme, the data communication switches between two transmission modes: source transmission and relay transmission. The transmission mode is determined based on the selected link. If the selected link is an SR link, node S broadcasts a frame to node D and relay R_i^*, otherwise, relay R_i^* transmits a frame to node D. The received signals at R_i^* and D (in the first and second time slots) are respectively given by

$$y_{SR_i^*} = \sqrt{P} h_{SR_i^*} x + n_{SR_i^*}, \tag{5.5}$$

$$y_{SD} = \sqrt{P} h_{SD} x_{+} n_{SD}, \tag{5.6}$$

$$y_{R_i^*D} = \sqrt{P} h_{R_i^*D} \tilde{x} + n_{R_i^*D}, \tag{5.7}$$

where x and $\tilde{x}$ denote the BPSK modulated symbol transmitted from the source and the relay nodes, respectively, $n_{SR_i^*}, n_{SD}$, and $n_{R_i^*D}$ denote the AWGN. To ensure the successful reception of the data, ACK/NACK signaling is used between nodes, through an error-free feedback link. In the source transmission mode, where both D and R_i^* receive the same frame, if D successfully decodes the received frame, it sends an ACK signal to R_i^*, and R_i^* discards the received frame. In the case of unsuccessful decoding at node D, a NACK signal is sent to R_i^*, at which time, if the frame is successfully decoded at R_i^*, it is stored in its buffer, and an ACK signal is sent to node S. In the relay transmission mode, the relay R_i^* transmits one of its stored frames to node D, and if it is received successfully, an ACK is sent to the R_i^*, therefore R_i^* drops the frame from its buffer.

We consider three channel coding and transmission schemes: convolutional code, Turbo codes and DTC. Fig. 5.2 shows the block diagrams of these schemes. In the convolutionally coded scheme, the source and the relay nodes use the same convolutional encoder to encode a K-bit message into an N-bit codeword. The selected relay and the destination node decode the received signal by a Viterbi decoder. The success of the decoding process is determined by the Cyclic Redundancy Check (CRC) code. The selected relay then, uses the same convolutional encoder to re-encode the received K-bit message if NACK signal is received.

In the Turbo-coded scheme, the source and the relay nodes use the same Turbo encoder to encode a K-bit message into an N-bit codeword. The Turbo encoder with rate $R_T = 1/3$, consists of the parallel concatenation of two RSC encoders with rate $R_C = 1/2$, separated by a random interleaver. The received signal is decoded by a Turbo decoder and consists of two constituent soft-input soft-output RSC decoders that exchange extrinsic information, iteratively.

In the DTC scheme, the source node uses an RSC encoder with rate $R_C = 1/2$ to generate the first constituent of a Turbo-coded codeword. The received frames, at nodes R_i^* and D, are decoded by a conventional Viterbi decoder. If the decoding process at node D is unsuccessful, then the relay node R_i^*, using the same RSC encoder with the source node and a random interleaver, generates the second constituent of a Turbo-coded codeword. The turbo decoding is performed at node D by combining the first and the second constituent of a Turbo-coded codeword.

It should be noted that in the Turbo-coded and DTC scheme, at node D the received frame from the relay is combined with the frame directly received from node S by a maximal-ratio combining

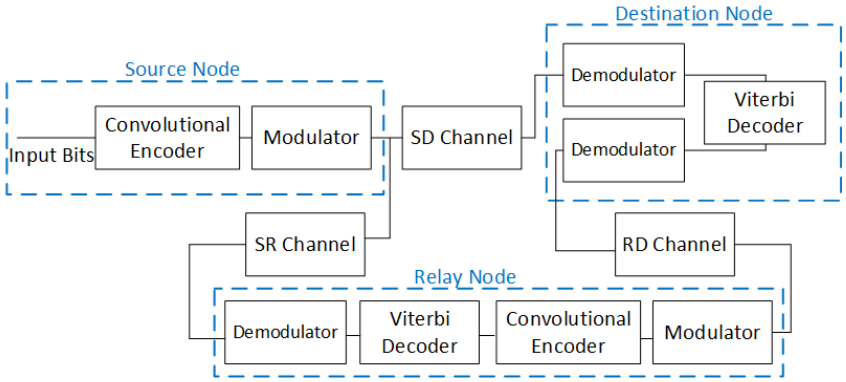

(a) Convolutionally coded scheme

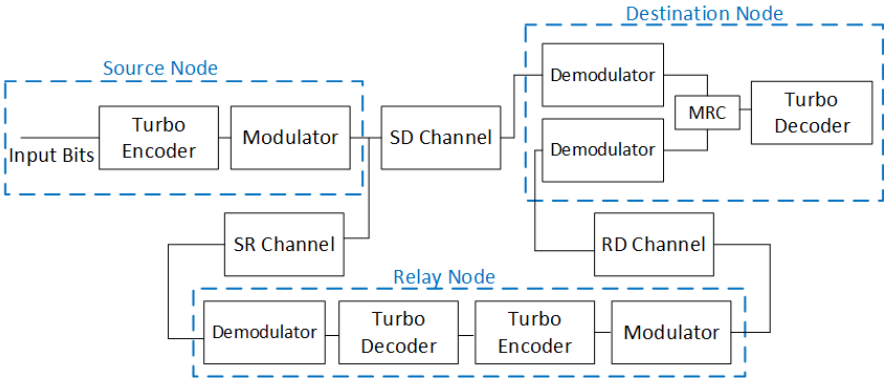

(b) Turbo coding scheme

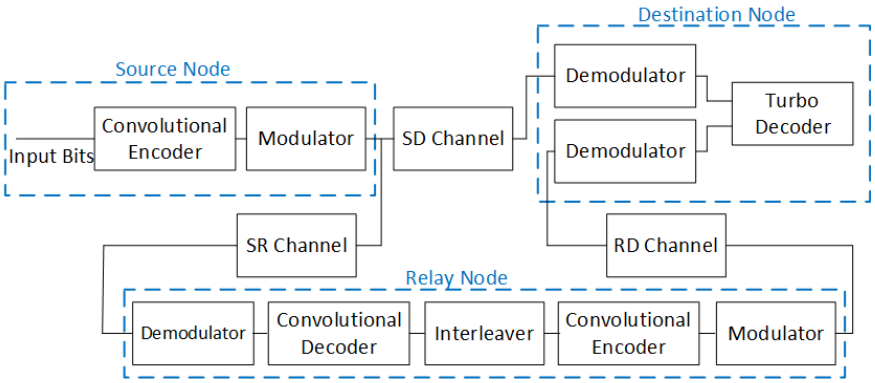

(c) DTC scheme

Figure 5.2: Block diagram of the system with three coding schemes

(MRC). However, in the convolutionally-coded scheme, MRC is not used. Although it is possible to use MRC in all three schemes, not using it results in a simpler expression for the average throughput. Therefore, we present the analysis for the convolutionally coded scheme without MRC, and the other two schemes with MRC.

5.3 Performance Analysis

In this section, we analyze the performance of the system model presented in Section II in terms of the average throughput. We define the throughput as number of error-free frames over the total number of frames, received by node D. Considering this definition, throughput is given as

$$\eta = R_0(1 - P_{SD})\mathfrak{p}_{\mathfrak{s}} + \frac{1}{2}R_0(1 - P_{RD})(1 - \mathfrak{p}_{\mathfrak{s}}), \tag{5.8}$$

where R_0 is the source transmission data rate, P_{SD} is the probability that an error occurs at node D in the source transmission mode, P_{RD} is the probability that an error occurs at node D in the relay transmission mode, and $\mathfrak{p}_{\mathfrak{s}}$ is the probability of the source transmission mode. Note that in the relay transmission mode,

5.3.1 Throughput Analysis of the Buffer-aided Relay Selection scheme

In what follows, we use a Markov chain analysis to study the performance of the coded system. In an L-relay system whereby each relay is equipped with a buffer of size Q, each state of the Markov chain is denoted by $Z_u = (\rho, q_1, q_2, ..., q_L)$, $1 \leq u \leq 2(1+Q)^L$, where $\rho \in \{0, 1\}$ is a binary variable that changes value when the direct transmission from S to D is successful.

In the construction of the Markov chain, we follow the following rules:

Rule 1) In the relay transmission mode, if node D successfully decodes the received frame, q_i is decremented.

Rule 2) In the source transmission mode, if the direct transmission from S to D fails, but R_i^* successfully decodes the frame, q_i is incremented.

Rule 3) In the source transmission mode, if the direct transmission from S to D is successful, ρ changes from 0 to 1, or 1 to 0, depending on its current value, and q_i stays unchanged.

As an example, in TABLE I, states $S_1 - S_9$ of Markov chain for a system with $L = 2, Q = 2$ are shown. It should be noted that this Markov chain has $2(1+Q)^L = 18$ states. States $S_{10} - S_{18}$ are not shown in the table, since they have similar buffer status as $S_1 - S_9$, however the value of the variable s_D is $s_D = 1$. The transition matrix of the Markov chain is denoted by $\boldsymbol{T} \in \mathbb{R}^{2(1+Q)^L \times 2(1+Q)^L}$, in

Table 5.1: States of Markov chain for a system with $L = 2, Q = 2$

S_i	$s_D q_1 q_2$	$A_{\mathcal{NF}}(i)$	$A_{\mathcal{NE}}(i)$
S_1	000	2	0
S_2	001	2	1
S_3	010	2	1
S_4	002	1	1
S_5	011	2	2
S_6	020	1	1
S_7	012	1	2
S_8	021	1	2
S_9	022	0	2

which the entry

$$T_{uv} = \mathbb{P}(Z_v \to Z_u), \tag{5.9}$$

is the probability of moving from state Z_v to state Z_u, and $\mathbb{P}\{\bullet\}$ denotes the probability operator. For each state, $A_{\mathcal{NF}}$ and $A_{\mathcal{NE}}$ denote the number of relays with non-full and non-empty buffers, respectively. The transition probabilities from state Z_v to state Z_u, following each rule, for $u \neq v$ are given by

$$\begin{cases} C_{RD}(1 - P_{RD}), & \text{Rule 1} \\ C_{SR}(1 - P_{SR})P_{SD}, & \text{Rule 2} \\ C_{SR}A_{\mathcal{NF}}(1 - P_{SD}), & \text{Rule 3} \\ 0, & \text{O.W.} \end{cases} \tag{5.10}$$

and for the case $u = v$

$$T_{vv} = 1 - \sum_{v \neq u} T_{uv} = 1 - A_{\mathcal{NE}}C_{RD}(1 - P_{RD}) - A_{\mathcal{NF}}C_{SR}\big(1 - P_{SD}P_{SR}\big), \tag{5.11}$$

where C_{SR} and C_{RD} are probabilities that a certain SR or RD link is selected for the transmission, P_{SR} and P_{RD} are the average frame error rate (FER) over the selected SR or RD channel, P_{SD}

is the average FER over the SD channel. The expressions for P_{SR}, P_{RD} and P_{SD} depend on the coded scheme. We derive these expressions in the following sections. Considering that SR and RD channels are independent and non-identically distributed, C_{SR} and C_{RD} are calculated as

$$C_{SR} = \int_0^\infty \bar{\gamma}_{SR} \left(1 - e^{\frac{-\gamma}{\bar{\gamma}_{SR}}}\right)^{A_{\mathcal{NF}}-1} \left(1 - e^{\frac{-\gamma}{\bar{\gamma}_{RD}}}\right)^{A_{\mathcal{NE}}} e^{\frac{-\gamma^*}{\bar{\gamma}_{SR}}} d\gamma, \tag{5.12}$$

$$C_{RD} = \int_0^\infty \bar{\gamma}_{RD} \left(1 - e^{\frac{-\gamma}{\bar{\gamma}_{SR}}}\right)^{A_{\mathcal{NF}}} \left(1 - e^{\frac{-\gamma}{\bar{\gamma}_{RD}}}\right)^{A_{\mathcal{NE}}-1} e^{\frac{-\gamma^*}{\bar{\gamma}_{RD}}} d\gamma, \tag{5.13}$$

where $\bar{\gamma}_\kappa = \mathbb{E}\{\gamma_\kappa\}$ is the average SNR with $\mathbb{E}\{\bullet\}$ denoting the expectation operator, and $\kappa = \{SR, RD\}$. With some manipulations, we have

$$C_{SR} = \sum_{i=0}^{A_{\mathcal{NF}}-1} \sum_{j=0}^{A_{\mathcal{NE}}} \binom{A_{\mathcal{NF}}-1}{i} \binom{A_{\mathcal{NE}}}{j} \frac{(-1)^{i+j}\bar{\gamma}_{RD}}{(i+1)\bar{\gamma}_{RD} + j\bar{\gamma}_{SR}}, \tag{5.14}$$

$$C_{RD} = \sum_{i=0}^{A_{\mathcal{NF}}} \sum_{j=0}^{A_{\mathcal{NE}}-1} \binom{A_{\mathcal{NF}}}{i} \binom{A_{\mathcal{NE}}-1}{j} \frac{(-1)^{i+j}\bar{\gamma}_{SR}}{i\bar{\gamma}_{RD} + (j+1)\bar{\gamma}_{SR}}. \tag{5.15}$$

Note that if the SR and RD channels are independent and identically distributed (i.i.d.), (5.14) and (5.15) can be simplified to

$$C_{RD} = C_{SR} = \frac{1}{A}, \tag{5.16}$$

where $A = A_{\mathcal{NF}} + A_{\mathcal{NE}}$.

It is to be noted that the transition matrix is stationary, irreducible and aperiodic, therefore a steady state $\boldsymbol{\pi} \in \mathbb{R}^{2(1+Q)^L}$ exists; $\boldsymbol{\pi}\boldsymbol{T} = \boldsymbol{\pi}$. Therefore, it is given as

$$\begin{aligned} \boldsymbol{\pi} &= (\boldsymbol{T} - \boldsymbol{I} + \boldsymbol{B})^{-1}\boldsymbol{b}, \\ B_{ij} &= 1 \quad \forall i, j, \\ \boldsymbol{b} &= [1, 1, ..., 1]^\intercal, \end{aligned} \tag{5.17}$$

where $\boldsymbol{I}$ is identity matrix and $\intercal$ is transpose operator [55]. Each entity of $\boldsymbol{\pi}$, denoted by π_u approximates the probability of being at state Z_u in the long run.

In order to calculate $\boldsymbol{\pi}$ in (5.17), the inverse of a square matrix of size $2(1+Q)^L$ should be calculated. For large values of buffer size and large number of relays, the inverse calculation is complicated. To address this problem, an efficient way to calculate the steady state probabilities is proposed in [55]. For each state u, π_u is given by

$$\pi_u = \left[\sum_{v=1}^{2(1+Q)^L} \frac{\prod_{t \in \Psi(u,\theta_v)} T_{ut}}{\prod_{w \in \Psi(v,\theta_u)} T_{vw}} \right]^{-1}, \tag{5.18}$$

where θ_u is a set of states u for which the steady state probability is the same, and $\Psi(v, \theta_u)$ denotes a set of states that state v has to pass through to reach state $u \in \theta_u$.

According to the definition of η, the throughput at each state Z_u is given as

$$\eta_u = R_0 A_{\mathcal{NF}} C_{SR}(1 - P_{SD}) + \frac{R_0}{2} A_{\mathcal{NE}} C_{RD}(1 - P_{RD}). \tag{5.19}$$

Therefore, the average throughput can then be calculated as

$$\begin{aligned} \bar{\eta} &= \sum_{u=1}^{2(1+Q)^L} \pi_u \eta_u \\ &= \sum_{u=1}^{2(1+Q)^L} \pi_u \Big(R_0 A_{\mathcal{NF}} C_{SR}(1 - P_{SD}) + \frac{R_0}{2} A_{\mathcal{NE}} C_{RD}(1 - P_{RD}) \Big). \end{aligned} \tag{5.20}$$

5.3.2 Performance Analysis of the Convolutionally coded Scheme

In this section, we derive an approximation of the FER for a convolutional code in a Rayleigh block fading channel. The exact evaluation of FER in a block fading channel is complicated. The commonly used bounding methods for FER are the Jenson's inequality and the Chernoff upper bound [111], where these bounds are shown to be loose. In [111], a tight bound on FER is proposed for both uncoded and coded schemes. This bound is tight only in the high-SNR regime. In [112], an approximation of the FER for an uncoded system in a block fading channel using Extreme value theory is proposed. This method proposes a tight approximation of the FER for any value of SNR and packet length. Using the same method, we calculate a bound on the FER of a convolutional

code in a block fading Rayleigh channel. The FER of a convolutional code over a quasi-static fading channel is bounded by [112]

$$P_{SR,RD} \leq 1 - \int \left(1 - P_e(\gamma^*)\right)^K f_{SR,RD}(\gamma^*) d\gamma^*, \tag{5.21}$$

$$P_{SD} \leq 1 - \int \left(1 - P_e(\gamma_{SD})\right)^K f_{SD}(\gamma_{SD}) d\gamma_{SD}, \tag{5.22}$$

where K is the message length. $P_e(\gamma \in \{\gamma^*, \gamma_{SD}\})$ denotes the error event probability which is upper bounded by

$$P_e(\gamma) \leq \sum_{d=d_{\text{free}}}^{\infty} a(d) P_2(d|\gamma), \tag{5.23}$$

where $a(d)$ represents the number of error events with distance d, d_{free} is the minimum free distance, and $P_2(d|h)$ is the conditional pairwise error probability given by

$$P_2(d|\gamma) = Q\left(\sqrt{2R_c\gamma d}\right). \tag{5.24}$$

For large values of SNR, $P_e(\gamma)$ in (5.23) can be approximated by its dominant term, when $d = d_{\text{free}}$. Using the Extreme value theory as in [112], the P_{SD} can further be expressed as

$$P_{SD} \leq 1 - e^{-\frac{\alpha}{\bar{\gamma}_{SD}}} \Gamma\left(1 + \frac{\beta}{\bar{\gamma}_{SD}}\right), \tag{5.25}$$

where $\Gamma(\bullet)$ is the standard Gamma function, α and β are given by

$$\begin{aligned} \alpha &= \frac{1}{R_c d_{\text{free}}} \left(\text{erf}^{-1}\left(1 - \frac{2}{K a(d_{\text{free}})}\right)\right)^2, \\ \beta &= \frac{1}{R_c d_{\text{free}}} \left(\text{erf}^{-1}\left(1 - \frac{2}{K a(d_{\text{free}}) e}\right)\right)^2 - \alpha, \end{aligned} \tag{5.26}$$

where $\text{erf}(\bullet)$ denotes the error function, and e is the Euler's number. The expression for $P_{SR,RD}$ is given in (5.27).

$$
\begin{aligned}
P_{SR,RD} \leq \bar{\gamma}_{RD} A_{\mathcal{NF}} & \sum_{i=0}^{A_{\mathcal{NF}}-1} \sum_{j=0}^{A_{\mathcal{NE}}} \binom{A_{\mathcal{NF}}-1}{i} \binom{A_{\mathcal{NE}}}{j} \frac{(-1)^{i+j}}{(i+1)\bar{\gamma}_{RD} + j\bar{\gamma}_{SR}} \\
& \times \left[1 - e^{\frac{-\alpha}{\bar{\gamma}_{RD}\bar{\gamma}_{SR}}((i+1)\bar{\gamma}_{RD} + j\bar{\gamma}_{SR})} \Gamma\left(1 + \beta \frac{(i+1)\bar{\gamma}_{RD} + j\bar{\gamma}_{SR}}{\bar{\gamma}_{RD}\bar{\gamma}_{SR}}\right)\right] \\
& + \bar{\gamma}_{SR} A_{\mathcal{NE}} \sum_{i=0}^{A_{\mathcal{NF}}} \sum_{j=0}^{A_{\mathcal{NE}}-1} \binom{A_{\mathcal{NF}}}{i} \binom{A_{\mathcal{NE}}-1}{j} \frac{(-1)^{i+j}}{i\bar{\gamma}_{RD} + (j+1)\bar{\gamma}_{SR}} \\
& \times \left[1 - e^{\frac{-\alpha}{\bar{\gamma}_{RD}\bar{\gamma}_{SR}}(i\bar{\gamma}_{RD} + (j+1)\bar{\gamma}_{SR})} \Gamma\left(1 + \beta \frac{i\bar{\gamma}_{RD} + (j+1)\bar{\gamma}_{SR}}{\bar{\gamma}_{RD}\bar{\gamma}_{SR}}\right)\right].
\end{aligned}
\tag{5.27}
$$

By substituting (5.25) and (5.27) in (5.20), the average throughput of the system is calculated.

If the source-relay and relay-destination channels are i.i.d., $\bar{\gamma}_{SR} = \bar{\gamma}_{RD} = \bar{\gamma}$, (5.27) could be further simplified as

$$
P_{SR,RD} \leq \sum_{i=0}^{A-1} \binom{A}{i+1} (-1)^i \left[1 - e^{-\frac{\alpha(i+1)}{\bar{\gamma}}} \Gamma\left(1 + \frac{\beta(i+1)}{\bar{\gamma}}\right)\right]. \tag{5.28}
$$

Using (5.10) and (5.18) and after some manipulations, the steady state probability of state i is given by

$$
\pi_i = \left[\frac{1 - P_{SR,RD}}{A(i)} \sum_{j=1}^{2(1+Q)^L} \frac{A(j)}{1 - P_{SR,RD}} P_{SD}^{\delta_{ij}}\right]^{-1}, \tag{5.29}
$$

where $\delta_{ij} = \delta_j - \delta_i$, and δ_i denotes the number of packets stored in all buffers in state i.

Using (5.20),(5.28), and (5.29), the average throughput is given by

$$
\bar{\eta} = \sum_{i=1}^{2(1+Q)^L} \frac{(1 - P_{SD})\, A_{\mathcal{NF}(i)} + 0.5(1 - P_{SR,RD}) A_{\mathcal{NE}(i)}}{1 - P_{SR,RD}} \left[\sum_{j=1}^{2(1+Q)^L} \frac{A(j)}{1 - P_{SR,RD}} P_{SD}^{\delta_{ij}}\right]^{-1} R_0. \tag{5.30}
$$

Diversity Analysis

Having obtained an analytical expression of the $\bar{\eta}$, one can evaluate the asymptotic behavior of the $\bar{\eta}$, as $\bar{\gamma}_{SR} = \bar{\gamma}_{SR} = \bar{\gamma}_{SD} = \bar{\gamma} \to \infty$, and assuming that all buffers are never full or empty, therefore, all the relays are available for transmission and reception. This assumption is made in the

literature to simplify the mathematical framework [54]. For all states $A_{\mathcal{NF}}(u) = A_{\mathcal{NE}}(u) = L$ and $A(u) = 2L$. Under these assumptions, the steady state distribution is uniform and the probabilities for all $u \in \{1, ..., 2(1+Q)^L\}$ are given by [55]

$$\pi_u = \frac{1}{2(1+Q)^L}, \tag{5.31}$$

the $\bar{\eta}$ is written as

$$\bar{\eta} = \frac{R_0}{2}(1 - \mathcal{P}_{SD}) + \frac{R_0}{4}(1 - \mathcal{P}_{RD}), \tag{5.32}$$

For large values of $\bar{\gamma}$, the expression of P_{SD} in (5.25) and $P_{SR,RD}$ in (5.28) can be approximated as

$$P_{SD} \approx 1 - e^{-\frac{\alpha}{\bar{\gamma}}}, \tag{5.33}$$

$$P_{SR,RD} \approx (1 - e^{-\frac{\alpha}{\bar{\gamma}}2L})(1 - e^{-\frac{\alpha}{\bar{\gamma}}})^{2L}. \tag{5.34}$$

Using $1 - e^{-x} \approx x$, when $x \to 0$, (5.34) becomes $P_{SR,RD} \approx (\frac{\alpha}{\bar{\gamma}})^{2L+1}$. Therefore, the diversity order of $\mathcal{D} \approx 2L + 1$ is achieved. This maximum achievable diversity given is attained when all the SR and RD links are available and can participate in the selection process. The diversity gain offered by these links is twice the number of relays, in addition to the source-destination link.

Buffer Size Analysis

Diversity analysis showed that buffering improves the diversity order. The maximum diversity order is achieved when all the SR and RD links are available to participate in the relay selection scheme. In other words, none of the buffers are full or empty. We denote by π_f the probability that all the buffers are full. This probability is given by

$$\pi_f = \left[\frac{1 - P_{SR,RD}}{L} \sum_{j=1}^{2(1+Q)^L} \frac{A(j)}{1 - P_{SR,RD}} P_{SD}^{\delta f}\right]^{-1}, \tag{5.35}$$

$$\delta_f = \delta(j) - QL. \tag{5.36}$$

For large values of $\bar{\gamma}$, π_f can be approximated by

$$\pi_f \approx LP_{SD}^{QL}\left[\sum_{j=1}^{2(1+Q)^L} A(j)P_{SD}^{\delta j}\right]^{-1}. \tag{5.37}$$

As shown in (5.37), in a system with L relays, π_f is a function of P_{SD} and Q. It is obvious in (5.37) that π_f increases as the SNR of the SD channels decreases. In a system with low SNR SD link, the probability of having full buffers is higher than a system with high SNR SD link. That is, having full buffers decreases the number of available links in the selection process. Therefore, the offered diversity gain degrades. On the other hand, an increase in buffer size can compensate for this degradation, where the performance of the system improves as buffer size increases, at the expense of an increased transmission delay.

5.3.3 Performance Analysis of the Turbo coded Scheme

In [113], an analytical approximation for the FER of the Turbo code over the quasi-static Rayleigh fading channel is obtained, and is given by

$$P_f = \mathbb{P}(\gamma \leq \gamma_{\text{th}}), \tag{5.38}$$

where γ is the instantaneous channel SNR, and γ_{th} is the minimum SNR required for iterative decoder convergence in AWGN channel [113]. Given (5.38), for each state, the FER over the selected SR or RD channel, and over the SD channel are given by

$$\begin{aligned} P_{SR} &= \mathbb{P}(\gamma_{SR} \leq \gamma_{\text{th}}) \\ &= \int_0^{\gamma_{\text{th}}} f_{SR}(\gamma_{SR})d\gamma_{SR}, \end{aligned} \tag{5.39}$$

$$\begin{aligned} P_{RD} &= \mathbb{P}(\gamma_{RD} + \gamma_{SD} \leq \gamma_{\text{th}}) \\ &= \int_0^{\gamma_{\text{th}}}\int_0^{\gamma_{\text{th}}} f_{RD}(\gamma_{RD})f_{SD}(\gamma_{SD})d\gamma_{RD}d\gamma_{SD}, \end{aligned} \tag{5.40}$$

$$P_{SD} = \int_0^{\gamma_{\text{th}}} f_{SD}(\gamma_{SD})d\gamma_{SD}, \tag{5.41}$$

respectively. Hence, the average $P_{SR,RD}$ and P_{SD} can further be obtained in closed-form as

$$P_{SR} = \left(1 - e^{-\frac{\gamma_{\text{th}}}{\bar{\gamma}_{SR}}}\right)^{A_{\mathcal{NF}}} \left(1 - e^{-\frac{\gamma_{\text{th}}}{\bar{\gamma}_{RD}}}\right)^{A_{\mathcal{NE}}}, \tag{5.42}$$

$$P_{RD} = \sum_{i=0}^{A_{\mathcal{NF}}} \sum_{j=0}^{A_{\mathcal{NE}}} \binom{A_{\mathcal{NF}}}{i} \binom{A_{\mathcal{NE}}}{j} (-1)^{i+j} \bar{\gamma}_{SD}^{-1} \left(\frac{i}{\bar{\gamma}_{SR}} + \frac{j}{\bar{\gamma}_{RD}} - \frac{1}{\bar{\gamma}_{SD}}\right)^{-1} \left(e^{\frac{-\gamma_{th}}{\bar{\gamma}_{SD}}} - e^{\frac{-\gamma_{th}i}{\bar{\gamma}_{SR}} - \frac{\gamma_{th}j}{\bar{\gamma}_{RD}}}\right), \tag{5.43}$$

$$P_{SD} = 1 - e^{-\frac{\gamma_{\text{th}}}{\bar{\gamma}_{SD}}}. \tag{5.44}$$

The average throughput of the system is achieved by putting (5.42)-(5.44)in (5.20)and (5.18).

Diversity Analysis

Similar to the convolutionally-coded scheme, we evaluate the asymptotic behavior of $\bar{\eta}$ of the Turbo-coded scheme, under the same assumptions. The steady state probabilities are given as in (5.31), and the $\bar{\eta}$ is written as

$$\bar{\eta} = \frac{R_0}{2}(1 - \mathcal{P}_{SD}) + \frac{R_0}{4}(1 - \mathcal{P}_{RD}), \tag{5.45}$$

where

$$\mathcal{P}_{RD} \approx \frac{1}{2L+1} \left(\frac{\gamma_{\text{th}}}{\bar{\gamma}}\right)^{2L+1}, \tag{5.46}$$

$$\mathcal{P}_{SD} \approx \frac{\gamma_{\text{th}}}{\bar{\gamma}}. \tag{5.47}$$

Approximations (5.46) and (5.47) emerge from: $1 - e^{-x} \approx x$, when $x \to 0$. By substituting (5.46) and (5.47) into (5.20), the asymptotic throughput is approximated by

$$\bar{\eta} \approx \frac{R_0}{2}\left(1 - \frac{\gamma_{\text{th}}}{\bar{\gamma}}\right) + \frac{R_0}{4}\left(1 - \frac{1}{2L+1}\left(\frac{\gamma_{\text{th}}}{\bar{\gamma}}\right)^{2L+1}\right). \tag{5.48}$$

According to (5.48), the $\bar{\eta}$ is approximated by the average of two terms. The first term representing the direct SD transmission, and the second term representing the relay transmission mode. It is important to note that (5.48) shows that in relay transmission mode, the diversity order of $2L+1$ is achieved. By equipping relays with buffers, $2L$ links participate in the selection process. Therefore, the diversity order is twice the number of relays in addition to the SD link.

5.3.4 Performance Analysis of the DTC Scheme

In the performance analysis of the DTC scheme, the Markov chain is constructed by following the same rules as the Turbo-coded scheme, however, the transition probabilities are different. In this case, the transition probabilities from state Z_v to state Z_u, for $u \neq v$, are given by

$$T_{uv} = \begin{cases} C_{RD}(1 - P_{DTC}), & \text{Rule 1} \\ C_{SR}(1 - P_{conv})P_{SD}, & \text{Rule 2} \\ C_{SR}A_{\mathcal{NF}}(1 - P_{SD}), & \text{Rule 3} \\ 0, & \text{O.W.} \end{cases} \tag{5.49}$$

and for $u = v$

$$T_{vv} = 1 - A_{\mathcal{NE}}C_{RD}(1 - P_{DTC}) - A_{\mathcal{NF}}C_{SR}(1 - P_{conv}P_{SD}), \tag{5.50}$$

where C_{RD} and C_{SR} are defined according to (5.14) and (5.15), respectively. P_{conv} is the average FER of convolutional code over the selected SR or RD channel, P_{SD} is the average FER of convolutional code over the SD channel, and P_{DTC} is the average FER of the DTC at node D. By calculating the transition matrix T, following the transition rules and using (5.18), the steady state $\boldsymbol{\pi}$ is calculated. The probability of error for each state Z_u is given as

$$\eta_u = R_0 A_{\mathcal{NF}}C_{SR}(1 - P_{SD}) + \frac{R_0}{2}A_{\mathcal{NE}}C_{RD}(1 - P_{DTC}). \tag{5.51}$$

Given (5.18) and (5.51), the $\bar{\eta}$ for DTC scheme can be calculated as

$$\begin{aligned}\bar{\eta} &= \sum_{u=1}^{2(1+Q)^L} \pi_u \eta_u \\ &= \sum_{u=1}^{2(1+Q)^L} \pi_u \Big(R_0 A_{\mathcal{NF}} C_{SR}(1-P_{SD}) + \frac{R_0}{2} A_{\mathcal{NE}} C_{RD}(1-P_{DTC}) \Big).\end{aligned} \tag{5.52}$$

The P_{conv} is calculated similar to (5.27). In the following, we derive the bounds on P_{DTC}.

Bound on P_{DTC} We derive the upper bound on FER of the DTC scheme using the union bound given by

$$P_{DTC} \leq \sum_{d=d_{min}} \lambda_d P_2(d), \tag{5.53}$$

where λ_d represents the number of codewords with Hamming weight d, d_{min} represents the minimum free distance of the Turbo code, and $P_2(d)$ denotes the pairwise error probability (PEP) between the all-zero sequence and a sequence with weight d.

On the quasi-static channel with known CSI, the conditional PEP at node D, can be written as [114]

$$P_2(d|\gamma_{SD}, \gamma^*) = Q\Bigg(\sqrt{2R_C\big(\gamma_{SD}(d_0+d_1) + \gamma^*(d_0+d_2)\big)} \Bigg), \tag{5.54}$$

where d_0 denotes the Hamming weight of the systematic bits, d_1 and d_2 denote the Hamming weight of the parity bits sent through the SD and RD channels, respectively, $d = d_0 + d_1 + d_2$, and $Q(\bullet)$ is the tail integral of a standard Gaussian distribution defined as $Q(x) = \int_x^\infty \frac{1}{\sqrt{2\pi}} e^{-z^2/2} dz$. To simplify (5.54), we consider the Q-function bound,

$$Q\big(\sqrt{x+y}\big) \leq \frac{1}{2} Q\big(\sqrt{x}\big) e^{-y/2}, \tag{5.55}$$

and use the Q-function representation from [115],

$$Q(x) = \frac{1}{\pi} \int_0^{\pi/2} e^{-\frac{x^2}{2\sin^2\phi}} d\phi. \tag{5.56}$$

By substituting (5.55) and (5.56) into (5.54), we have

$$P_2(d|\gamma_{SD}, \gamma^*) \leq \frac{1}{2\pi} \int_0^{\pi/2} e^{\frac{-R_C\gamma_{SD}(d_0+d_1)}{\sin^2\phi}} e^{-R_T\gamma^*(d_0+d_2)} d\phi. \tag{5.57}$$

The unconditional PEP is obtained by averaging (5.57) over the fading distributions, and it is given by

$$P_2(d) = \int_0^{\infty} \int_0^{\infty} P_2(d|\gamma_{SD}, \gamma^*) f_{SD}(\gamma_{SD}) f_{SR,RD}(\gamma^*) d\gamma_{SD} d\gamma^*. \tag{5.58}$$

By substituting (5.3), (5.4), and (5.57) into (5.58), and evaluating the integrals, the closed-form expression of the upper bound for $P_2(d)$ is given by (5.59).

$$\begin{aligned} P_2(d) \leq \frac{1}{4} &\left(1 - \sqrt{\frac{R_C(d_0+d_1)\bar{\gamma}_{SD}}{1+R_C(d_0+d_1)\bar{\gamma}_{SD}}}\right) \\ &\times \left[\sum_{i=0}^{A_{\mathcal{NF}}-1} \sum_{j=0}^{A_{\mathcal{NE}}} \binom{A_{\mathcal{NF}}-1}{i} \binom{A_{\mathcal{NE}}}{j} \frac{(-1)^{i+j} A_{\mathcal{NF}} \bar{\gamma}_{RD}}{(i+1)\bar{\gamma}_{RD} + j\bar{\gamma}_{SR} + R_C(d_0+d_2)} \right. \\ &\left. + \sum_{i=0}^{A_{\mathcal{NF}}} \sum_{j=0}^{A_{\mathcal{NE}}-1} \binom{A_{\mathcal{NF}}}{i} \binom{A_{\mathcal{NE}}-1}{j} \frac{(-1)^{i+j} A_{\mathcal{NE}} \bar{\gamma}_{SR}}{i\bar{\gamma}_{SR} + (j+1)\bar{\gamma}_{RD} + R_C(d_0+d_2)} \right] \end{aligned} \tag{5.59}$$

The upper bound in (5.53) is tight for the AWGN channels, however, for a quasi-static Rayleigh channel, it provides a loose bound. To get a tighter bound, one can use the limit-before-averaging method proposed in [116]. The P_{DTC} using limit-before-averaging method is written as

$$P_{DTC} \leq \int_0^{\infty} \int_0^{\infty} \min \left\{ 1, \sum_{d=d_{min}} \lambda_d P_2(d|\gamma_{SD}, \gamma^*) \right\} f_{SD}(\gamma_{SD}) f_{SR,RD}(\gamma^*) d\gamma_{SD} d\gamma^*. \tag{5.60}$$

This integration is calculated numerically as no closed form expression can be obtained. It should be noted that in (5.60), the order of integration and summation cannot be interchanged, due to the

minimization. Nevertheless, the analytical expression of the average PEP given in (5.59) is helpful, since it presents insight into the asymptotic behavior of the performance of the coding scheme.

Diversity Analysis

Similar to the Turbo-coded scheme, we evaluate the asymptotic behavior of $\bar{\eta}$ of the DTC scheme, under the same assumptions. The steady state probabilities are given as in (5.31), and the $\bar{\eta}$ is written as

$$\bar{\eta} = \frac{R_0}{2}(1 - \mathcal{P}_{SD}) + \frac{R_0}{4}(1 - \mathcal{P}_{DTC}), \tag{5.61}$$

where

$$\mathcal{P}_{SD} \approx \frac{\alpha}{\bar{\gamma}}, \tag{5.62}$$

$$\mathcal{P}_{DTC} \leq \sum_{d=d_{min}} \lambda_d \mathcal{P}_2(d), \tag{5.63}$$

$$\mathcal{P}_2(d) \approx \frac{2L\Gamma(2L)}{(d_0 + d_1)(d_0 + d_2)^{2L} \left(R_c\bar{\gamma}\right)^{2L+1}}. \tag{5.64}$$

Given the expression in (5.64), the diversity order for the relay transmission mode is $2L + 1$.

5.4 Simulations and Results

In this section, we present the simulation results in terms of the average throughput for all three coding schemes, under various system parameters. The model used in the simulations complies with the system model presented in Section 5.2. In the convolutionally-coded scheme, we considered an 8-state $(13, 15)$ convolutional encoder with rate of $R_c = 1/2$, at source and relay nodes. In the Turbo-coded scheme, we considered a 4-state $(1, 5/7)_8$ Turbo code with overall rate $R_T = 1/3$, whereas in the DTC scheme, we consider a 4-state $(1, 5/7)_8$ convolutional encoder with rate $R_c = 1/2$, at source and relay nodes. For all three schemes, we consider message block length $K = 1000$. For the Turbo-coded and DTC scheme the interleaver size is 1000. It is assumed that the source and relay nodes transmit with normalized power $P = 1$. Channels are modeled as quasi-static Rayleigh

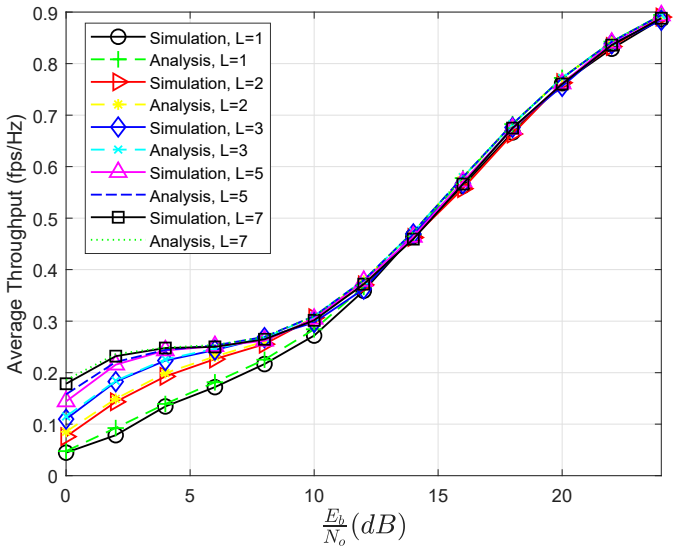

Figure 5.3: The average throughput of the convolutionally coded scheme versus SNR, $L = \{1, 2, 3, 5, 7\}$, $Q = 2$

fading with $\mathbb{E}\{|h_{SR_i}|^2\} = \mathbb{E}\{|h_{R_iD}|^2\} = 1, \mathbb{E}\{|h_{SD}|^2\} = 0.1$. The value of γ_{thr} for $(1, 5/7)_8$ Turbo code is 0.134 dB, according to [113].

5.4.1 Simulation and Results for the convolutionally coded scheme

In Fig. 5.3, for the convolutionally coded scheme, the analytical results of the average throughput are compared with simulation results. The number of relays are $L = \{1, 2, 3, 5, 7\}$ and buffer size is $Q = 2$ for all relays. It is clear from these results that our analytical results match perfectly with the simulated ones. As it can be observed from Fig. 5.3, increasing the number of relays improves the average throughput, since more links are available for selection. It can also be seen that in high SNRs, the average throughput converges to one, due to the successful transmission through the SD link.

Fig. 5.4 plots the average throughput versus SNR for different buffer sizes. Systems with two relays and buffer sizes of $Q = \{1, 2, 4, 12\}$ are considered. As we can see in Fig. 5.4, increasing the buffer size improves the average throughput. The reason is that increasing buffer size decreases the probability of buffers being full. Therefore, more links are available for selection. As the buffer size increases, the average throughput approaches the case where $Q \to \infty$. Moreover, we can see

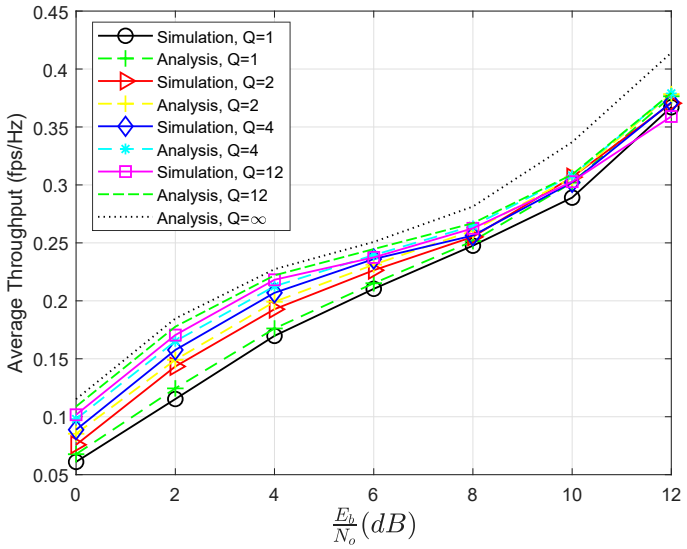

Figure 5.4: The average of the convolutionally coded scheme throughput versus SNR, $L = 2$, $Q = \{1, 2, 4, 12, \infty\}$

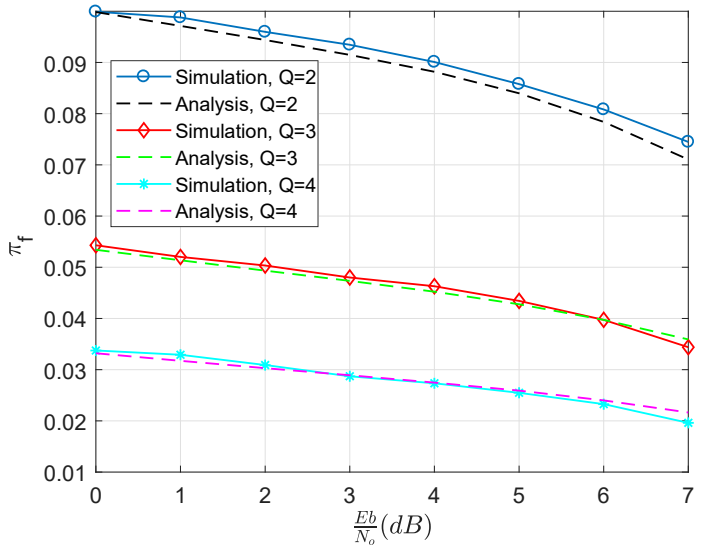

Figure 5.5: The probability of buffers being full, $L = 2$, $Q = \{2, 3, 4\}$

that the analytical results closely follows the simulated ones.

In Fig. 5.5, we show the probability of buffers being full versus the SD channel SNR, in a system with two relays and different buffer sizes. We compare the simulation results to the analytical ones given in (5.37). In addition to the accurate analytical results, Fig. 5.5 shows that in a system with

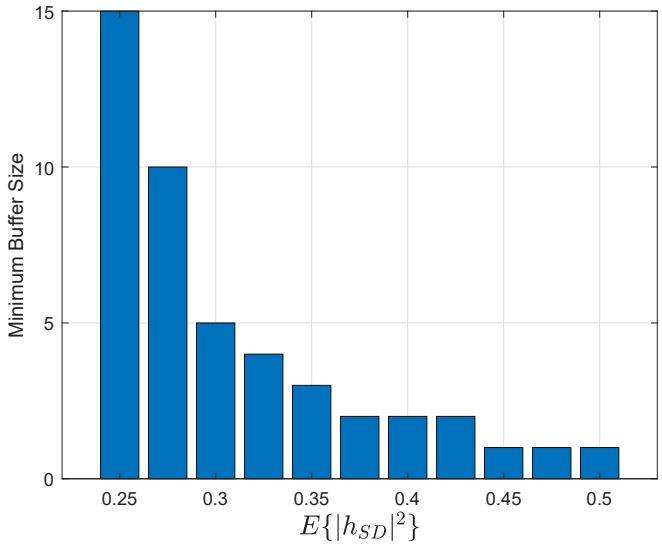

Figure 5.6: Minimum required buffer size to achieve $\bar{\eta} \geq 0.25$, $L = 2$

low SNR SD channel the value of π_f is larger compared to high SNR channels. One can note that in a low SNR channel, the probability that the transmission through the direct link fails is higher. Hence, the transmitted packets are stored in the buffers more often. As a final remark, one can see that increasing buffer size decreases the probability of buffers being full, π_f. As a result, the total number of the channels available in the selection process increases, therefore higher diversity gain is achieved as shown in Fig. 5.4.

In Fig. 5.6 we show the minimum required buffer size versus $\mathbb{E}\{|h_{SD}|^2\}$, to achieve a fixed average throughput $\bar{\eta} \geq 0.25$. In these results, we consider a system with two relays, and the channels are modeled as $\frac{Eb}{N_o} = 4dB$, and $\mathbb{E}\{|h_{SR}|^2\} = \mathbb{E}\{|h_{SR}|^2\} = 1$. Fig. 5.6 shows the minimum required buffer size for different values of $\mathbb{E}\{|h_{SD}|^2\}$, in order to maintain the system performance at $\bar{\eta} \geq 0.25$. We can see that smaller buffer size is required when the SD channel has higher SNR. This becomes an important issue as determining the minimum required buffer size is important since it minimizes the transmission delay.

5.4.2 Simulation and Results for the Turbo coded scheme

In Fig. 5.7, the performance of the Turbo-coded system is shown in terms of the average throughput versus the average SNR for different number of relays $L = \{1, 2, 3, 5\}$, and buffer size

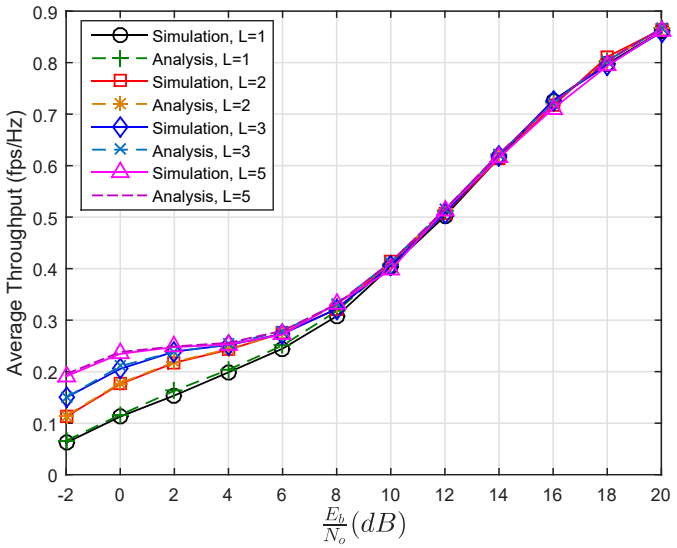

Figure 5.7: Average throughput for Turbo-coded scheme for a system with $L = 1, 2, 3, 5$, and $Q = 2$

$Q = 2$. The analytical results obtained in section 5.3.3 are compared with the simulation results. It is evident from these results that the simulated throughput corroborates our analytical framework as an approximation on the throughput is seen to be tight over the entire SNR regime. We also note that in low SNR regime, as the number of relays increases, the throughput performance improves, as expected. However, as illustrated in Fig. 5.7, in high SNR regime the curves corresponding to various relays converge. The reason is that in high SNR regime, the error probabilities in S-R and R-D links are very low. Thus, the throughput in (5.19) can be approximated as a function of P_{SD}, and independent of the number of relays. Moreover, due to the dominance of the direct link transmission in high SNR regime, full throughput is achieved.

In Fig. 5.8, we investigate the impact of relay buffer size on the average throughput of the underlying system. Here, we consider a system with two relay nodes, i.e. $L = 2$, and buffer sizes $Q = 1, 2, 6, 12$ and $Q = \infty$. As can be observed in Fig. 5.8, in low SNR regime, the average throughput improves as the buffer size increases. The reason is that buffers increase the number of available links for selection. Each relay can provide two available links when the related buffer is neither full nor empty. The probability of buffers being full is diminished by increasing the buffer size. Therefore, performance improvement is achieved. However, for sufficiently large buffer sizes,

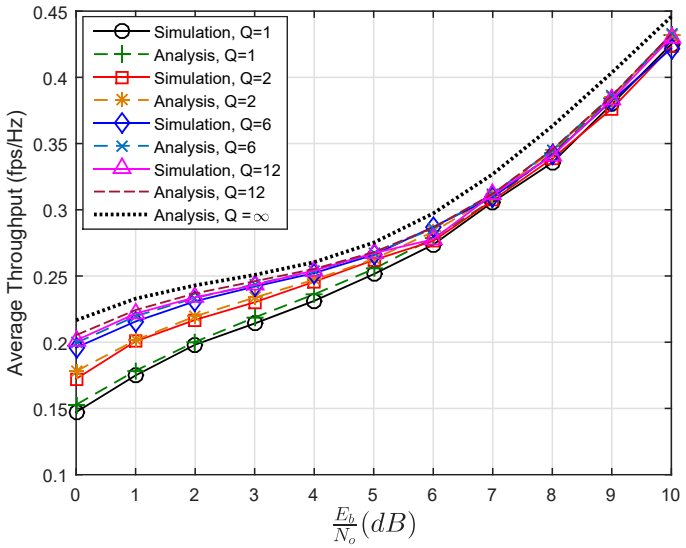

Figure 5.8: Average throughput for Turbo-coded scheme for a system with $L = 2$, and $Q = 1, 2, 6, 12, \infty$

when the probability of buffers being full is very small, increasing the buffer size further, would result in insignificant performance improvement. As depicted in Fig. 5.8, the achieved gain when increasing buffer size from $Q = 6$ to $Q = 12$ is insignificant. Fig. 5.8 also shows that for different buffer sizes, the analytical results closely follow the simulated ones.

In Fig. 5.9, we plot the average delay of the Turbo coded scheme. The average delay is measured in terms of the number of time slots required for each packet to reach the destination node. It is shown in Fig. 5.9 that the average delay increases with an increase in the buffer size and the number of relays. It can also be observed that as SNR increases, the average delay decreases. The reason is that in high SNR regime, the FER decreases. Thus, fewer time slots are required to successfully deliver a frame to the destination node. As it was shown in Fig. 5.8, in a system with $\mathbb{E}\{|h_{SR_i}|^2\} = \mathbb{E}\{|h_{R_iD}|^2\} = 1, \mathbb{E}\{|h_{SD}|^2\} = 0.1$ and $L = 2$, increasing buffer size more than $Q = 6$ results in insignificant improvement in average throughput. In Fig. 5.9, it can be seen that average delay continues to increase for buffer sizes larger than $Q = 6$. Therefore, in system design it is better to maintain the buffer size to a minimum when the throughput requirement is satisfied.

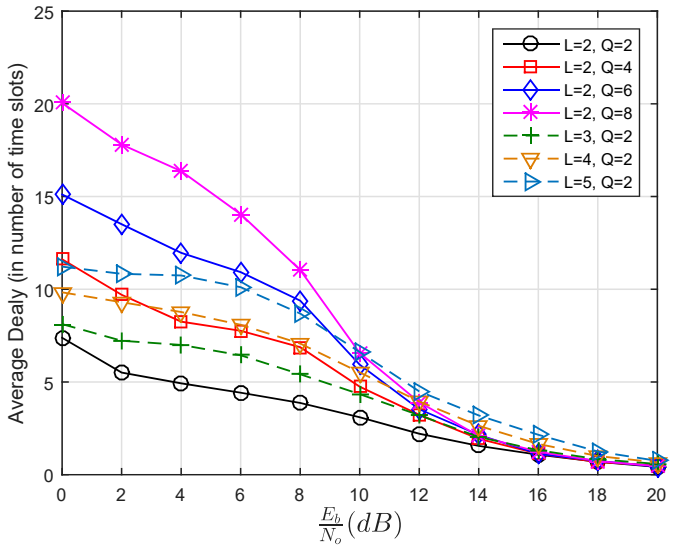

Figure 5.9: Average delay of Turbo coded scheme for a system with $L = 2, 3, 4, 5$, and $Q = 2, 4, 6, 8$

5.4.3 Simulation and Results for the DTC scheme

In Fig. 5.10, we compare the average throughput of the DTC scheme with a system with convolutional encoders at the source and relay nodes, and no interleaver. In the convolutional scheme, the received signals at node D are combined by a MRC and sent to a Viterbi decoder. We consider a system with $L = \{1, 2, 4\}$, and buffer size $Q = 2$. We can see that significant performance improvement is achieved at the expense of higher complexity at the destination node decoder. The importance of this comparison is that both the DTC and convolutionally coded schemes use the same code rate $1/2$, therefore, the extra coding gain achieved by the DTC scheme is the result of the interleaver at R_i^* and an iterative decoder at node D.

In Fig. 5.11 and 5.12, we present the average throughput of the DTC in buffer-aided relay system versus the average SNR for various number of relays and different buffer sizes. We show a comparison between the simulation and analytical results. It should be noted that the analytical throughput is calculated from the general formula given in (5.20), and the analytical expression of the P_{DTC} is calculated by the limit-before-averaging method, given in (5.60). It can be observed in Fig. 5.11 and 5.12, that analytical results follow the simulated ones, after the divergence at low SNR values. This divergence is due to the false convergence behavior region of the union upper

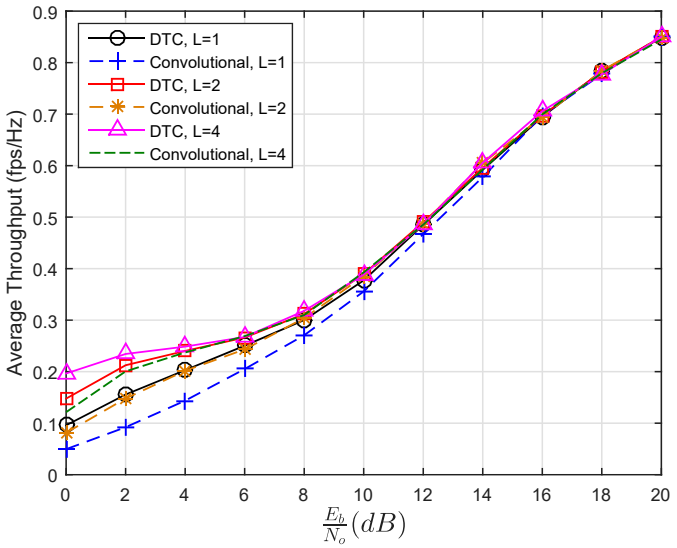

Figure 5.10: Average throughput for the DTC scheme compared to the convolutionally coded scheme, for a system with $L = 1 - 3$, and $Q = 2$

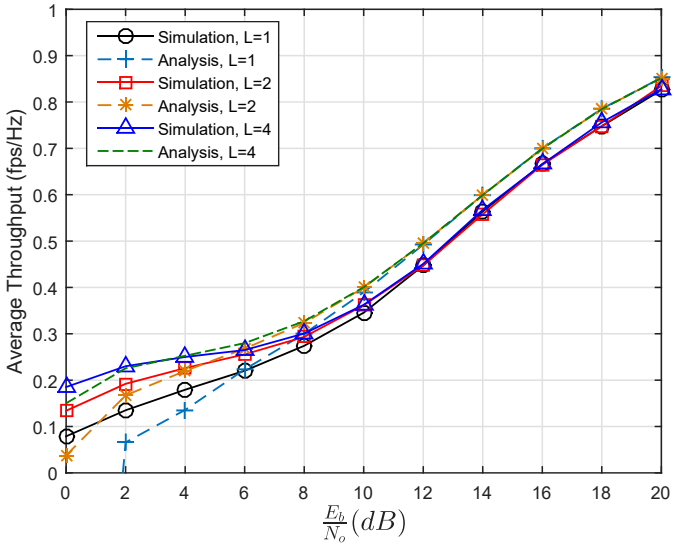

Figure 5.11: Average throughput of DTC scheme for a system with $L = 1, 2, 4$, and $Q = 2$

bound on the Turbo code. At high SNR values, the analytical results follow the simulation ones. It can be seen that the analytical framework describes the behavior of the DTC scheme for different number of relays and buffers. As seen in these figures, the performance improves when the number of relays or buffer size increases.

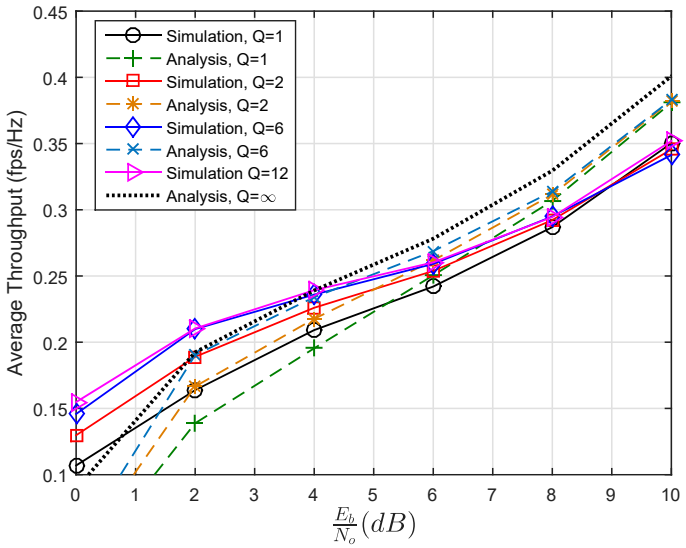

Figure 5.12: Average throughput of DTC scheme for a system with $L = 2$, and $Q = 1, 2, 6, 12, \infty$

In Fig. 5.13, the average delay of the DTC scheme is compared with the convolutionally coded scheme vs channel SNR. As it can be seen, in all the cases the convolutionally coded scheme has higher delay than the DTC scheme. The average delay of the two schemes converge in high SNRs. This is because in high SNR regime, the frames are delivered to the destination node successfully through the SD channel.

In Fig. 5.14, we compare the average delay of the DTC scheme and the convolutionally coded scheme for different buffer sizes. The channel SNR is set to $2dB$. It can be observed that the average delay increases linearly with an increase in buffer size. Also, it is shown that for the convolutionally coded scheme, the average delay increases with a higher rate compared to the DTC scheme.

5.5 Conclusion

In this chapter, we studied a buffer-aided relay selection scheme, in a multi-relay network with coded transmissions. We considered three coding schemes: convolutionally coded, Turbo-coded and DTC. For each scheme, we analyzed the performance of the system in terms of the average throughput. By providing the Monte-Carlo simulation results, we showed that the analytical results closely follow the simulation ones, for all the values of SNR, and various number of relays and

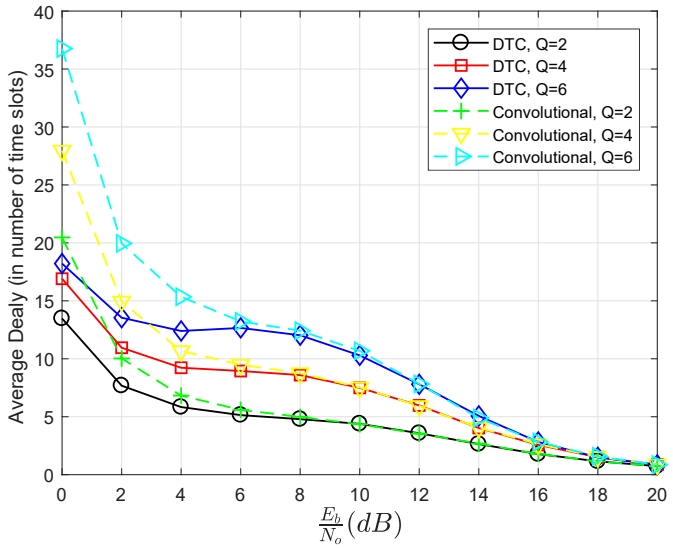

Figure 5.13: Average delay of the DTC scheme compared to the convolutionally coded scheme, for a system with $L = 2$, and $Q = 2, 4, 6$

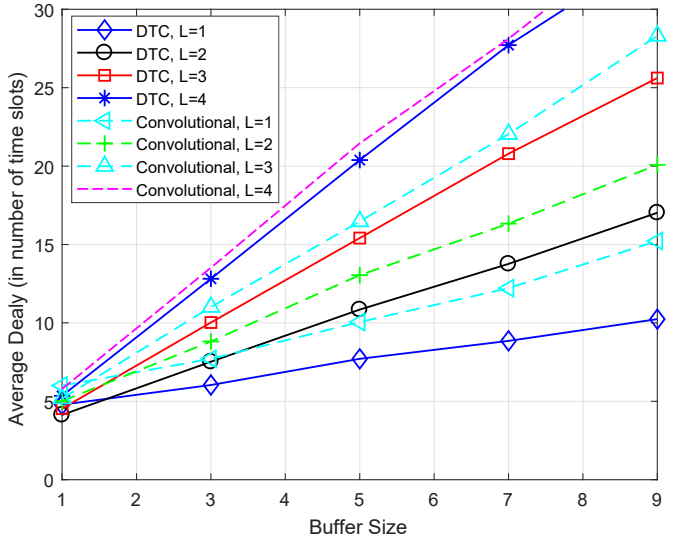

Figure 5.14: Average delay of the DTC scheme compared to the convolutionally coded scheme, for a system with $L = 1, 2, 3, 4$

buffer sizes. In the DTC scheme we observed a gap between the analytical results and the simulation ones, due to the false convergence behavior region of the union upper bound. However, it can be observed that the analytical results follow the similar trend as the simulation ones. By further investigating the analytical results in high-SNR regime and infinite buffer size, we obtained the

achievable diversity order of the system. We showed that the achievable diversity order is twice the number of relays, plus the additional direct link. For finite buffer sizes, we analyzed the probability of buffers being full. We showed the impact of buffer size and different system parameters on this probability. We also investigated the minimum required buffer size for achieving a certain average throughput. Since one of the parameters of concern in buffer-aided relaying network is the inevitable transmission delay, we demonstrated the average delay in different schemes and for different values of SNR and various number of relays and buffer sized. Finally, we provided a comparison between the DTC and convolutionally coded schemes in buffer-aided relaying network, in terms of the average throughput and average delay. We showed that in all cases the DTC scheme outperforms the convolutionally coded one.

Chapter 6

Conclusions and Future Work

6.1 Conclusions

The application of cooperative relaying in LTE-A standard is suggested by 3GPP in order to improve the performance of the cellular networks. Equipping a network with relays alleviates the effect of multipath fading by establishing independent channels. Moreover, the communication distance is shortened by adding relay nodes. Therefore, the effect of path loss becomes less destructive. As a result, the network coverage is expanded and the number of under coverage users are augmented. In this thesis, we have tackled the problem of resource allocation in relay networks. We proposed efficient algorithms for resource allocation to improve the performance of the cooperative network and supported them with the analytical and simulation frameworks. Firstly, we proposed an optimal algorithm for joint subcarrier-relay assignment and power allocation. Secondly, we proposed a cross-layer design for throughput maximization. Lastly, we provided analysis framework for coded buffer-aided relay selection system. In what follows, we summarize the contributions of this thesis.

In Chapter 3, we considered a cooperative network combined with OFDM. We investigated the problem of joint power allocation and subcarrier-relay assignment. The objective of this allocation problem is to find the best subcarrier-relay assignment and power allocation, that maximizes the minimum received SNR, representing the cell-edge users with weakest channels. This optimization problem is non-convex, and the optimal solution can be obtained through an exhaustive search. However, the time complexity of the exhaustive search increases exponentially with an increase in

the number of subcarriers and relays, hence, making it impractical for cellular network applications. We provided a simple and practical algorithm with polynomial time complexity that finds the optimal solution. We proved the optimality of the proposed algorithm and assessed its performance for different system parameters and provided comparisons with two other algorithms. The simulation results showed the superiority of our algorithm.

While in Chapter 3 we focused on maximizing the physical layer characteristics, in Chapter 4 we considered both the physical and link-layer characteristics. We considered a relaying network where channels are equally spatially correlated. We proposed a cross-layer algorithm, where by considering the physical and link layer characteristics, one or multiple relays are selected in order to maximize the link layer throughput. We provided simulation results to compare the performance of the proposed scheme with the capacity-based scheme. We showed that the cross-layer design significantly improves the system performance compared to the capacity-based design, for different values of SNR and correlation coefficients. We investigated the performance of the cross-layer-based algorithm in various network models, including AF and DF relaying networks. Furthermore, we investigated the performance of the cross-layer based algorithm for relay selection and subcarrier allocation in an OFDM-based system. Finally, we studied the optimum number of relays required for cooperation in order to achieve maximum throughput, for different values of SNR.

In chapter 5, we considered a buffer-aided multi-relay network with coded transmissions. We considered a network with independent but non-identically distributed links and assumed that channels undergo quasi-static Rayleigh fading. We looked at three different coding schemes: convolutional codes, Turbo codes and DTC. For each coding scheme, we studied the performance analysis of the system in terms of the average throughput and derived a closed-form expression. Furthermore, by analyzing the asymptotic behavior of the average throughput for infinite buffer size and in the high-SNR regime, we obtained an approximation on the maximum achievable diversity gain of the system. We provided the Monte-Carlo simulations to corroborate the derived analytical framework. We showed that analytical average throughput follows the simulation results under different system parameters, such as channel SNR, number of relays and buffer sized. Finally, we investigated the average delay in different scheme and for different values of SNR and various number of relays and buffer sized.

6.2 Future Work

In this thesis, we have studied the challenges in the cooperative network and designed algorithms for performance improvement. We considered a cooperative network with one source and one destination nodes where all the nodes are equipped with single antenna. These assumptions limit the applicability of the scheme in practical applications. Considering a multi-user network with multi-antenna nodes can be an extension to this work.

The relay selection schemes that we proposed are based on the availability of the perfect and instantaneous CSI estimation, which is not always feasible in practical applications, due to the high amount of overhead. Thus, it is useful to investigate the performance of the network under statistical CSI or under the impact of outdated channel estimation. Furthermore, we considered Rayleigh flat fading channels. Study on the performance of the proposed algorithms on other fading channels like Nakagami-fading is of interest.

For the system with coded transmissions, we assumed fixed rate and fixed packet length during the transmission. However, in actual communication systems such as the LTE-A standard, different code rates and packet sizes are supported. Thus, investigating the adaptability of the system to variable rate and packet lengths can be considered in the future work. Furthermore, in this work, the BPSK modulation scheme is employed. Considering higher level modulations might be part of the future work.

In this thesis, we mainly put focus on improving the physical layer or data link layer characteristics. In more practical situations, the energy efficiency is considered an issue of concern. Designing an energy efficient network is challenging and requires significant modifications to the algorithms at each layer. Studying these challenges and proposing an energy efficient algorithm can be considered a possible direction to the future work. Moreover, in this work we considered orthogonal channels in frequency. However, such schemes suffer a poor spectral efficiency. Since the spectrum is a scarce and valuable resource considering the problem of resource allocation in a cooperative network with non-orthogonal channels is another direction to the future work.

Bibliography

[1] Future mobile data usage and traffic growth. [Online]. Available: https://www.ericsson.com/en/mobility-report/future-mobile-data-usage-and-traffic-growth

[2] A. Goldsmith, *Wireless Communications*. Cambridge University Press, 2005.

[3] "3rd Generation Pertnership Project; technical specification group radio access network; Evolved Universal Terrestrial Radio Access (E-UTRA); relay architecture for E-UTRA (LTE-Advanced)(release 9)," 3GPP, Tech. Rep. TR 36.806 V9.0.0, 2010.

[4] N. Nomikos, T. Charalambous, I. Krikidis, D. N. Skoutas, D. Vouyioukas, M. Johansson, and C. Skianis, "A survey on buffer-aided relay selection," *IEEE Commun. Surveys Tutorials*, vol. 18, no. 2, pp. 1073–1097, Second Quarter 2016.

[5] A. Attarkashani and W. Hamouda, "Performance analysis of power allocation and relay assignment in OFDM systems," in *2016 IEEE International Conference on Communications (ICC)*, May 2016, pp. 1–6.

[6] ——, "Joint power allocation and subcarrier-relay assignment for OFDM-based decode-and-forward relay networks," *IEEE Communications Letters*, vol. 20, no. 11, pp. 2312–2315, Nov 2016.

[7] ——, "Throughput maximization using cross-layer design in wireless sensor networks," in *2017 IEEE International Conference on Communications (ICC)*, May 2017, pp. 1–6.

[8] A. Attarkashani, W. Hamouda, and J. M. Moualeu, "Performance analysis of coded buffer-aided relay systems," 2018, manuscript submitted for publication.

[9] A. Attarkashani, W. Hamouda, J. M. Moualeu, and J. Haghighat, "Performance analysis of Turbo codes and distributed Turbo codes in buffer-aided relay systems," 2018, manuscript submitted for publication.

[10] T. Cover and A. E. Gamal, "Capacity theorems for the relay channel," *IEEE Transactions on Information Theory*, vol. 25, no. 5, pp. 572–584, September 1979.

[11] J. N. Laneman and G. W. Wornell, "Energy-efficient antenna sharing and relaying for wireless networks," in *2000 IEEE Wireless Communications and Networking Conference. Conference Record (Cat. No.00TH8540)*, vol. 1, Sept. 2000, pp. 7–12 vol.1.

[12] A. Sendonaris, E. Erkip, and B. Aazhang, "Increasing uplink capacity via user cooperation diversity," in *Proceedings. 1998 IEEE International Symposium on Information Theory (Cat. No.98CH36252)*, Aug 1998, pp. 156–.

[13] A. Bletsas, A. Khisti, D. P. Reed, and A. Lippman, "A simple cooperative diversity method based on network path selection," *IEEE J. Sel. Areas Commun.*, vol. 24, no. 3, pp. 659–672, Mar. 2006.

[14] S. S. Ikki and M. H. Ahmed, "Performance analysis of generalized selection combining for amplify-and-forward cooperative-diversity networks," in *2009 IEEE Int. Conf. Communications*, Dresden, June 2009, pp. 1–6.

[15] T. Hesketh, R. C. de Lamare, and S. Wales, "Joint partial relay selection, power allocation and cooperative maximum likelihood detection for mimo relay systems with limited feedback," in *2013 IEEE 77th Vehicular Technology Conference (VTC Spring)*, 2013, pp. 1–5.

[16] Y. Jing and H. Jafarkhani, "Single and multiple relay selection schemes and their achievable diversity orders," *IEEE Transactions on Wireless Communications*, vol. 8, no. 3, pp. 1414–1423, March 2009.

[17] Q. Jiang, X. Liao, and H. Chen, "Joint power allocation and subcarrier assignment for two-way OFDM multi-relay system," in *2013 IEEE Wireless Communications and Networking Conference (WCNC)*, April 2013, pp. 709–714.

[18] K. Xiong, P. Fan, K. B. Letaief, S. Yi, and M. Lei, "Joint subcarrier-pairing and resource allocation for two-way multi-relay OFDM networks," in *2012 IEEE Global Communications Conference (GLOBECOM)*, Dec 2012, pp. 4874–4879.

[19] H. Mu, M. Tao, W. Dang, and Y. Xiao, "Joint subcarrier-relay assignment and power allocation for decode-and-forward multi-relay OFDM systems," in *2009 Fourth International Conference on Communications and Networking in China*, Aug 2009, pp. 1–6.

[20] T. Kim and M. Dong, "An iterative hungarian method to joint relay selection and resource allocation for D2D communications," *IEEE Wireless Communications Letters*, vol. 3, no. 6, pp. 625–628, Dec 2014.

[21] A. K. Sadek, Z. Han, and K. J. R. Liu, "Distributed relay-assignment protocols for coverage expansion in cooperative wireless networks," *IEEE Transactions on Mobile Computing*, vol. 9, no. 4, pp. 505–515, April 2010.

[22] S. R. Cho, W. Choi, and K. Huang, "QoS provisioning relay selection in random relay networks," *IEEE Transactions on Vehicular Technology*, vol. 60, no. 6, pp. 2680–2689, July 2011.

[23] K. R. Reddy and A. Rajesh, "Best relay selection using co-operative game theory: Manets," in *2016 International Conference on Communication and Signal Processing (ICCSP)*, 2016, pp. 1347–1351.

[24] A. S. Mohamed, M. Abd-Elnaby, and S. A. El-dolil, "Performance evaluation of adaptive modulation decode-and-forward cooperative wireless communication system with best-relay selection," in *2014 International Conference on Engineering and Technology (ICET)*, April 2014, pp. 1–7.

[25] Y. Hu, C. Schnelling, Y. Amraue, and A. Schmeink, "Finite blocklength performance of a multi-relay network with best single relay selection," in *2017 International Symposium on Wireless Communication Systems (ISWCS)*, Aug 2017, pp. 122–127.

[26] J. N. Laneman and G. W. Wornell, "Distributed space-time-coded protocols for exploiting cooperative diversity in wireless networks," *IEEE Transactions on Information Theory*, vol. 49, no. 10, pp. 2415–2425, Oct 2003.

[27] K. Azarian, H. E. Gamal, and P. Schniter, "Achievable diversity-vs-multiplexing tradeoffs in half-duplex cooperative channels," in *Information Theory Workshop*, 2004, pp. 292–297.

[28] C. Jishi, L. Kongshui, C. Wenjing, and M. Dongtang, "A decentralized multiple relay selection scheme for cooperative relay networks with distributed space-time coding," in *2013 8th International Conference on Communications and Networking in China (CHINACOM)*, Aug 2013, pp. 979–982.

[29] T. Zhang, "Distributed space-time coding with decode-and-forward-amplify-and-forward selection relaying protocol in cooperative wireless sensor networks," *IET Wireless Sensor Systems*, vol. 3, no. 1, pp. 9–15, March 2013.

[30] F. Verde, "Performance analysis of randomised space-time block codes for amplify-and-forward cooperative relaying," *IET Communications*, vol. 7, no. 17, pp. 1883–1898, Nov 2013.

[31] H. V. Khuong, P. C. Sofotasios, V. Q. Son, L. T. Tra, and P. H. Lien, "Analysis of cognitive cooperative networks with best relay selection and diversity reception," in *2015 International Conference on Advanced Technologies for Communications (ATC)*, Oct 2015, pp. 651–656.

[32] S. R. Hussain, S. Shakeera, and K. R. Naidu, "BER analysis of amplify and forward scheme with best relay selection in space shift keying system," in *2015 International Conference on Communications and Signal Processing (ICCSP)*, April 2015, pp. 1722–1726.

[33] G. A. Sukkar, Z. A. Shafeeq, and A. A. Amayreh, "Best relay selection in a multi-relay nodes system under the concept of cognitive radio," in *2015 6th International Conference on Information and Communication Systems (ICICS)*, April 2015, pp. 177–181.

[34] N. Hidayati, Suwadi, and Wirawan, "Performance of best relay selection in single relay selection scheme with network coding," in *2017 2nd International conferences on Information Technology, Information Systems and Electrical Engineering (ICITISEE)*, Nov 2017, pp. 388–391.

[35] D. Yang, X. Fang, and G. Xue, "OPRA: Optimal relay assignment for capacity maximization in cooperative networks," in *2011 IEEE International Conference on Communications (ICC)*, June 2011, pp. 1–6.

[36] K. Hosseini and R. Adve, "Comprehensive node selection and power allocation in multi-source cooperative mesh networks," in *2010 44th Annual Conference on Information Sciences and Systems (CISS)*, March 2010, pp. 1–6.

[37] D. Lee and S. Choi, "Low-complexity interference-aware single relay selection in multi-source multi-destination cooperative networks," in *2012 6th International Conference on Signal Processing and Communication Systems*, Dec 2012, pp. 1–5.

[38] J. B. Kim, M. S. Song, and I. H. Lee, "Achievable rate of best relay selection for non-orthogonal multiple access-based cooperative relaying systems," in *2016 International Conference on Information and Communication Technology Convergence (ICTC)*, Oct 2016, pp. 960–962.

[39] S. Sharma, Y. Shi, Y. T. Hou, and S. Kompella, "An optimal algorithm for relay node assignment in cooperative ad hoc networks," *IEEE/ACM Transactions on Networking*, vol. 19, no. 3, pp. 879–892, June 2011.

[40] I. Krikidis, J. S. Thompson, S. Mclaughlin, and N. Goertz, "Max-min relay selection for legacy amplify-and-forward systems with interference," *IEEE Transactions on Wireless Communications*, vol. 8, no. 6, pp. 3016–3027, June 2009.

[41] M. J. Taghiyar, S. Muhaidat, and J. Liang, "Max-min relay selection in bidirectional cooperative networks with imperfect channel estimation," *IET Communications*, vol. 6, no. 15, pp. 2497–2502, October 2012.

[42] I. Ahmed, A. Nasri, D. S. Michalopoulos, R. Schober, and R. K. Mallik, "Relay subset selection and fair power allocation for best and partial relay selection in generic noise and interference," *IEEE Transactions on Wireless Communications*, vol. 11, no. 5, pp. 1828–1839, May 2012.

[43] R. Burkard, M. DellAmico, , and S. Martello, *Assignment Problems*. SIAM, 2012, vol. 2.

[44] H. W. Kuhn, *The Hungarian method for the assignment problem*. Naval Research Logistics Quarterly, 1955, vol. 2.

[45] E. Lawler, *Combinatorial Optimization: Networks and Matroids*. New York: Dover Publications, Inc., 2011.

[46] H. Alt, N. Blum, K. Mehlhorn, and M. Paul, "Computing a maximum cardinality matching in a bipartite graph in time $o(n^{1.5}\sqrt{\frac{m}{\log(n)}})$," *Information Processing Letters*, vol. 37, no. 4, pp. 237,240, Feb. 1991.

[47] F.-L. Luo and C. Zhang, Eds., *Signal Processing for 5G: Algorithms and Implementations*, 1st ed. John Wiley and Sons, Ltd, 2016.

[48] Z. Fei, B. Li, S. Yang, C. Xing, H. Chen, and L. Hanzo, "A survey of multi-objective optimization in wireless sensor networks: Metrics, algorithms and open problems," *IEEE Communications Surveys Tutorials*, vol. PP, no. 99, pp. 1–1, 2016.

[49] A. Bari, "Relay nodes in wireless sensor networks: A survey," University of Windsor, Windsor, ON, Tech. Rep., Nov. 2005.

[50] A. Vallimayil, K. M. K. Raghunath, V. R. S. Dhulipala, and R. M. Chandrasekaran, "Role of relay node in wireless sensor network: A survey," in *2011 3rd Int. Conf. Electronics Computer Technology (ICECT)*, vol. 5, April 2011, pp. 160–167.

[51] N. Zlatanov, R. Schober, and P. Popovski, "Throughput and diversity gain of buffer-aided relaying," in *2011 IEEE Global Telecommunications Conference - GLOBECOM 2011*, Dec 2011, pp. 1–6.

[52] ——, "Buffer-aided relaying with adaptive link selection," *IEEE Journal on Selected Areas in Communications*, vol. 31, no. 8, pp. 1530–1542, August 2013.

[53] N. Zlatanov and R. Schober, "Buffer-aided relaying with adaptive link selection ;fixed and mixed rate transmission," *IEEE Transactions on Information Theory*, vol. 59, no. 5, pp. 2816–2840, May 2013.

[54] A. Ikhlef, D. S. Michalopoulos, and R. Schober, "Max-max relay selection for relays with buffers," *IEEE Trans. Wireless Commun.*, vol. 11, no. 3, pp. 1124–1135, Mar. 2012.

[55] I. Krikidis, T. Charalambous, and J. S. Thompson, "Buffer-aided relay selection for cooperative diversity systems without delay constraints," *IEEE Trans. Wireless Commun.*, vol. 11, no. 5, pp. 1957–1967, May 2012.

[56] T. Charalambous, N. Nomikos, I. Krikidis, D. Vouyioukas, and M. Johansson, "Modeling buffer-aided relay selection in networks with direct transmission capability," *IEEE Commun. Lett.*, vol. 19, no. 4, pp. 649–652, April 2015.

[57] N. Zlatanov, V. Jamali, and R. Schober, "Achievable rates for the fading half-duplex single relay selection network using buffer-aided relaying," in *2014 IEEE Global Communications Conference*, Dec 2014, pp. 4156–4161.

[58] G. Chen, Z. Tian, Y. Gong, Z. Chen, and J. A. Chambers, "Max-ratio relay selection in secure buffer-aided cooperative wireless networks," *IEEE Transactions on Information Forensics and Security*, vol. 9, no. 4, pp. 719–729, April 2014.

[59] A. A. M. Siddig and M. F. M. Salleh, "Balancing buffer-aided relay selection for cooperative relaying systems," *IEEE Transactions on Vehicular Technology*, vol. 66, no. 9, pp. 8276–8290, Sept 2017.

[60] B. R. Manoj, R. K. Mallik, and M. R. Bhatnagar, "Priority-based max-link relay selection scheme for buffer-aided df cooperative networks," in *2018 IEEE Wireless Communications and Networking Conference (WCNC)*, April 2018, pp. 1–6.

[61] ——, "Performance analysis of buffer-aided priority-based max-link relay selection in df cooperative networks," *IEEE Transactions on Communications*, pp. 1–1, 2018.

[62] P. Xu, Z. Ding, I. Krikidis, and X. Dai, "Achieving optimal diversity gain in buffer-aided relay networks with small buffer size," *IEEE Transactions on Vehicular Technology*, vol. 65, no. 10, pp. 8788–8794, Oct 2016.

[63] W. Raza, N. Javaid, H. Nasir, N. Alrajeh, and N. Guizani, "Buffer-aided relay selection with equal-weight links in cooperative wireless networks," *IEEE Communications Letters*, vol. 22, no. 1, pp. 133–136, Jan 2018.

[64] R. Nakai, M. Oiwa, and S. Sugiura, "Generalized buffer-state-based relay selection for fixed-rate buffer-aided cooperative systems," in *2017 IEEE 85th Vehicular Technology Conference (VTC Spring)*, 2017, pp. 1–5.

[65] R. A. Sultan, A. K. Sultan, and M. Youssef, "Buffered-relay selection in an underlay cognitive radio network," in *2013 11th International Symposium and Workshops on Modeling and Optimization in Mobile, Ad Hoc and Wireless Networks (WiOpt)*, May 2013, pp. 201–207.

[66] G. Chen, Z. Tian, Y. Gong, and J. Chambers, "Decode-and-forward buffer-aided relay selection in cognitive relay networks," *IEEE Transactions on Vehicular Technology*, vol. 63, no. 9, pp. 4723–4728, Nov 2014.

[67] S. Haykin, *Communication Systems*, 4th ed. John Wiley and Sons, Inc., 2000.

[68] P. Robertson, "Illuminating the structure of code and decoder of parallel concatenated recursive systematic (turbo) codes," in *1994 IEEE GLOBECOM. Communications: The Global Bridge*, vol. 3, Nov 1994, pp. 1298–1303 vol.3.

[69] D. Divsalar, S. Dolinar, R. J. McEliece, and F. Pollara, "Transfer Function Bounds on the Performance of Turbo Codes," *Telecommunications and Data Acquisition Progress Report*, vol. 122, pp. 44–55, Apr. 1995.

[70] S. Yiu, R. Schober, and L. Lampe, "Distributed space-time block coding," *IEEE Transactions on Communications*, vol. 54, no. 7, pp. 1195–1206, July 2006.

[71] J. Hu and T. M. Duman, "Low density parity check codes over wireless relay channels," *IEEE Transactions on Wireless Communications*, vol. 6, no. 9, pp. 3384–3394, September 2007.

[72] A. Chakrabarti, A. D. Baynast, A. Sabharwal, and B. Aazhang, "Low density parity check codes for the relay channel," *IEEE Journal on Selected Areas in Communications*, vol. 25, no. 2, pp. 280–291, February 2007.

[73] B. Zhao and M. C. Valenti, "Distributed Turbo coded diversity for relay channel," *Electronics Letters*, vol. 39, no. 10, pp. 786–787, May 2003.

[74] M. C. Valenti and B. Zhao, "Distributed Turbo codes: towards the capacity of the relay channel," in *2003 IEEE 58th Vehicular Technology Conference. VTC 2003-Fall (IEEE Cat. No.03CH37484)*, vol. 1, Oct 2003, pp. 322–326 Vol.1.

[75] Y. Li, B. Vucetic, T. F. Wong, and M. Dohler, "Distributed Turbo coding with soft information relaying in multihop relay networks," *IEEE Journal on Selected Areas in Communications*, vol. 24, no. 11, pp. 2040–2050, Nov 2006.

[76] G. Al-Habian, A. Ghrayeb, M. Hasna, and A. Abu-Dayya, "Distributed Turbo coding using log-likelihood thresholding for cooperative communications," in *2008 42nd Asilomar Conference on Signals, Systems and Computers*, Oct 2008, pp. 1005–1009.

[77] Y. Li, B. Vucetic, and J. Yuan, "Distributed Turbo coding with hybrid relaying protocols," in *2008 IEEE 19th International Symposium on Personal, Indoor and Mobile Radio Communications*, Sept 2008, pp. 1–6.

[78] C. M. Grinstead and J. L. Snell, *Introduction to Probability*, 2nd ed. American Mathematical Society, 1997.

[79] Y. J. Kuo, S. I. Sou, and Y. Lee, "Heuristic approach for subcarrier assignment in relay based femtocell with threshold constraint," in *2014 IEEE International Conference on Communication Systems*, Nov 2014.

[80] N. Parveen, D. S. Venkateswarlu, and B. N. Bhandari, "Implementation of OFDM-based multi-relay multi-pair two-way communication network," in *2014 Eleventh International*

Conference on Wireless and Optical Communications Networks (WOCN), Sept 2014, pp. 1–4.

[81] Y. Fu and Q. Zhu, "Joint optimization methods for nonconvex resource allocation problems of decode-and-forward relay-based OFDM networks," *IEEE Transactions on Vehicular Technology*, vol. 65, no. 7, pp. 4993–5006, July 2016.

[82] Q. Jiang, X. Liao, and H. Chen, "Joint power allocation and subcarrier assignment for two-way OFDM multi-relay system," in *2013 IEEE Wireless Communications and Networking Conference (WCNC)*, April 2013, pp. 709–714.

[83] X. Zhang, X. S. Shen, and L. L. Xie, "Joint subcarrier and power allocation for cooperative communications in LTE-Advanced networks," *IEEE Trans. Wireless Commun.*, vol. 13, no. 2, pp. 658–668, February 2014.

[84] P. Li, S. Guo, W. Zhuang, and B. Ye, "On efficient resource allocation for cognitive and cooperative communications," *IEEE J. Sel. Areas Commun.*, vol. 32, no. 2, pp. 264–273, February 2014.

[85] Y. Li, M. Sheng, C. W. Tan, Y. Zhang, Y. Sun, X. Wang, Y. Shi, and J. Li, "Energy-efficient subcarrier assignment and power allocation in OFDMA systems with max-min fairness guarantees," *IEEE Trans. Commun.*, vol. 63, no. 9, pp. 3183–3195, Sept 2015.

[86] A. M. Jalil and W. Hamouda, "Optimal solution for a joint power allocation and relay assignment problem," *IEEE Trans. Veh. Technol.*, vol. 65, no. 8, pp. 6497–6507, Aug 2016.

[87] J. Kennington and Z. Wang, "A shortest augmenting path algorithm for the semiassignment problem," *J. Operations Research*, vol. 40, no. 1, pp. 178–187, 1992.

[88] A. Mehrabi and K. Kim, "Maximizing data collection throughput on a path in energy harvesting sensor networks using a mobile sink," *IEEE Transactions on Mobile Computing*, vol. 15, no. 3, pp. 690–704, March 2016.

[89] K. Jain, J. Padhye, V. N. Padmanabhan, and L. Qiu, "Impact of interference on multi-hop wireless network performance," *Wireless Networks*, vol. 11, no. 4, pp. 471–487, 2005.

[90] A. Karnik, A. Iyer, and C. Rosenberg, "Throughput-optimal configuration of fixed wireless networks," *IEEE/ACM Transactions on Networking*, vol. 16, no. 5, pp. 1161–1174, Oct 2008.

[91] M. M. Miao, J. Sun, and S. X. Shao, "A cross-layer relay selection algorithm for D2D communication system," in *2014 Int. Conf. Wireless Communication and Sensor Network (WCSN)*, Dec 2014, pp. 448–453.

[92] J. M. Moualeu, W. Hamouda, H. Xu, and F. Takawira, "Cross-layer relay selection criterion for cooperative-diversity networks," in *2012 IEEE Int. Conf. Communications (ICC)*, June 2012, pp. 5075–5079.

[93] A. Saha, A. Ghosh, and W. Hamouda, "Learning-based relay selection for cooperative networks," in *2014 IEEE Global Communications Conf.*, Dec 2014, pp. 386–391.

[94] D. Chen and H. Ji, "QoS oriented cross-layer design for improving multimedia transmissions over cooperative relaying networks," in *2011 IEEE Global Telecommunications Conf. (GLOBECOM 2011)*, Dec 2011, pp. 1–5.

[95] D. Wu, G. Zhu, D. Zhao, and L. Liu, "Cross-layer design of joint relay selection and power control scheme in relay-based multi-cell networks," in *2011 IEEE Wireless Communications and Networking Conf.*, March 2011, pp. 251–256.

[96] S. Efazati and P. Azmi, "Effective capacity maximization in multirelay networks with a novel cross-layer transmission framework and power-allocation scheme," *IEEE Trans. Veh. Technol.*, vol. 63, no. 4, pp. 1691–1702, May 2014.

[97] B. V. Nguyen, R. O. Afolabi, and K. Kim, "Dependence of outage probability of cooperative systems with single relay selection on channel correlation," *IEEE Commun. Lett.*, vol. 17, no. 11, pp. 2060–2063, November 2013.

[98] R. Swaminathan, R. Roy, and M. D. Selvaraj, "Performance analysis of triple correlated selection combining for cooperative diversity systems," in *2013 IEEE Int. Conf. Communications (ICC)*, June 2013, pp. 5483–5488.

[99] S. Dang, J. P. Coon, and G. Chen, "An equivalence principle for OFDM-based combined bulk/per-subcarrier relay selection over equally spatially correlated channels," *IEEE Trans. Veh. Technol.*, vol. PP, no. 99, pp. 1–1, 2016.

[100] Y. Chen and C. Tellambura, "Distribution functions of selection combiner output in equally correlated Rayleigh, Rician, and Nakagami-m fading channels," *IEEE Trans. Commun.*, vol. 52, no. 11, pp. 1948–1956, Nov 2004.

[101] P. Herhold, E. Zimmermann, and G. Fettweis, "On the performance of cooperative amplify-and-forward relay networks," in *5th Int. ITG Conf. Source and Channel Coding*, Jan 2004, pp. 451–458.

[102] T. M. C. Chu, H. Phan, and H. J. Zepernick, "Adaptive modulation and coding with queue awareness in cognitive incremental decode-and-forward relay networks," in *2014 IEEE International Conference on Communications (ICC)*, June 2014, pp. 1453–1459.

[103] T. Islam, A. Ikhlef, R. Schober, and V. K. Bhargava, "Diversity and delay analysis of buffer-aided BICM-OFDM relaying," *IEEE Transactions on Wireless Communications*, vol. 12, no. 11, pp. 5506–5519, Nov. 2013.

[104] M. Marey, H. Mostafa, O. A. Dobre, and M. H. Ahmed, "Data detection algorithms for BICM alternate-relaying cooperative systems with multiple-antenna destination," *IEEE Transactions on Vehicular Technology*, vol. 65, no. 5, pp. 3802–3807, May 2016.

[105] T. E. Hunter and A. Nosratinia, "Diversity through coded cooperation," *IEEE Transactions on Wireless Communications*, vol. 5, no. 2, pp. 283–289, Feb 2006.

[106] J. M. Moualeu, W. Hamouda, H. Xu, and F. Takawira, "Multi-relay Turbo-coded cooperative diversity networks over Nakagami- m fading channels," *IEEE Trans. Veh. Technol.*, vol. 62, no. 9, pp. 4458–4470, Nov. 2013.

[107] J. M. Moualeu, W. Hamouda, and F. Takawira, "AF Turbo-coded selective relaying with imperfect channel state information," in *2014 IEEE International Conference on Communications (ICC)*, June 2014, pp. 5443–5448.

[108] ——, "Selection relaying in coded cooperation with delayed CSI over Rayleigh fading channels," in *2014 IEEE Wireless Communications Networking Conf. (WCNC)*, April 2014, pp. 881–886.

[109] ——, "Relay selection for coded cooperative networks with outdated CSI over Nakagami-m fading channels," *IEEE Transactions on Wireless Communications*, vol. 13, no. 5, pp. 2362–2373, May 2014.

[110] H. Kaya and E. Öztürk, "Performance analysis of distributed Turbo coded scheme with two ordered best relays," *IET Communications*, vol. 9, no. 5, pp. 638–648, 2015.

[111] Y. Liu and M. Tao, "Optimal channel and relay assignment in OFDM-based multi-relay multi-pair two-way communication networks," *IEEE Transactions on Communications*, vol. 60, no. 2, pp. 317–321, February 2012.

[112] A. Mahmood and R. Jantti, "Packet error rate analysis of uncoded schemes in block-fading channels using extreme value theory," *IEEE Commun. Lett.*, vol. 21, no. 1, pp. 208–211, Jan. 2017.

[113] H. E. Gamal and A. R. Hammons, "Analyzing the Turbo decoder using the Gaussian approximation," *IEEE Transactions on Information Theory*, vol. 47, no. 2, pp. 671–686, Feb 2001.

[114] M. K. Simon and M.-S. Alouini, *Digital Communications Over Fading Channels: A Unified Approach to Performance Analysis*. New York, NY, USA: Wiley, 2000.

[115] J. W. Craig, "A new, simple and exact result for calculating the probability of error for two-dimensional signal constellations," in *MILCOM 91 - Conference record*, Nov 1991, pp. 571–575 vol.2.

[116] E. Malkamaki and H. Leib, "Evaluating the performance of convolutional codes over block fading channels," *IEEE Transactions on Information Theory*, vol. 45, no. 5, pp. 1643–1646, Jul 1999.